University of Bahrain

College of Engineering

Department of Electrical and Electronics Engineering

Feasibility of Using Off-Grid PV Powered Atmospheric Water Generating System via Underground Condensation in Bahrain

A Thesis Submitted in Partial Fulfillment of the Requirements for A Degree in Master of Science in Renewable Energy Engineering

Prepared by:

Yusuf Ahmed Alawi

20146996

Supervised by:

Supervisor - Dr. Maamar Taleb, Associate Professor

Co. Supervisor - Dr. Omar Alabbasi, Associate Professor

Kingdom of Bahrain

12 January 2023

University of Bahrain

College of Engineering

Department of Electrical and Electronics Engineering

Feasibility of Using Off-Grid PV Powered Atmospheric Water Generating System via Underground Condensation in Bahrain

A Thesis Submitted in Partial Fulfillment of the Requirements for A Degree in Master of Science in Renewable Energy Engineering

Prepared by:

Yusuf Ahmed Alawi

20146996

Supervised by:

Supervisor - Dr. Maamar Taleb, Associate Professor

Co. Supervisor - Dr. Omar Alabbasi, Associate Professor

Kingdom of Bahrain

12 January 2023

University of Bahrain
College of Engineering
Department of Electrical and Electronics Engineering

Thesis Defense Committee Approval

The student Yusuf Ahmed Alawi, student ID 20146996, has defended the thesis by which he partially fulfilled the requirement for the degree of Master of science entitled "Feasibility of Using an Off-Grid PV Powered Atmospheric Water Generating System via Underground Condensation in Bahrain" on 05/01/2023

Name	**Signature**
Dr. Maamar Taleb *(Supervisor)*	
Dr. Omar Alabbasi *(Co-Supervisor)*	
Prof. Mohamed Abdelkarim Antar (External Examiner)	
Prof. Ahmed Yousif (Internal Examiner)	

Academic Department's Stamp

ELECTRICAL & ELECTRONIC ENGINEERING
UNIVERSITY OF BAHRAIN

Acknowledgments

I would like to express my deepest and sincerest appreciation for all of the great individuals who have supported me through my thesis journey in various ways and phases, as this allowed me to reach such a fruitful outcome.

Firstly, my profound admiration to all my academic tutors that have passed me the knowledge to attain this thesis. This includes my tutors at both my bachelor's and master's level studies at Bahrain Polytechnic and the University of Bahrain, respectively.

I am indebted to my thesis supervisors, Dr. Omar Al-Abbasi and Dr. Maamar Taleb, for always being supportive and guiding me along this journey successfully. You are great leaders that I learnt a lot from you.

Secondly, I would like to pay my regards to my family that being my parents, siblings and wife who have aided me in every way possible throughout my journey by always showing me the utmost support, care, continuous motivation, and sacrifices when times were challenging. You have contributed to make me what I am today. I am grateful and blessed for having you as my backbone.

Last but not least, I would express my gratitude to my tutors from my bachelors' studies from Bahrain Polytechnic, Mr. Nikolaos Vasilikos, Dr. Christina Georgantopoulou, Mrs. Payal Modi and Dr. Sam Chehab for always being supportive mentors as to always providing me with enriching opportunities and experiences where I was able to discover my true hidden strengths and accordingly make them grow all while overcoming my weaknesses. Thank you for motivating me to purse my higher education.

Abstract

Water Scarcity is a worldwide dilemma, thus, investigating sustainable methods of water production is one of the sustainable development goals. The following thesis investigates capability of creating an off-grid photovoltaic powered atmospheric water generating system that operates via underground region condensation in Bahrain (shallow subsurface).

The principle is to have a system which produces water from thin air through forcing warm-humid atmospheric air underground at colder shallow depths, causing water vapor to condense by reaching the dew point due to heat transfer. Consequently, the main objective is to analyze if it is theoretically viable and if so, how much water can be generated in a year.

The methodology closely mimics the shallow underground temperature profile in Bahrain through simulating a 3D model in COMSOL Software by deducing necessary Multiphysics and boundary conditions. To then pair it with a copper pipe and inject within it annual atmospheric air weather records and obverse thermodynamics behavior. Sample COMSOL results are compared with the simplified model to detect deviation between the quantity of water generated. Finally, to size required PV system components.

Hence, underground temperature profile at the surface ranged from 58 and 18 °C during the hottest and coldest intervals of the year while starting to stabilize annually at set temperature boundary conditions of 25 °C at 6-7m depth. Also, after using a 34m long copper pipe of 32.4mm ID with coil design, results were a total 29.2kg of water could be produced for 69 days/yr or 0.42 l/day. The average deviation between models was 43.4% due to volumetric flow rate integration. Sized PV system was a 50 Ah battery, 40W Panel and 5A SCC. Lastly, Recommendations for future work provided.

Table of Contents

Chapter 1 Introduction to the Study **1**

1.1 Introduction **2**

1.2 Research Problem **4**

1.3 Research Questions **4**

1.4 Research Objectives **5**

1.5 Research Significance **7**

1.6 Thesis Outline **8**

1.7 Terminologies **9**

Chapter 2 Theory and Literature Review **11**

2.1 Geothermal Energy **14**

2.1.1 History of Geothermal Energy 15

2.1.2 Geothermal Energy Applications 17

2.1.3 Shallow Subsurface Temperature Modeling 20

2.2 Psychrometric Chart **28**

2.2.1 Relevant Thermodynamics Properties 29

2.3 Atmospheric Water Generator (AWG) and Estimating Water Production **31**

2.3.1 Heat Transfer Rate Required for Condensation 35

2.3.2 Actual Heat Transfer Rate Occurring 38

2.3.3 Calculating Mass Flow Rate of Air and Water 42

2.3.4 Mass of Water to be Generated Per Day 42

2.4 Renewable Energy (RE) and Solar PV Systems **43**

2.4.1 Reason for Selecting Solar PV RE Source 47

2.4.2 Classification of Solar PV Systems 48

2.4.3 Off-Grid PV System Components and Details 49

2.4.4 Off-Grid Solar PV System Sizing Equations 53

2.4.5 Estimating Payback Period of PV Systems 58

2.5 Additional Equations **59**
2.5.1 Helical Coil Pipe Length Formula 59
Chapter 3 Methodology and Procedure **61**
3.1 Methodology and Procedural **62**
3.2 Mathematical Model **64**
3.2.1 Heat Transfer in Solids 64
3.2.2 Surface to Surface Radiation 65
3.2.3 Fluid Flow 66
3.2.4 Moisture Transport in Air – Diluted Species 68
3.3 Parameters and Component Definitions **69**
3.3.1 Building the 3D Geometry 70
3.3.2 Mesh Generation 71
3.4 Transient Study **72**
3.5 AWG Simplified Model **72**
Chapter 4 Results, Discussion and Recommendations **74**
4.1 Shallow Underground Temperature Profile **75**
4.2 Initial Analysis of AWG Feasibility **78**
4.3 Annual Water Production Rate **79**
4.3.1 Assumptions and Variables Utilized 79
4.3.2 Water Production Rate – COMSOL 80
4.3.3 Design Modification to Increase Yield 82
4.3.4 Water Production Rate – Simplified Model 85
4.3.5 Comparison of Water Production Rates 87
4.4 Off-Grid PV System Sizing **89**
4.4.1 Assumptions and Variables Utilized 89
4.4.2 Load Estimate 90
4.4.3 Sizing of Components 90
4.4.4 Payback Period 92

4.5 Conclusion 94

4.6 Recommendations and Future Work 96

References 97

APPENDICES i

APPENDIX A. Mathematical Modelling (COMSOL) ii

APPENDIX B. COMSOL Condensation Result xxii

APPENDIX C. Sample Simplified Model Calculation Result (Excel) xxv

APPENDIX D. Load Estimation - PV System Sizing xxvi

List of Tables

TABLE 1, TYPES OF SOLAR PANELS (DESCRIPTION, PROS AND CONS) – (TALEB, 2020). 51
TABLE 2, TYPES BATTERIES (DESCRIPTION, PROS AND CONS) – (UNBOUNDSOLAR, 2020). 52
TABLE 3, PROCEDURAL FOR SIMPLIFIED MODEL. 72
TABLE 4, CONSIDERED VARIABLES USED FOR GROUND SIMULATION 75
TABLE 5, CONSIDERED VARIABLES USED FOR AWG SIMULATION....79
TABLE 6, WATER CONDENSED/PRODUCED AT A VELOCITY OF 4.25 M/S – COMSOL RESULT. 82
TABLE 7, CONSIDERED VARIABLES USED FOR AWG SIMPLIFIED MODEL....85
TABLE 8, WATER CONDENSED/PRODUCED @4.25 M/S – SIMPLIFIED MODEL SAMPLE RESULT 86
TABLE 9, COMPARISON OF WATER CONDENSATION RESULTS....88
TABLE 10, OFF-GRID PV SYSTEM SIZING VARIABLES 89
TABLE 11, PV SYSTEM LOAD ESTIMATE. 90
TABLE 12, RESULTS OF OFF-GRID SOLAR PV COMPONENT SIZING 91
TABLE 13, ESTIMATING THE PV SYSTEM PAY BACK PERIOD (PBP)....93
TABLE 14, COMSOL CONDENSATION RESULT @4.25 M/S. XXII
TABLE 15, LOAD ESTIMATE FORMULAS USED FOR SIZING PV SYSTEM (FANS AND PUMP)....XXVI

List of Figures

Fig. 1: Earth Cross Section (E. Yahkontova, 2020). 14

Fig. 2: Natural Sources of Geothermal Energy: A – Hot Springs, B – Steam Vents and C- Geysers 15

Fig. 3: History of Geothermal Energy (Links, 2014): A- Paleo American Indians, B - Prince Piero in Italy with Geothermal Power Plant Invention and C - First Commercial Geothermal Power Station in Italy. 16

Fig. 4: Predicted Geothermal Energy Capacity and Growth 2017-2023 (IEA, 2018). 16

Fig. 7: Ground Source Heat Pumps (GHP). 18

Fig. 8: Slink Loops. 18

Fig. 9: Earth Air Heat Exchangers. 19

Fig. 10: Ground samples at different elevations, (a) Physical Model, (b) Computational Domain (NIT, 2017). 21

Fig. 11: Interaction of the Major Factors in the Soil and Mesh Division in the Computation Domain (Tong, 2020). 23

Fig. 12: Annual Soil Temperature Profile of Four Cities (Tong, 2020). 27

Fig. 13, Annual Variation of Soil Temperature at different depths (NIT, 2017). 27

Fig. 14, Soil Temperature difference between Summer and Winter (Sofyan, 2020). 28

Fig. 15: Psychrometric Chart (EngineeringToolbox). 29

Fig. 16: Dry Bulb Temperature DBT vs Wet Bulb Temperature WBT (Alj, 2021) 30

Fig. 17: Simple General Representation of the Atmospheric Water Generating System showcasing its Working Principle. 32

Fig. 18: MOF Atmospheric Water Generator (UC Berkely, 2020). 33

Fig. 19: Water Scarcity Map (Gido, 2016). 35

Fig. 20: Sensible Heat (Quora, 2017) 36

Fig. 21: Latent Heat (Quora, 2017) 37

Fig. 22: Radial Conduction (Meier, 2009). 38

Fig. 23: Forced Convection (Mhhe, 2019). 39

FIG. 24: RESISTANCE NETWORK DIAGRAM OF ACTUAL HEAT TRANSFER RATE OCCURRING 40
FIG. 25: BAHRAIN NATIONAL EE AND RE TARGETS – 2ND ANNUAL INTERNATIONAL SUSTAINABLE ENERGY EVENT (ISEE) (H.E DR. MIRZA, 2021). 44
FIG. 26: RENEWABLE ENERGY (RE) SOURCES 45
FIG. 27: ESTIMATED RENEWABLE ENERGY SHARE OF GLOBAL ELECTRICITY PRODUCTION AT END OF 2019 (IRENA, 2020) 46
FIG. 28: ANNUAL ADDITIONS OF RENEWABLE POWER CAPACITY 2013-2019 (IRENA, 2020) 46
FIG. 29: GLOBAL LEVELIZED COST OF ELECTRICITY OF ELECTRICITY FROM NEWLEY COMMISSIONED, UTILITY-SCALE RENEWABLE POWER GENERATION TECHNOLOGIES (IRENA, 2020) 47
FIG. 30: ON-GRID PV SOLAR SYSTEMS (MEPCELL, 2018) 48
FIG. 31: OFF-GRID PV SOLAR SYSTEMS (MEPCELL, 2018) 49
FIG. 32: DIAGRAM SHOWING MAIN COMPONENTS FOR OFF-GRID PV SYSTEM (BHGPOWER, 2020) 50
FIG. 33: SERIES VS PARALLEL STRING ARRANGEMENT (MINDER, 2022) 55
FIG. 34: SUMMARIZED DIAGRAM OF THESIS METHODOLOGY AND PROCEDURAL. 63
FIG. 35: ILLUSTRATION OF THE 3D DOMAIN CONFIGURATION – GROUND AND PIPE PROFILE 71
FIG. 36: MESH SETTINGS IN COMSOL. 71
FIG. 37: COMSOL SHALLOW UNDERGROUND TEMPERATURE PROFILE SAMPLE RESULT DAY 226. 76
FIG. 38: COMSOL SHALLOW UNDERGROUND TEMPERATURE PROFILE RESULT (TEMP VS DEPTH) 77
FIG. 39: INITIAL AWG ANALYSIS - AMBIENT PROPERTIES & GROUND TEMP (HIGH DWPNT). 78
FIG. 40: CONDENSATION INDICATOR @4.25M/S. 80
FIG. 41: CONDENSATION RATE @4.25M/S. 81
FIG. 42: CONDENSATION TREND AT VARIOUS VELOCITIES FOR SIMILAR PIPE DESIGN. 84
FIG. 43: COMPARISON OF WATER CONDENSATION RESULTS. 88
FIG. 44: COMSOL STUDY SETTINGS (MULTIPHYSICS MODEL BUILDER). II
FIG. 45: COMPONENT DEFINITIONS – AMBIENT PROPERTIES. II
FIG. 46: COMSOL TIME DEPENDANT STUDY SETTINGS. III
FIG. 47: UTILIZED PARAMETERS SETTINGS IN COMSOL III
FIG. 48: AMBIENT PROPERTIES SETTINGS IN COMSOL. IV
FIG. 49: NONLOCAL COUPLINGS AND PROPERTIES SETTINGS IN COMSOL. V

FIG. 50: BUILDING GEOMETRY IN COMSOL – GROUND BLOCK SETTINGS V
FIG. 51: BUILDING GEOMETRY IN COMSOL – PIPE DESIGN HELIX SETTINGS. VI
FIG. 52: SETTING SOIL MATERIAL FOR GROUND DOMAIN - COMSOL VI
FIG. 53: SETTING COPPER MATERIAL FOR PIPE DOMAIN - COMSOL VII
FIG. 54: SETTING COPPER MATERIAL FOR AIR DOMAIN – COMSOL VII
FIG. 55: COMSOL HEAT TRANSFER IN SOLIDS PHYSICS SETTINGS VIII
FIG. 56: COMSOL HEAT TRANSFER IN SOLIDS PHYSICS – SOLID GROUND SETTINGS VIII
FIG. 57: COMSOL HEAT TRANSFER IN SOLIDS PHYSICS – INITIAL VALUES SETTINGS IX
FIG. 58: COMSOL HEAT TRANSFER IN SOLIDS PHYSICS – HEAT FLUX SETTINGS PART 1 IX
FIG. 59: COMSOL HEAT TRANSFER IN SOLIDS PHYSICS – HEAT FLUX SETTINGS PART 2 X
FIG. 60: COMSOL HEAT TRANSFER IN SOLIDS PHYSICS – MOIST AIR SETTINGS X
FIG. 61: COMSOL HEAT TRANSFER IN SOLIDS PHYSICS – THIN LAYER PIPE SHELL SETTINGS XI
FIG. 62: COMSOL HEAT TRANSFER IN SOLIDS PHYSICS – INFLOW SETTINGS XI
FIG. 63: COMSOL HEAT TRANSFER IN SOLIDS PHYSICS – OUTFLOW SETTINGS XII
FIG. 64: COMSOL SURFACE TO SURFACE RADIATION SETTINGS XII
FIG. 65: COMSOL SURFACE TO SURFACE RADIATION – DIFFUSE SURFACE SETTINGS XIII
FIG. 66: COMSOL SURFACE TO SURFACE RADIATION – INITIAL VALUES SETTINGS XIV
FIG. 67: COMSOL SURFACE TO SURFACE RADIATION – OPACITY SETTINGS XIV
FIG. 68: COMSOL SURFACE TO SURFACE RADIATION – EXTERNAL RADIATION SOURCE SETTINGS XV
FIG. 69: COMSOL LAMINAR FLOW PHYSICS SETTINGS. XV
FIGURE 70, DIAGRAM SHOWING INLET AIR FLOW AND COLLECT CONDENSED WATER REGION XVI
FIG. 71: COMSOL LAMINAR FLOW PHYSICS – FLUID PROPERTIES SETTINGS. XVII
FIG. 72: COMSOL LAMINAR FLOW PHYSICS – INITIAL VALUES SETTINGS. XVII
FIG. 73: COMSOL LAMINAR FLOW PHYSICS – WALL SETTINGS. XVIII
FIG. 74: COMSOL LAMINAR FLOW PHYSICS – INLET SETTINGS. XVIII
FIG. 75: COMSOL LAMINAR FLOW PHYSICS – OUTLET SETTINGS. XIX
FIG. 76: COMSOL MOISTURE TRANSPORT IN AIR PHYSICS SETTINGS. XIX
FIG. 77: COMSOL MOISTURE TRANSPORT IN AIR PHYSICS – MOIST AIR SETTINGS. XX
FIG. 78: COMSOL MOISTURE TRANSPORT IN AIR PHYSICS – INITIAL VALUES SETTINGS. XX

Fig. 79: COMSOL Moisture Transport in Air Physics – Insulation Settings. xx
Fig. 80: COMSOL Moisture Transport in Air Physics – Inflow Settings. xxi
Fig. 81: COMSOL Moisture Transport in Air Physics – Outflow Settings. xxi
Fig. 82: Sample Simplified Model Calculation to Estimate Water Condensation in day/step # 210.667 of the year in Excel. xxv
Fig. 83, Diagram of Sized PV System xxvii

Chapter 1 Introduction to the Study

1.1 Introduction 2

1.2 Research Problem 4

1.3 Research Questions 4

1.4 Research Objectives 5

1.5 Research Significance 7

1.6 Thesis Outline 8

1.7 Terminologies 9

1.1 Introduction

Water is a highly valuable natural resource of which all living beings require it to survive, However, its scarcity is continuously increasing, causing worldwide related shortages threatening sustainable living, which might be via decrease in agriculture activities, shortage of clean water supply for hygiene, or drinking and hence, causing diseases or even deaths in cases of presence of unsafe water or no water supply at all (Science Daily, 2022).

Four billion people experience severe water scarcity for at least one month each year. Also, two billion people live in countries where the water supply is inadequate. Furthermore, half of the world's population could be living in areas facing water scarcity by as early as 2025, and around 700 million people by 2030 may be displaced due to the intense water scarcity faced. To add, it is also expected that by 2040, approximately ¼ of children worldwide will be living in areas of extreme water scarcity (UNICEF, 2010).

Thus, to tackle various sustainable development goals (SDG's), it is vitally important to endlessly research and investigate new sustainable methods of water productions as the two typical temperature and pressure driven water purification methods that being boiling and evaporation as well as reverse osmosis (RO) have several negative impacts to various sectors such as environment, healthy, food and energy (F. Bensebaa, 2013).

That said, the present thesis investigates the theoretical analysis and design to the feasibility of creating a sustainable off-grid photovoltaic (PV) powered atmospheric water generating (AWG) system functioning via condensation in Bahrain in the underground region (shallow subsurface).

The system's basic theoretical operating principle revolves around the idea of having a fan that forces high temperature and humid atmospheric air

at a specific volumetric flow rate from above ground through the inlet of a copper pipe design leading to underground at specific shallow depths reaching -10m where temperature is stable throughout the year and it is also lower during the summer relative to the temperature above ground. Hence, because of the temperature difference, the warm and moist atmospheric air rejects some of its thermal energy to the surrounding soil via combined radial conduction and forced convection heat transfer to eventually reach the dew point temperature (DWPNT) hence water condenses reaching 100% relative humidity (RH). The condensed water droplets are then formed and collected at the bottom of the system, which can then be pumped above ground for access. It is vital to stress that the psychrometric chart is the foundation to understand thermodynamics and heat transfer behaviors as it identifies various thermodynamics properties such as dry bulb temperature (DBT), relative and specific humidity (RH and SH), and humidity ratio.

The idea is that such system could be fully operated via properly sizing an off-grid PV system for sourcing power to operate the appliances in the worst-case remote application. Also, on the fact that in various regions of the world, shallow subsurface or underground applications of Ground Source Heat Pumps (GHP) and earth air heat exchanger is common which will somewhat serve us for similar use. GHP's are systems in which holes are drilled at shallow depths and pipes are connected in a continuous loop called a slinky loop which circles underground to increase the heat transfer rate. In such systems, water or other liquid flows through the loop during the winter season and absorbs heat from underground and such heated fluid is then pumped above ground and is used for heating houses, water tanks etc., to reduce electricity consumption. In contrast, during the summer season, the reverse application is utilized (O. Sullivan, 2022).

1.2 Research Problem

There are various key problems and constraints to the thesis topic, and such is invadable in every thesis, or else the topic and its objectives serve no real challenge or benefit to the research community. That said, thesis includes problems such being that no similar work has been published of shallow underground temperature profile modelling in Bahrain whether it be via actual experimental readings or utilizing computer aided drawing (CAD) software's to mimic behaviour so, attempting this research to place a foundation could be somewhat challenging to attempt it accurately. In addition to the latter, such research in other countries is available, but either rare to find or very little of information is available on it. It contains questionable results like idealistic temperatures ranges, or following a different complex modelling method making it challenging to interpret, such includes using other software, environmental variables and constraints are different etc.

To add, other problems include the complexity of deriving the appropriate engineering formulas to suit the application researched. This includes combining formulas from various courses such as thermodynamics, heat transfer, and fluid mechanic to account for countless variables such as pipe length, combined heat transfers, volumetric flow rate.

1.3 Research Questions

There are several important questions about the research topic that arises which must be critically acknowledged to optimistically overcome of which some being the following:

1. Is the temperature difference between shallow underground and atmospheric air sufficient for permitting the atmospheric air to reach

the DWPNT throughout the year allowing water to reach 100% RH to achieve condensation?

2. Can sufficient water be produced annually? What design element can be modified to improve the result if not?
3. Will there be any concrete literature review that can be efficiently utilized to be of significance, especially for subsurface shallow temperature profile modeling?
4. How long will the CAD simulation take for such complicated computation, especially with trial and error, and will it be viable?
5. To what extent will the utilized CAD Software be accurate, especially to the simplified model?

1.4 Research Objectives

After clearly discussing the research motivation within the introduction in section 1.1, along with the research problems and mainly research questions in sections 1.2 and 1.3, the research objectives can be clearly summarized to further paint a clearer picture of the deliverables. That said, the main thesis topic deliverables include:

1. The first objective is computing a 3D model of a shallow underground temperature profile in Bahrain:

- Approached via utilizing COMSOL Software with necessary Multiphysics to mimic real-life conditions.
- Depict and analyze annual temperature profile and fluctuation as function of depth for logical interpretation to verify with other available literature.

- Observe at which depth the temperature stays stable throughout the year with the least fluctuation, which will be a depth greatly focused on for water generation due to the constant soil temperature variable.
- Aids is an early portrayal of whether AWG system is feasible DWPNT > temperature shallow below ground.

2. The second objective is continuity of computer computation to determine the amount of water to be generated annually:

- Continue using COMSOL software to couple the shallow subsurface temperature profile 3D Model of Bahrain with a 3D pipe that stretches from surface level to the required depth underground.
- Utilize COMSOL Multiphysics to mimic forced flow of atmospheric air within the pipe having annual atmospheric air weather records extracted directly from COMSOL feature based on Bahrain's geographical coordinates.
- Water generation to be determined via running diluted species and heat transfer through solids and fluids Multiphysics on COMSOL.
- Fine tune parameters like pipe length, air volumetric flow rate etc to increase yield of water production results.

3. The third objective is to compare the results of simplified model calculation to that of results obtained from COMSOL simulations:

- To note deviation and accuracy of the water generated sample results between mathemtical model and COMSOL results via utilizing heat transfer and theoretical thermodynamics formulas and using modeled underground temperature and COMSOL ambient properties.

4. The final objective includes sizing the required off-grid PV system components to supply the necessary power to operate all devices of

the AWG in remote applications in the form of sustainable renewable energy (RE) systems:

- Estimate loads of the AWG system to allow operation.
- Proper sizing of PV system includes PV panels, batteries, solar charge controller (SCC) is all required.
- An alternating current (AC) to direct current (DC) inverter will not be necessary to be sized as the aim is to efficiently utilize DC devices directly to cut cost of necessary off grid solar PV system.

1.5 Research Significance

With the research objectives clearly discussed above, along with the problems and questions, the thesis significance can be explained below:

- Lack of Similar Work – The research topic is of great importance due to that it was not explored before in Bahrain as well as various other countries, which will be clear at the literature review stage. Therefore, this exploration can be regarded as a strong foundation for similar scopes of work locally or internationally, which includes future project piloting if the system is deemed feasible and also, utilizing shallow subsurface ground temperature modelling for any relevant analysis such as GHP's or earth air heat exchangers, and even mimicking similar feasibility study of such AWG system in countries with extreme water scarcity like Somalia, Chad and Niger within the African continent for possible application (UNDRR, 2022).
- Sustainable Technology – If such a system is theoretically deemed feasible to produce a significant amount of water per unit time, it is a positive milestone of which this system can be looked at upon as a

possible technology which can mitigate water scarcity to help reduce its impact along with the impacts of conventional water production techniques and sustain the biosphere to a certain extent after further development and actual piloting on real-life basis.

- SDG's and Bahrain 2030 Vision – The research topic is significant due to the fact that, if proven functional, it could directly contribute to and align to the various SDG's and Bahrain 2030 visions such being Sustainable Clean Water SDG 6, Affordable and clean Energy SDG 7, Innovation SDG 9, Sustainable Cities and Communities SDG 11 and life on land SDG 15 (Bahrain, 2008).

1.6 Thesis Outline

The thesis is segregated into four chapters where the content is as follows:

- Chapter 1 – Introduction to the Study: chapter of which we are currently within it discusses 7 elements that being an introduction to the thesis, research problems, questions, objectives and research significance. To add, other than the thesis setting section that we are currently within, it also encompasses the various research terminologies proceeding it.
- Chapter 2 – Theory and Literature Review: chapter includes clear and concise theoretical explanation of the thesis topic and relevant information required for processing results of which includes geothermal energy, psychrometric graph, necessary thermodynamics and heat transfer theories and formulas required to estimate water production rate and, RE, off grid PV systems sizing etc. Chapter 2

also includes relevant supporting literature review to highlight what was previously done about such topic being shallow subsurface temperature profiling and AWGs to focus on the extent of benefits.

- Chapter 3 – Methods and Procedures: This chapter tackles the methodology, research tools, and data collection procedures. This mainly revolves around how theory and problems are taken into account and applied respectively through COMSOL and attempting simplified model to attain thesis objectives.
- Chapter 4 – Results, Discussion, Conclusion and Recommendations: Chapter will showcase and discuss the results of the shallow underground temperature profile obtained from COMSOL Multiphysics 3D simulation as well as showcasing the total amount of water that can be theoretically generated annually via COMSOL to then compare it with sample results of mathemtical model. To add, required sized off-grid solar system components will be emphasized. Finally, recommendations on the thesis work done to be honestly declared in aims of future use and developments.

Nonetheless, after the fourth chapter, there will be dedicated references sections to include all of the used references in APA Style sixth edition as well as an appendices section to include any additional work that was not included in the main body of the thesis.

1.7 Terminologies

AC	Alternating Current
3D	Three Dimensional
AWG	Atmospheric Water Generator
CAD	Computer Aided Drawing

DBT	Dry Bulb Temperature
DC	Direct Current
DOD	Depth of Discharge
DWPNT	Dew Point Temperature
GHP	Geothermal Heat Pump
ID	Inside Diameter
Impp	Optimum Operating Current Corresponding to Maximum Power Point
Isc	Short Circuit Current
OD	Outside Diameter
PBP	Pay Back Period
PV	Photovoltaic
RE	Renewable Energy
RH	Relative Humidity
SCC	Solar Charge Controller
SDG's	Sustainable Development Goals
SH	Specific Humidity
VMP	Optimum Operating Voltage Corresponding to Maximum Power Point
VOC	Open Circuit Voltage
WBT	Wet Bulb Temperature

Chapter 2 Theory and Literature Review

2.1 Geothermal Energy 14

2.1.1 History of Geothermal Energy 15

2.1.2 Geothermal Energy Applications 17

2.1.3 Shallow Subsurface Temperature Modeling 20

2.1.3.1 COMSOL Modeling 26

2.2 Psychrometric Chart 28

2.2.1 Relevant Thermodynamics Properties 29

2.3 Atmospheric Water Generator (AWG) and Estimating Water Production 31

2.3.1 Heat Transfer Rate Required for Condensation 35

2.3.1.1 Sensible Heat Transfer Rate Required 35

2.3.1.2 Latent Heat Transfer Rate Required 36

2.3.1.3 Sum of Heat Transfer Rate Required 37

2.3.2 Actual Heat Transfer Rate Occurring 38

2.3.2.1 Radial Conduction and Forced Convection 38

2.3.2.2 Actual Heat Transfer Rate Formula 39

2.3.2.3 Radial Conduction Resistance Formula 40

2.3.2.4 Forced Convection Resistance Formula 41

2.3.3 Calculating Mass Flow Rate of Air and Water 42

2.3.4 Mass of Water to be Generated Per Day 42

2.4 Renewable Energy (RE) and Solar PV Systems 43

2.4.1 Reason for Selecting Solar PV RE Source 47

2.4.2 Classification of Solar PV Systems 48

2.4.3 Off-Grid PV System Components and Details 49

2.4.4 Off-Grid Solar PV System Sizing Equations 53

2.4.4.1 Load Estimate Including Wiring Efficiency 53

2.4.4.2 Battery Sizing 54

2.4.4.3 PV Panel Sizing 56

2.4.4.4 SCC Sizing 58
2.4.5 Estimating Payback Period of PV Systems 58
2.5 Additional Equations 59
2.5.1 Helical Coil Pipe Length Formula 59

The following chapter disucssed the theoretical framework and background of the researched topic including relevant literature review to summarize what has been previously and how it has been beneficial to this research. Thus, chapter will critically include the following:

- Geothermal Energy – Section highlights relevancy to investigated topic, general information, history and applications to focus on shallow crust region, and most importantly how to mimic shallow subsurface temperature modelling and profiling where this includes looking at the relevant physics being solar radiation, long wave radiation, combined convection and conduction heat transfer.
- Psychrometric Chart – To stress the relevance of the psychrometric chart to the investigated topic. To also discussing various specific thermodynamic properties such as DBT, DWPNT, RH and SH.
- AWG's and Estimating Water Production – This segment argues the AWG studied with extra details about functionality as well as arguing what has been previously done about AWG's. This segment also mainly includes the bounding theoretical formulas to estimate water production which contains various thermodynamics and heat transfer formulas like sensible and latent heat, radial conduction, forced convection and dimensionless numbers ex Reynolds, Nusselt and Heat Transfer Coefficient.
- Solar PV Systems – This section includes general classification of solar PV systems to dissect associated systems components to mainly highlight the focus on off-grid systems and the necessary formulas and calculations to size the system for the intended AWG application. To add, estimating the payback period (PBP) of the system.

- Additional Equations – Helical coil length formula used to estimate the length of the copper helical coil pipe design.

2.1 Geothermal Energy

Geothermal energy is simply the thermal energy that is generated/stored below land surfaces Fig. 1 (Nat Geo, 2012).

Nevertheless, considering how such energy is generated, a small fraction of the thermal energy is produced as a result of friction occurring between the rocks deep beneath the crust. Also, a small fraction is due to gravitational pull formed when the earth was formed approx. 4 billion years ago. Yet, the majority of the heat is generated due to nuclear reactions occurring and the decay of radioactive materials. Moreover, not to forget, it is important to stress and clarify that some of the heat that is stored at extreme shallow's levels being the upper part of the crust/land, is due to the solar radiation received from the sun. The latter is of our crucial focus in this thesis as we intent on tackling such region of the geosphere layer being crust to access for our type of application which is similar to ground source heat pump application as will be discussed clearly in the geothermal energy application section below.

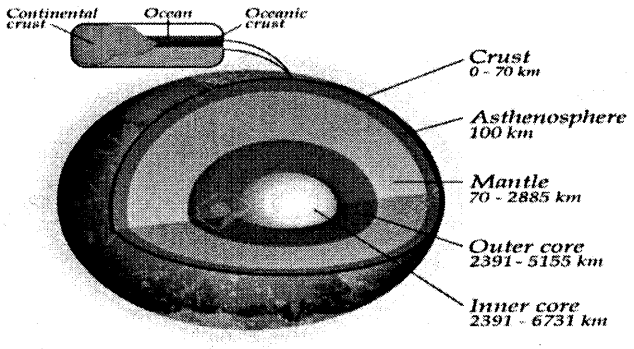


Fig. 1: Earth Cross Section (E. Yahkontova, 2020).

Geothermal Energy, as will be discussed later, is mainly used for power generation and heat and cooling purposes nowadays. However, there are naturally occurring sources of geothermal energy such as hot springs, steam vents, lava and geysers as shown Fig. 2. Nonetheless, geothermal energy is considered a clean and renewable energy source which is utilized in a particular application that is to be clarified in subsection below 2.1.2.



Fig. 2: Natural Sources of Geothermal Energy: A – Hot Springs, B – Steam Vents and C- Geysers

2.1.1 History of Geothermal Energy

A short summary of some history to present related encounters to geothermal energy can be seen provided (Links, 2014):

- The First Encounter: based on archaeologists, the first human and geothermal energy sources interaction occurred in North America estimated to be +10,000 years ago by Paleo American Indians via the use of hot springs for cooking, bathing and cleaning (Fig. 3 - A).
- 1807 - City of Hot Springs, Arkansas: European settlers moved west and encountered hot springs.
- 1892 – Low-Temperature Geothermal District Heating System: hot springs were pumped to heat 450 homes and buildings in Idaho.
- 4th July 1904 – First Geothermal Power Plant: invented by Prince Piero Conti in Tuscan, Italy after lighting four light bulbs (Fig. 3-B).

- 1911 – First Commercial Geothermal Power Station Built in Italy: after the success of Prince Piero Conti in Tuscan Italy, a larger geothermal power plant was constructed in Italy (Fig. 3-C).
- 2017 – 14GW Geothermal Energy Capacity in more than 24 countries worldwide: with development in technology, estimated growth is 4.7%, to reach 18GW by 2023 (Fig. 4).

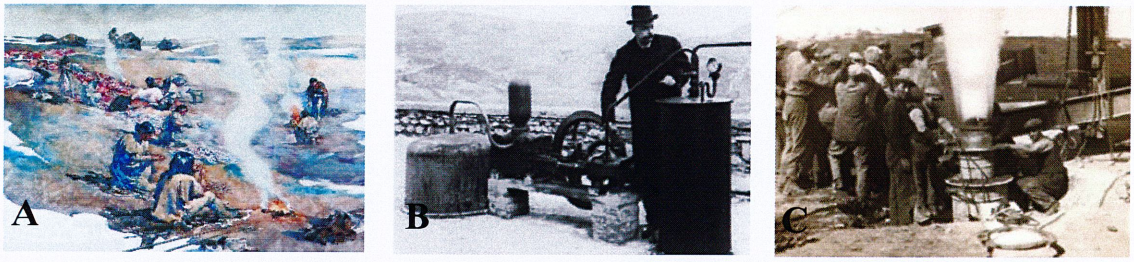


Fig. 3: History of Geothermal Energy (Links, 2014): A- Paleo American Indians, B - Prince Piero in Italy with Geothermal Power Plant Invention and C - First Commercial Geothermal Power Station in Italy.

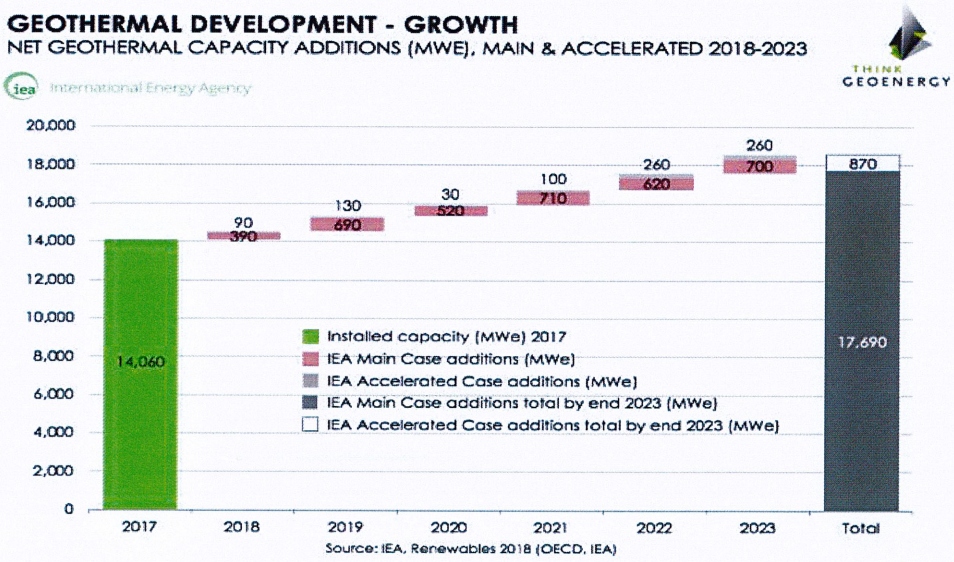


Fig. 4: Predicted Geothermal Energy Capacity and Growth 2017-2023 (IEA, 2018).

2.1.2 Geothermal Energy Applications

There are two main uses or applications of geothermal energy which can be classified into electricity generation and heating/cooling applications (Nat Geo, 2012). Electricity generation applications are differentiated into 4 various types of power plants such being dry steam, flash steam, binary cycle and finally enhanced geothermal systems. On the other hand, heating and cooling applications uses include low-temperature geothermal energy, coproduced geothermal energy, ground heat pumps and earth air heat exchangers. Hence, since our investigated topic is not considering electricity generation via geothermal energy application, our main area of focus is on the second type of application.

1. Low-Temperature Geothermal Energy – accessed from underground pockets of heat around 150 °C or less. Pockets are found at shallow depths compared to electricity generation applications. Such thermal energy from pockets such as hot springs are then used for heating homes, industrial processes, cooking and even bathing. An example of these hot pockets is when it was used by paleo Indians as mentioned in the history section above as hot springs as well as in 1892 in Idaho being the first geothermal district heating system.
2. Groundsource Heat Pumps (GHP's) as illustrated in Fig. 5 – Accessible worldwide where holes are drilled at shallow depths of 3-90m. Pipes are connected to GHP in a slinky loop design, allowing increased heat transfer rate due to increased length see Fig. 6. Cold water or other liquid flows through the slink loop during the winter season and absorbs heat from underground. Heated fluid is pumped above ground and used for heating application to reduce electricity consumption. Oppositely,

during the summer, warm water from above ground is pumped underground to reject heat and cools as the temperature underground is lower. The largest GHP was constructed in 2012 in Ball state University Indiana, replacing a coal-fired boiler system, saving 2M$/yr in heating cost and CO_2 footprint (Nat Geo, 2012).

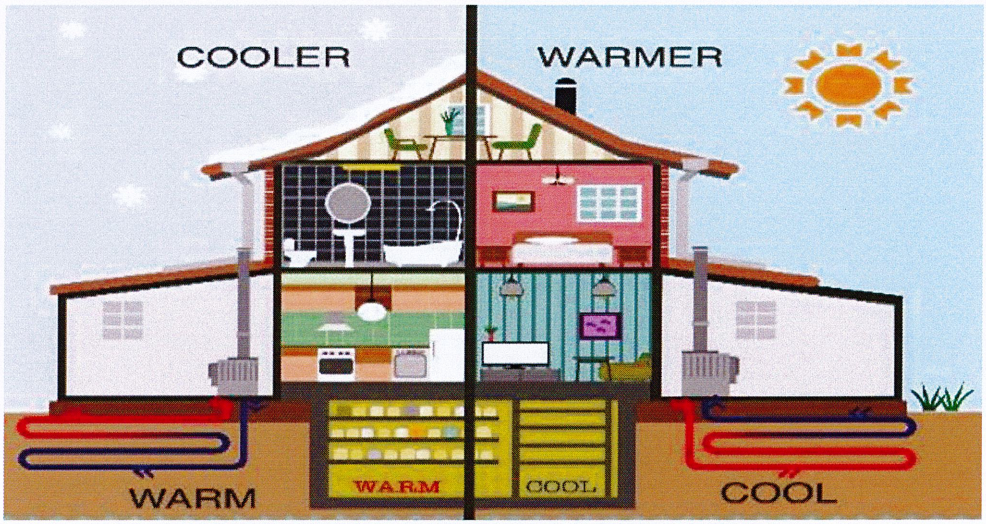


Fig. 5: Ground Source Heat Pumps (GHP).

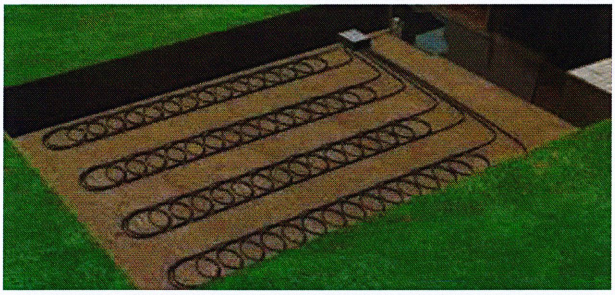


Fig. 6: Slink Loops.

3. Co-produced Geothermal Energy – hot water as a byproduct from oil and gas production is used to be further reinjected into geothermal wells to get further heated and used. The advantage is that previously such a byproduct of water was discarded, hence,

thermal energy loss. To showcase the protentional, 25 million Barrels of hot water is produced every year as a byproduct in USA (Nat Geo, 2012).

4. Earth Air Heat Exchangers illustrated in Fig. 7 – Functions similar to that of GHP's but instead of working fluid as liquids, the median fluid used is atmospheric air/gas.

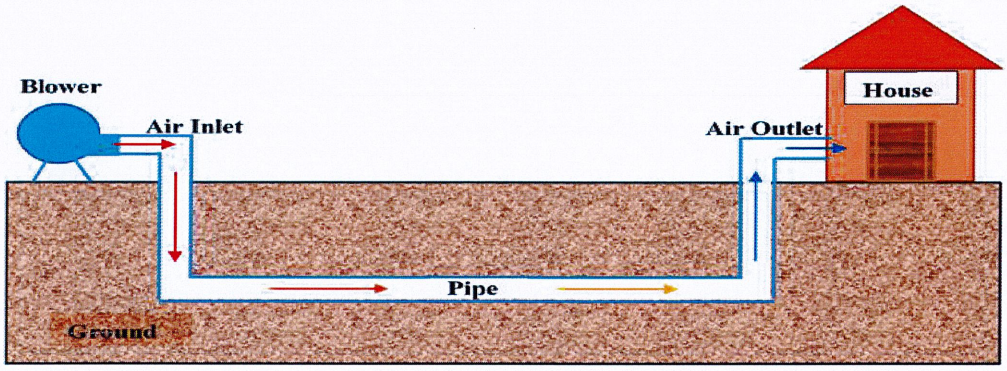


Fig. 7: Earth Air Heat Exchangers.

As seen above, the investigated AWG in this research topic has a similar approach to the working principle of GHP's and earth air heat exchangers as explained above of which will be further discussed in Chapter 2 below. The only difference is that instead of using the medium/working fluid to heat or cool a dedicated area, the cooled working fluid is atmospheric air for the purpose of harvesting moisture content. The application as will be seen is rather innovative and must be crucially analyzed to assess the feasibility and that is why temperature modeling of shallow subsurface/underground is of main importance.

2.1.3 Shallow Subsurface Temperature Modeling

As discussed, and also will be clearer later that in order to analyze the capability of the AWG system considered, shallow subsurface temperature modeling is a must to check if the temperature underground is sufficient to reach DWPNT. However, doing so without having any actual experimental readings to compare to is somewhat challenging given that there are multiple interacting physics. Nevertheless, the literature review is highly important in this section to consider note on its usefulness.

Firstly, Singh and Sharma (NIT, 2017) published a paper titled "Numerical Analysis for Ground Temperature Variation". The objective of the paper was to predict ground temperature variation in relation to depth for time-variant ambient air temperature and solar radiation data for their location. The methodology utilized to determine a numerical solution was via finite difference method to discretize the computational domain. The obtained numerical results were compared with experimental results of ground temperature. They computed diurnal temperature variation for the hottest day, coldest day, and annual variation for 2016. It was found that diurnal temperature variation is up to 0.4m depth and annual temperature variation is only up to 4m depth.

In summary, the mathematical formulation considered in the paper was a semi-infinite solid with one-dimensional (1D) coordinates as seen in Fig. 8 (a). They considered a variation of ground temperature following 1D transient heat conduction equation (2-1) by Carslaw and Jaeger (1980):

$$\frac{\partial^2 T(y,t)}{\partial y^2} = \frac{1}{\alpha}\frac{\partial T(y,t)}{\partial t} \qquad (2\text{-}1)$$

To add, equation (2-1) used was subjected to the first boundary condition at the ground surface by Bhardwaj and Bansal (1981) - (2-2):

$$\left(-k\,\frac{\partial T}{\partial y}\middle| y=0\right) = h\left(T_a - T_{y=0}\right) - \varepsilon\,\Delta R + \alpha_0 S. \qquad (2\text{-}2)$$

Considering the above equation (2-2), the thermal conductivity (k) through the ground surface is shown on the left term (solar radiation absorbitivity). The middle part of the formula takes into account the convective heat transfer (h) between ground surface ($T_{y=0}$) and air (T_a), temperatures whereas the last term on the right take into account the thermal radiation (ΔR), emissivity of soil ε and solar radiation level (S) absorbed by the ground surface with an absorptivity of soil = α_o.

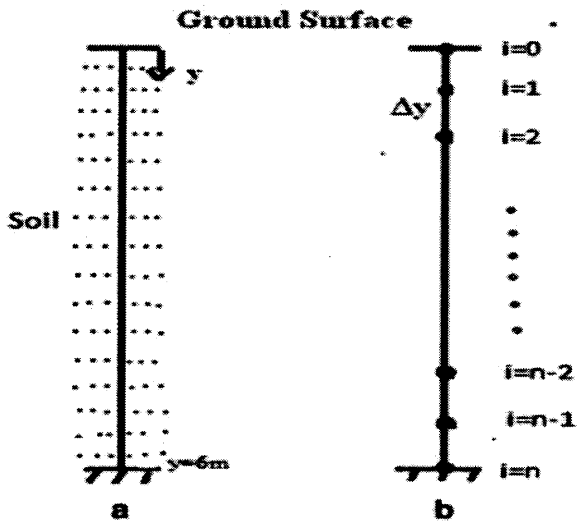


Fig. 8: Ground samples at different elevations, (a) Physical Model, (b) Computational Domain (NIT, 2017).

The main problem with their approach is that they had to use experimental data from underground to compare their numerical data and inject it into analysis, which is not similar to this research topic as no

experimental results are available for Bahrain. Moreover, the other setback is that they focused on one-dimensional (1D) modeling for a mathematical formulation which is not refined and precise for this research due to the fact that both ground temperature modeling, as well as water production rates, are all to be done via 3D analysis on COMSOL. Moreover, the methodology proved to have positive results, which motivates research, and that annual temperature variation underground is only up to 4m depth which means that for analyzing water production, it is ideal to reach depths more than 4m for stable temperature throughout the year.

Secondly, in 2020, Tong, Li, Duanmu and Wang, published a paper titled "Prediction of Temperature Profiles for Shallow Ground in Cold Region and Cold Winter Hot Summer Region of China". The motivation of the research is the lack of ground temperature data which prevented the development of underground engineering in China. The paper highlights how such analysis is crucially important to analyze applications of Groundsource heat pumps and earth air heat exchangers, so simplifying such analysis is vital for development. Researchers tried to overcome certain limitation of previous studies by considering surface radiation and evaporation and simplifying it as pure heat conduction then proposing a solution to ground modeling when the unavailability of ground temperature data, and avoiding 1D semi-infinite solid heat transfer model which provides a non refined and precise set of data etc.

The paper had the main objective to propose and validate a numerical prediction model that considers the effects of all physics and factors as shown in Fig. 9 and that they are necessary for ground modeling except moisture transport assumed fixed, such being short wave solar radiation absorbed by the soil, long wave radiation between sky and soil surface, latent evaporation energy of water in the soil surface, heat convection between air and soil

surface, heat conduction inside the ground, soil freezing and thawing latent heat of the water in soil on ground temperature along with the use of meteorological year databases to provide weather parameters for the numerical model. In addition, due to the long calculation time for numerical model, two harmonic analytic correlation (THAC) was introduced to obtain ground temperature rapidly and more accurately than kusada and bags correlation. Standard THAC for soil thermal diffusivity used was $8.13*10^{-2}m^2/day$.

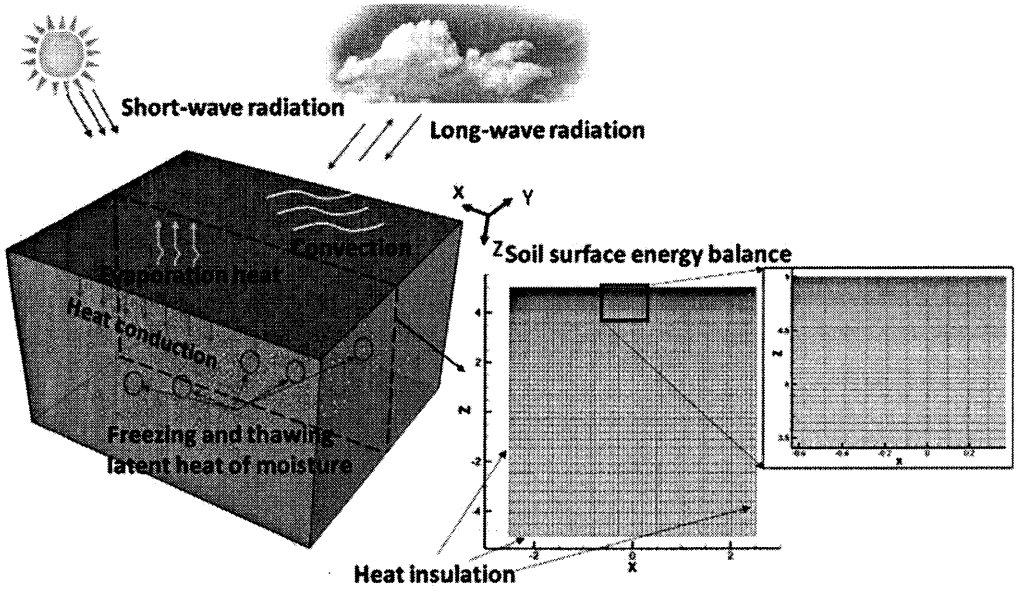


Fig. 9: Interaction of the Major Factors in the Soil and Mesh Division in the Computation Domain (Tong, 2020).

Nevertheless, the soil surface energy balance utilized by the paper is of great importance to us as it explains our whole temperature modeling for shallow subsurface as temperature variation is primarily caused due to temperature change of soil surface. Hence, the transient temperature of the soil surface is as seen below in equation (2-3):

$$q_c = \left(-k \frac{\partial T}{\partial z} \middle| z = 0\right) = q_s + q_k + q_a + q_e \quad (2\text{-}3)$$

where T is soil temperature in Celsius (°C), z is depth in meters (m), λ as heat conductivity W/(m °C), q_c is heat flux density transferred via conduction heat transfer from soil surface to soil interior per unit time, q_s being the short-wave solar radiation that is absorbed by the soil surface per unit area per unit time seen in equation (2-4), q_k represents the long wave radiation between sky and soil surface also per unit area per unit time seen in equation (2-5), q_a is the convection heat transfer between the air and soil surface per unit area per unit time seen later in equation (2-8) and finally q_e signifies the evaporation heat flux density of ground surface also per unit area and unit time seen in equation (2-10).

$$q_s = \alpha G \quad (2\text{-}4)$$

$$q_k = \varepsilon\sigma \left(T_{sur}^4 - T_{sky}^4\right) = h_{rad} \left(T_{sur} - T_{sky}\right) \quad (2\text{-}5)$$

In Which;

$$h_{rad} = \varepsilon\sigma(T_{sur} + T_{sky})(T_{sur}^2 + T_{sky}^2) \quad (2\text{-}6)$$

$$T_{sky} = 0.0552(T_a + 273.15)^{1.5} \quad (2\text{-}7)$$

where α is soil surface absorptivity assumed as 0.9, G is global solar radiation, σ as the soil surface emissivity, ε being Boltzmann constant = 5.67*10-8 W/m2K4, hrad represents the equivalent radiation heat transfer coefficient

(2-6), T_{sur} and T_{sky} are the temperatures of soil surface and sky both in kelvin (K) respectively. T_{sky} is computed via equation (2-7) by utilizing T_a which corresponds to atmospheric temperature.

$$q_a = h_{sur}(T_{air} - T_{sur}) \tag{2-8}$$

$$h_{sur} = \begin{cases} 5.7 + 3.8\, v_{wind}^{0.5} (v_{wind} \leq 4.88 m/s) \\ 7.2\, v_{wind}^{0.78} (v_{wind} > 4.88 m/s) \end{cases} \tag{2-9}$$

where h_{sur} represents convection heat transfer coefficient between air and soil surface seen in equation (2-9) and v_{wind} being wind velocity (m/s).

$$q_e = cfh_{sur}[(aT_{sur} + b) - r_a(aT_{air} + b)] \tag{2-10}$$

where a, b and c are 103 (Pa/K), 609(Pa) and 0.0168 (K/Pa) correspondingly, r_a or RH is the relativity humidity of the air. f is the coefficient of evaporation of which 0 for dry soil, 0.1-0.2 for arid soil, 0.4-0.5 for moist soil, 0.6-0.8 for wet soil and 1 for saturated soil. Nonetheless, the final soil surface energy balance equation can be derived as follows:

$$\lambda \frac{(T_{sur-1} - T_{sur})}{\partial x} + \alpha G + h_{rad}\left((T_{sky} - 237.15) - T_{sur}\right) + h_{sur}(T_{air} - T_{sur}) + cfh_{sur}[r_a(aT_{air} + b) - (aT_{sur} + b)] \tag{2-11}$$

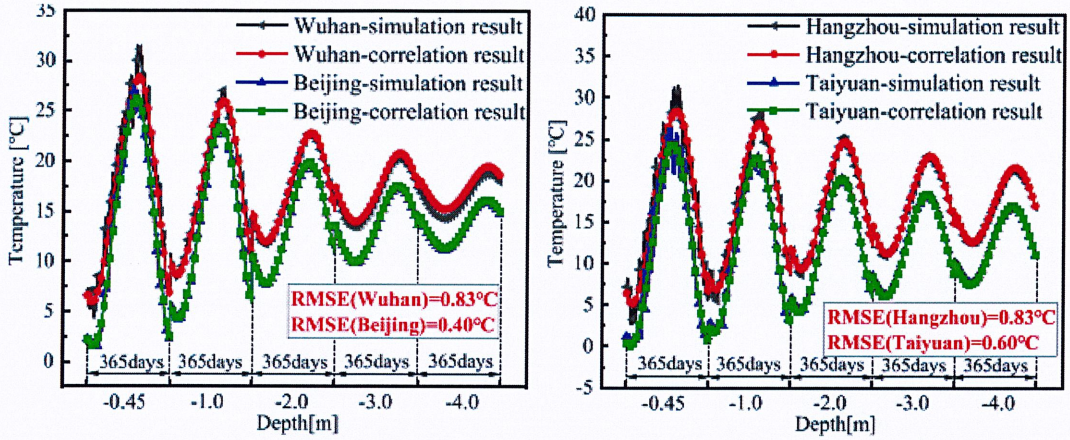
In this approach, no previous ground temperature data is required and it considers all necessary environmental effects and properties with great detail and accuracy. However, the paper considers model via complicated numerical analysis which cannot be verified unless actual experimental data is considered of underground. In contrast, our approach focuses on direct

Multiphysics integration in COMSOL Software to simplify the model as there are various deliverables and objectives set a part of the thesis and not only temperature modelling. Moreover, soil freezing and thawing latent heat will not be considered as in Bahrain, because such low temperatures are not reached. Finally, most of the theory from the above research is to be included in the COMSOL model for direct modeling.

2.1.3.1 COMSOL Modeling

With the literature review and theory clearly discussed above to understand the various effects and properties involved for accurate shallow subsurface modeling, most of this can be injected and applied directly into COMSOL via utilizing Multiphysics and ambient properties based on geographical location. Thus, procedural on how such is done, it is shared clearly in the next chapter. However, a crucial element for modeling shallow subsurface temperature profiles in COMSOL is setting the initial temperature condition for the 3D Soil. In our case, it is going to be assumed and set to 25 °C. This value cannot be accurately verified except with actual experimental tests. However, this assumption is amplified based on approximation while considering Fig. 10 and Fig. 11 below.

Fig. 10 below extracted from the works of Tong, Li, Duanmu and Wang, (2020) shared annual temperature profile of soil in four cities by considering at various depths and temperature at locations at deepest point around 20 °C @4m, but, those locations are colder than Bahrain during winter season and do not reach such concentrated high temperatures for long durations of summer. So, increasing to 25 °C for simulation on COMSOL is a realistic logical margin.



（a）Wuhan&Beijing　　（b）Hangzhou&Taiyuan

Fig. 10: Annual Soil Temperature Profile of Four Cities (Tong, 2020).

Secondly, seeing Fig. 11 below from the work of Singh and Sharma (NIT, 2017) shared the annual variation of soil temperature with depth change in Jamshedpur. It is noticed that temperature stabilizes at 6m depth around 29 °C throughout the seasons. The reflection of the above is that Bahrain's climate is somewhat similar to that of India (WorldData, 2022), but considering Jamshedpur in India, the average temperature is to a certain extent higher than that of Bahrain (Tomorrow, 2022). Additionally, the reason why 29 deg °C will not be selected is due to moisture content, as the soil tested in Jamshedpur is a fertile type of soil holding higher moisture content which traps more heat causing higher temperature readings.

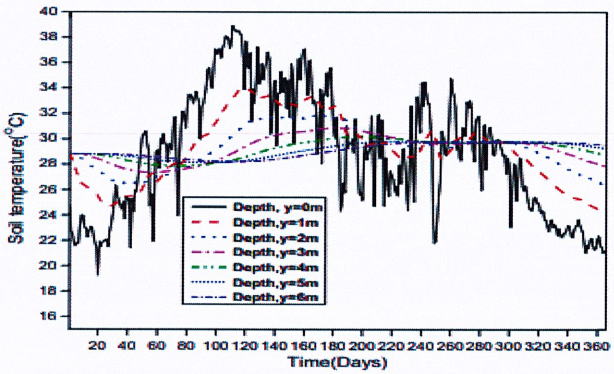


Fig. 11, Annual Variation of Soil Temperature at different depths (NIT, 2017).

Finally, initial boundary temperature is the temperature where there is no fluctuation throughout the year with a minimal difference of which occurs @9-10m depth with as little as 0.6 °C difference as seen presented by Sofyan, Hu, Kotousov, Riayatsyah, Khairil and Hamdani, (Sofyan, 2020) in Fig. 12 as apart of their thesis titled "A new approach to modeling of seasonal soil temperature fluctuations and their impact on the performance of a shallow borehole heat exchanger".

Soil layer	Soil temperature difference between summer and winter (°C)
1st soil layer (0–1 m)	15.1
2nd soil layer (1–2 m)	10.5
3rd soil layer (2–3 m)	7.3
4th soil layer (3–4 m)	5.1
5th soil layer (4–5 m)	3.5
6th soil layer (5–6 m)	2.4
7th soil layer (6–7 m)	1.7
8th soil layer (7–8 m)	1.2
9th soil layer (8–9 m)	0.8
10th soil layer (9–10 m)	0.6
11th soil layer (10–11 m)	0.4
12th soil layer (11–12 m)	0.3
13th soil layer (>12 m)	0

Fig. 12, Soil Temperature difference between Summer and Winter (Sofyan, 2020).

2.2 Psychrometric Chart

The term psychrometry or psychrometric is considered as the science and discipline to study and analyze various thermodynamic properties of humid air which is a mixture of dry air and water vapor (Purushothama, 2009). The chart is now considered a pillar tool for analyzing processes and properties of moist air by having the ability to determine thermodynamic properties for any related application.

The chart is crucial in our study topic as our application for the system is to condense the warm and humid atmospheric air above sea level hence,

understanding the related thermodynamics properties and what they are interpreted as allows successful analysis. That said, the relevant thermodynamic properties will be discussed in the next sub-section below:

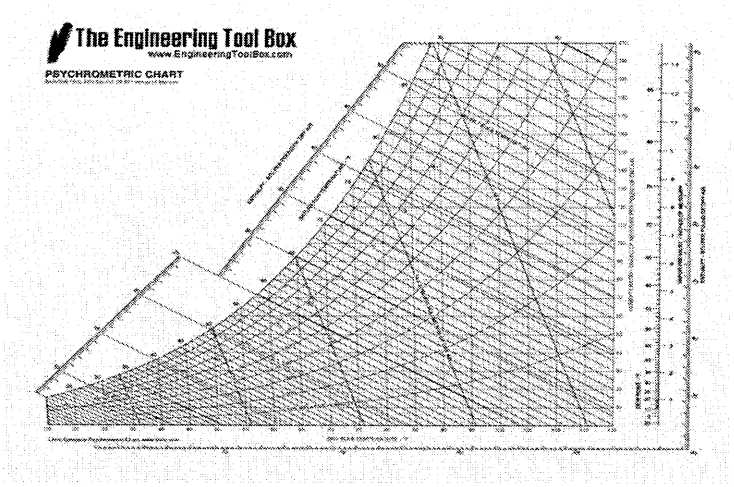


Fig. 13: Psychrometric Chart (EngineeringToolbox).

2.2.1 Relevant Thermodynamics Properties

The relevant thermodynamic properties are explained as the following:

- Dry Bulb Temperature (DBT) is the air temperature measured by a common thermometer that is freely exposed to air and is shielded from any moisture or radiation. DBT is the common temperature of air reading in degrees Celsius °C frequently measure and utilized also known as the true thermodynamics temp (EngTbx, 2004).
- Wet Bulb Temperature (WBT) differs from DBT as it is the temperature measured via thermometer covered with a damp cloth.

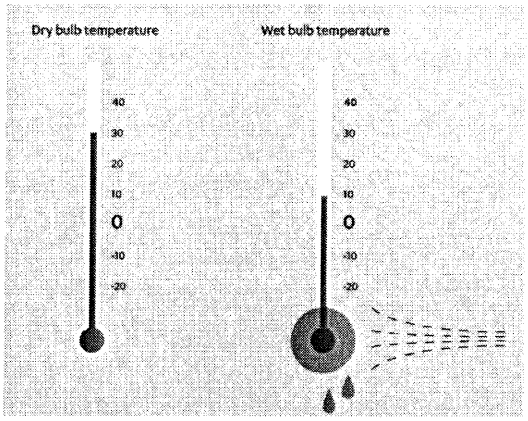


Fig. 14: Dry Bulb Temperature DBT vs Wet Bulb Temperature WBT (Alj, 2021)

- Relative Humidity (RH) measures the amount of water vapor that exists in the air sample compared to how much there could be. It is described from 0-1 or in percentage %. The RH and temperature properties are inversely proportional. A RH of 100% or 1 means that the air sample contains maximum possible amount of water vapor within it in (EngTbx, 2004).
- Specific Humidity (SH) is a measure of the mass of water vapor available in an air sample per unit mass of moist air of which units are g/kg or kg/kg etc. (EngTbx, 2004). SH is used to calculate rate of water generation with respect to volumetric air flow through the system.
- Dew Point Temperature (DWPNT) is the temperature °C where air sample can no more contain the water vapor present in it, causing such water vapor to condense into liquid (EngTbx, 2004). The basic principle is when air sample rejects enough heat/thermal energy to decrease its DBT, RH increases finally reaching 100% hence, achieving the DWPNT thus, water vapor condenses into liquid water.

Nevertheless, for analysing theoretical feasibility of water production via such underground condensation, in this thesis the psychrometric chart will be used to mainly obtain DWPNT of atmospheric air through using DBT and RH values available online and compare it to the shallow underground temperature to identify if temperature is sufficient to cause water condensation. The psychrometric chart will also be used to determine the SH of atmospheric air through also utilizing RH and DBT values to determine rate of water produced per unit time.

The latter utilization of the psychrometric chart is done via online computational calculators (FlyCarpet, 2019) to increase accuracy, reduce error and save time compared to the manual method.

2.3 Atmospheric Water Generator (AWG) and Estimating Water Production

The AWG operating principle analyzed in this thesis can be briefed by considering Fig. 15 as seen below. The system operates as deliberated earlier via having PV system operating a fan to direct hot and humid atmospheric air at specific volumetric flow rate through a pipe leading towards underground level at shallow depths were temperature is sufficient for allowing water vapor to DWPNT. Due to temperature difference, air rejects thermal energy underground, condenses and water is produced. Water can then be extracted for usage after being accumulated at the bottom of the system via a water pump. This system was firstly debated by Avdienko on TEDx talk (TEDx, 2016) which discussed the possibility of innovating a solution to water scarcity by simply proposing such device that can work with the similar principle investigated however, no concrete result or proof of work was

established as it was only a proposed idea by with no evidence of it being feasible obviously especially in Bahrain. To add, the depth up to which atmospheric air is going to be allowed to flow and cool underground is 10m and that is due to that the soil temperature throughout year is constant as seen previously in Fig. 12 thus, allowing min fluctuation in system design to occur.

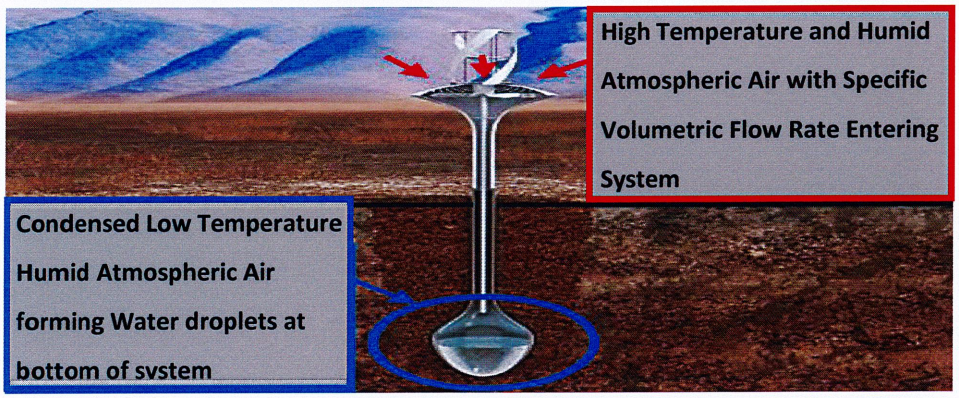


Fig. 15: Simple General Representation of the Atmospheric Water Generating System showcasing its Working Principle.

Yet, prior to exploring the theory related to the system investigated within this thesis topic, as a form of literature review, we can explore some of the various advancements or developments that have been done in relation to atmospheric water generators and whether they are or aren't relevant to us and also to which extent.

Firstly, Xu and Yaghi, (UC Berkley, 2020) published a paper titled as "Metal-Organic Frameworks for Water Harvesting from Air, Anywhere, Anytime". The motivation of the research is the projection of high-water scarcity expectation by the year 2050 as it will impact clean and safe water access to half of the world's population. Thus, the objective was to present a solution to combat the water scarcity challenge globally through having a globally applicable solution. Both Professors and their team at UC Berkley created an AWG system that functions by having a metal-organic framework

(MOF) as seen in Fig. 16 below. It consists of metal and organic mixture powder placed in a transparent box of which water vapor within the atmosphere gets trapped within the power as air flows within the box and accordingly due to the solar thermal energy, the MOF powder gains thermal energy causing the water droplets to evaporate and recondense to form and get collected. The results showed that such MOF systems can deliver 1 liter (lt) of water per kilogram (kg) of MOF and can be functional in even desert regions where RH of atmospheric air is as low as 10%.

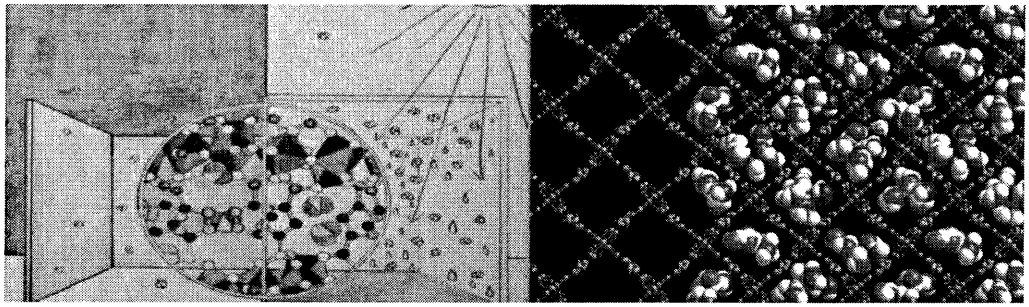


Fig. 16: MOF Atmospheric Water Generator (UC Berkely, 2020).

The main problem faced with their system is cost. The MOF material is reported by the team to be very expensive for large-scale implementation although it is showing great yielding amounts of water per mass of MOF thus, they are currently trying to develop cost effective materials to suit application through considering various material such as aluminum. The considered system investigated our research topic is well aware of possible barriers as it is kept in mind during the design stage. The system to produce water from thin air should be cost-effective through energy and material usage. That said, our design aims to battle such complications by utilizing sources of easily cost-effective material in every stage of the design process, including PV system components, piping material, etc.

Secondly, Gido, Broday and Friedler (Technion, 2016) have published a paper titled as "Assessment of Atmospheric Moisture Harvesting by Direct Cooling". The motivation of their research is to combat water scarcity Fig. 17 note that the weather and climate in Israel is high in moisture content, just like those in Bahrain. Nevertheless, the paper had the main objective to assess the feasibility and energy requirements of harvesting moisture from atmospheric air through a direct cooling process by considering moisture harvesting index (MHI). They summarized that the efficiency of harvesting moisture content from atmospheric air is highly weather and climate dependent of which Tropical areas like tropical regions of the Philippines could yield the highest results for instance. 0.23 kW of power is required to harvest 1 liter of water from atmospheric air. Whereas other less favorable regions require much more energy as investigated by the MHI deeming it a non feasible solution especially if time of operation is not suitable. Yet, the main conclusion provided is with the current type of technology of the direct cooling process, energy requirements to harvest moisture available in the atmosphere is drastically higher than desalination by reverse osmosis (RO). That said, our approach aims to overcome the latter summary of high energy requirement through direct conventional cooling as we aim to cool the atmospheric air through a non-conventional method being underground cooling and that is via allowing air to reject its thermal energy underground at shallow depths. This principle aims to reduce energy requirements significantly as technically speaking, shallow subsurface will be deemed as our natural thermal sink reservoir and the only energy requirement that being fan and water pump are satisfied via solar PV system to operate.

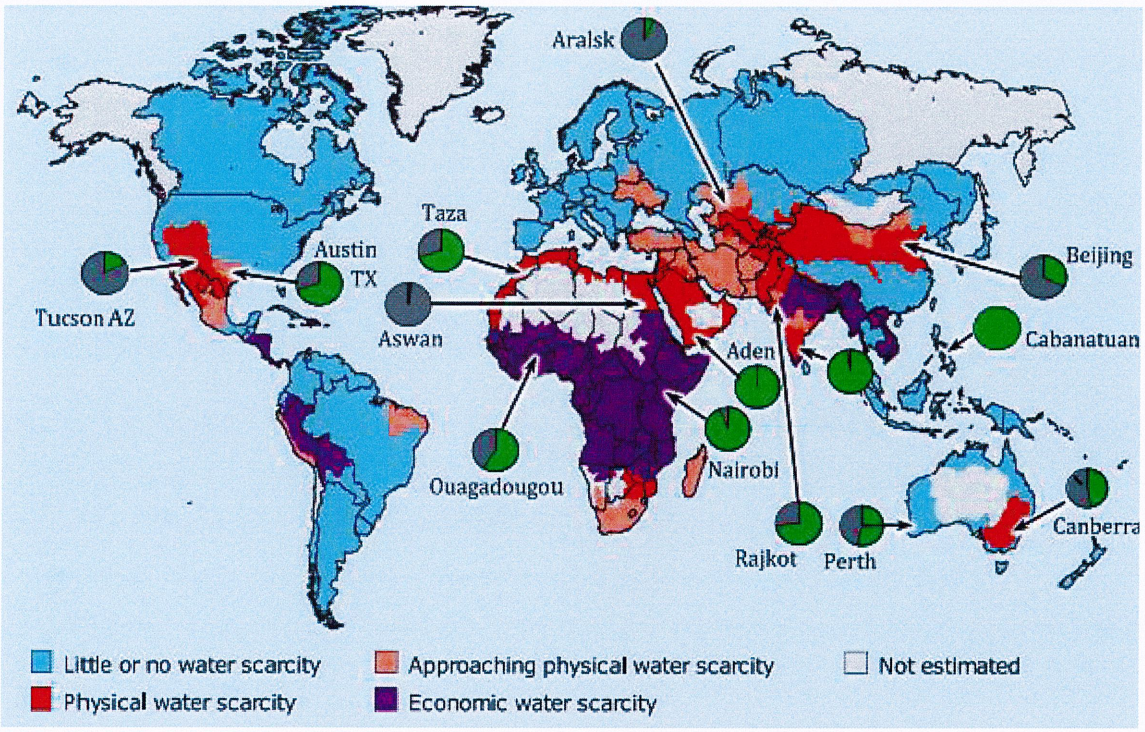


Fig. 17: Water Scarcity Map (Gido, 2016).

2.3.1 Heat Transfer Rate Required for Condensation

The first step of understanding the theory related to the system investigated to assess the feasibility of water production is to understand the concept related to the sum of the required heat transfer rate to reach the condensation phase of atmospheric air. It takes into consideration all of the required heat transfers to achieve condensation of water present within the atmospheric air, where it considers both sensible heats of air and water as well as latent heat of condensation of water. More details are indicated in the following subsections.

2.3.1.1 Sensible Heat Transfer Rate Required

Sensible Heat shown in Fig. 18 is the amount of Heat in Joules or Rate of Heat in Watts associated with the change of temperature of a body or fluid

at constant pressure and no change in phase (NCSU, 2020). To achieve condensation and produce water via our system, there is firstly two forms of sensible transfer processes required to occur that being the air (2-12) and water vapor (2-13) present in the air when DBT changes from atmospheric temperature to the DWPNT due to heat transfer (Modi, 2019).

$$\dot{Q}_{SA} = \dot{m}_A C_{p\,A} \Delta T_A = \dot{m}_A C_{p\,A} (T_{DWPNT} - T_{Atm\,DBT}) \tag{2-12}$$

$$\dot{Q}_{SW} = \dot{m}_W C_{p\,W} \Delta T_W = \dot{m}_W C_{p\,W} (T_{DWPNT} - T_{Atm\,DBT}) \tag{2-13}$$

where $\dot{Q}_{SA}$ and $\dot{Q}_{SW}$ are required sensible heat transfer rate for both air and water respectively (W), $\dot{m}_A$ and $\dot{m}_w$ are the mass flow rate of air and water (kg/s). $\dot{m}_A$ and $\dot{m}_w$ are calculated via equations (2-23) and (2-24) shown in coming sections. To add, $C_{p\,A}$ and $C_{p\,W}$ are specific heat capacity of air and water at constant pressure (J/kg K). $C_{p\,A}$ is obtained online via considering avg temperature between the atmosphere and underground soil (EngTbx, 2004) and for water it is 4186 J/kg K (EngTbx, 2004). Finally, T_{DWPNT} and $T_{Atm\,DBT}$ are DWPNT and DBT of the atmospheric air respectively (°C).

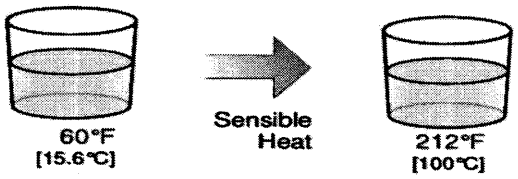


Fig. 18: Sensible Heat (Quora, 2017).

2.3.1.2 Latent Heat Transfer Rate Required

Latent Heat shown in Fig. 19 is the amount of Heat in Joules or Rate of Heat in Watts associated with the change of phase of a body or fluid at

constant pressure and temperature (NCSU, 2021). That said, to achieve condensation and produce water via our system, the third form of heat transfer required is latent heat of condensation of water (2-*14*) being when water vapor present within the air condenses into liquid water (Modi, 2019).

$$\dot{Q}_{LW} = \dot{m}_W L_C \tag{2-14}$$

where $\dot{Q}_{LW}$ is the latent heat transfer rate of water condensation required (W), L_C is the latent heat constant of condensation for water vapor to condense into liquid approx. 2500 kJ/kg (Socratic, 2017).

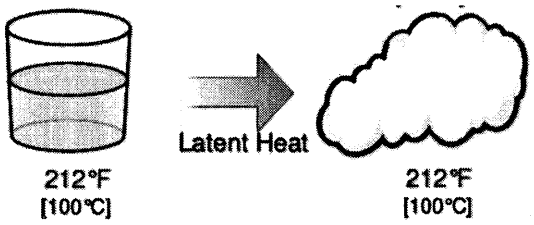


Fig. 19: Latent Heat (Quora, 2017).

2.3.1.3 Sum of Heat Transfer Rate Required

Upon considering equations (2-12), (2-13) and (2-14), the required heat transfer rates to achieve condensation of water vapor in atmospheric air can be summed as the following equation:

$$\dot{Q}_{Required} = \dot{Q}_{SA} + \dot{Q}_{SW} + \dot{Q}_{LW} \tag{2-15}$$

where $\dot{Q}_{Required}$ is the sum of all sensible and latent heats required to achieve condensation (W).

2.3.2 Actual Heat Transfer Rate Occurring

After discussing clearly in the previous section about the required heat transfer rate to achieve condensation which ultimately produce water, it is as important to understand the actual heat transfer rate occurring via our system design. The actual heat transfer rate that is occurring is a mixed mode heat transfer of both radial conduction and forced convection. The actual heat transfer rate occurring as will be seen later below must be more than or equal to that of the required heat transfer rate $\dot{Q}_{Actual} \geq \dot{Q}_{Required}$ so that water vapor present in atmospheric air will condense and water will be produced.

2.3.2.1 Radial Conduction and Forced Convection

Conduction is a form of heat transfer which occurs due to difference in temperature between two bodies in physical contact of which heat flows from high to low temperature body respsctively. Thus, radial conduction presented in Fig. 20 is when heat transfer occurs radially in a pipe (Nee, 2009). To be specific, in our case, radial conduction occurs via the pipe that is rejecting heat through its thickness from its inner diameter (ID) to the outer diameter (OD) where the inner surface at higher temperature due to atmospheric air flow and outer diameter lower is due to underground soil temperature.

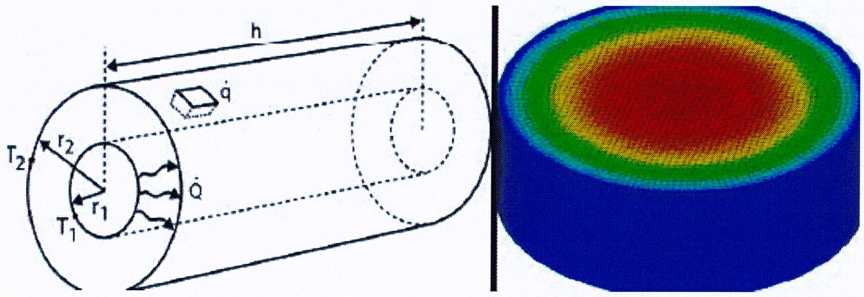


Fig. 20: Radial Conduction (Meier, 2009).

To add, convection is a form of heat transfer that occurs between a solid surface and adjacent fluid that is in motion (Modi, 2019). Forced convection as shown in Fig. 21 occurs when the fluid flow is forced as not occurring naturally due to density change (Mhhe, 2018). In our design, forced convection is occurring from atmospheric air forced underground via a fan, causing heat to transfer from flowing air to pipe respectively. That said, both radial conduction and forced convection are the heat transfer rates that are occurring within the system. Keeping in mind that there exists a third type of heat transfer occurring which is radial conduction between the outer pipe surface and underground soil, but that will not be considered in our analysis due to the assumption that the temperature of the outer surface of the pipe is equal to that of the temperature of soil underground.

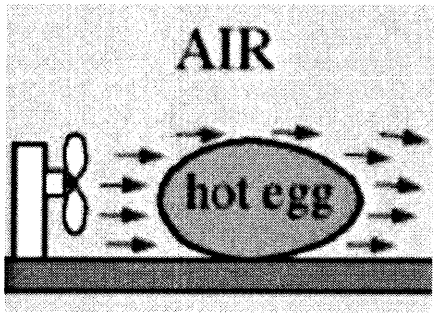


Fig. 21: Forced Convection (Mhhe, 2019).

2.3.2.2 Actual Heat Transfer Rate Formula

As disclosed, both mixed mode radial conduction and forced conduction heat transfer are occurring within the considered AWG represents the key to determine the feasibility of the system is by actual heat transfer being higher or equal to the sum of heat transfer required as discussed earlier $\dot{Q}_{Actual} \geq \dot{Q}_{Required}$. Nevertheless, the formula of $\dot{Q}_{Actual}$ is summarized via the resistance network diagram of Fig. 22 from which equation (2-16) is derived:

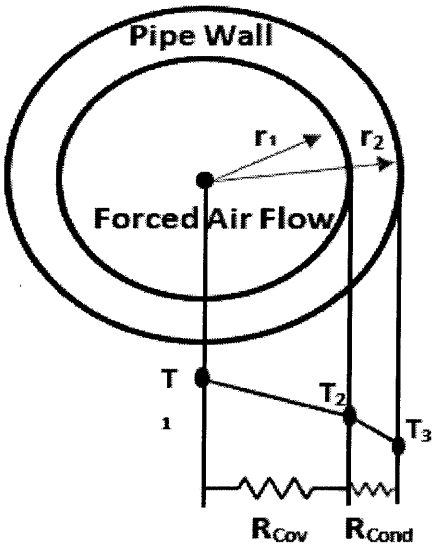


Fig. 22: Resistance Network Diagram of Actual Heat Transfer Rate Occurring

$$\dot{Q}_{Actual} = \frac{T_1 - T_3}{R_{FC} + R_{RC}} \tag{2-16}$$

$\dot{Q}_{Actual}$ is the actual heat transfer rate occurring in Watts (W), T_1 is the supplied atmospheric air temperature in Celsius (°C), T_3 is the outer surface pipe temperature assumed to be as average underground soil temperature in Celsius (°C) for simplification. R_{FC} and R_{RC} are the resistance due to forced convection and radial conduction respectively (°C/W) (Modi, 2019).

2.3.2.3 Radial Conduction Resistance Formula

$$R_{RC} = \frac{ln(\frac{r_2}{r_1})}{2 * \pi * L * k_{Pipe}} \tag{2-17}$$

Considering equation (2-17), r_2 and r_1 are outer and inner radius of selected pipe size correspondingly (m), L is the total length of pipe (m) and finally k_{Pipe} is thermal conductivity of pipe material selected (W/mK) (Modi, 2019) at an average underground temperature.

2.3.2.4 Forced Convection Resistance Formula

All of the equations related to R_{FC} can be derived as seen below from equations (2-*18*) and (2-*19*) (Modi, 2019):

$$R_{FC} = \frac{1}{h\,A_s} = \frac{1}{h*(\pi*D_1*L)} \qquad (2\text{-}18)$$

$$h = \frac{Nu*k_A}{D_1} \qquad (2\text{-}19)$$

where h is the heat transfer coefficient (W/m^2K) determined via estimation of various dimensional numbers by considering turbulent fluid flow like Reynolds Number (Re), Nusselt's Numbers (Nu) and Prandtl Number (Pr) seen in equations (2-20), (2-21) and (2-22) below. Nonetheless, A_s is the inner surface area of the pipe selected, D_1 is the inner diameter (ID) of the pipe (m) and finally k_A is the thermal conductivity of air (W/mK) at average temperature between atmospheric air and underground temperature.

$$Re = \frac{\rho_A*v_A*D_1}{\mu_A} \qquad (2\text{-}20)$$

Considering equation (2-20), Re defines the type of fluid flow occurring within the pipe where if Re<2300, flow is laminar and Re>2300 equates to a turbulent type of fluid flow, ρ_A is the density of the atmospheric air (kg/m^3) at average temperature (between underground and atmospheric air temperature), v_{air} is velocity of air (m/s) based on system operating design and dynamic viscosity μ_A at average temperature (Pa.s).

Our type of fluid flow as will be seen in result section is turbulent thus, Nu and Pr value estimation for turbulent type of flow is seen below:

$$Nu = 0.023Re^{0.8}Pr^{0.4} \quad (2\text{-}21)$$

$$Pr = \frac{\mu_A C_{pA}}{K_A} \quad (2\text{-}22)$$

2.3.3 Calculating Mass Flow Rate of Air and Water

Calculating mass flow rate of air and water can be estimated from equations (2-*23*) and (2-*24*) below:

$$\dot{m}_A = \rho_A * \pi r_1^2 * v_A \quad (2\text{-}23)$$

$$\dot{m}_W = \dot{m}_A * SH \quad (2\text{-}24)$$

where SH is the specific humidity of atmospheric air (kg/kg) at atmospheric air DBT.

2.3.4 Mass of Water to be Generated Per Day

If $\dot{Q}_{Actual} \geq \dot{Q}_{Required}$, amount of water generated per day via underground condensation can be estimated via equation (2-*25*) seen below:

$$m_{WG} = (\dot{m}_{Win} - \dot{m}_{Wout}) * 3600 * T \quad (2\text{-}25)$$

where $\dot{m}_{WG}$ is water generated per unit time in hours in kilograms or Liter as density of water 1000kg/m^3 (kg) = (Lt), 3600 converts from kg/s to kg/Hr and T is time operation (hrs). $\dot{m}_{Win}$ and $\dot{m}_{Wout}$ are mass flow rate of water in and out of the system at respective temperature, relative humidity (RH) and specific humidity (SH).

2.4 Renewable Energy (RE) and Solar PV Systems

There are various undesirable emissions with adverse effects that are produced by the combustion of fossil fuels to generate electricity which is also known as non-renewable energy sources among such adverse effects:

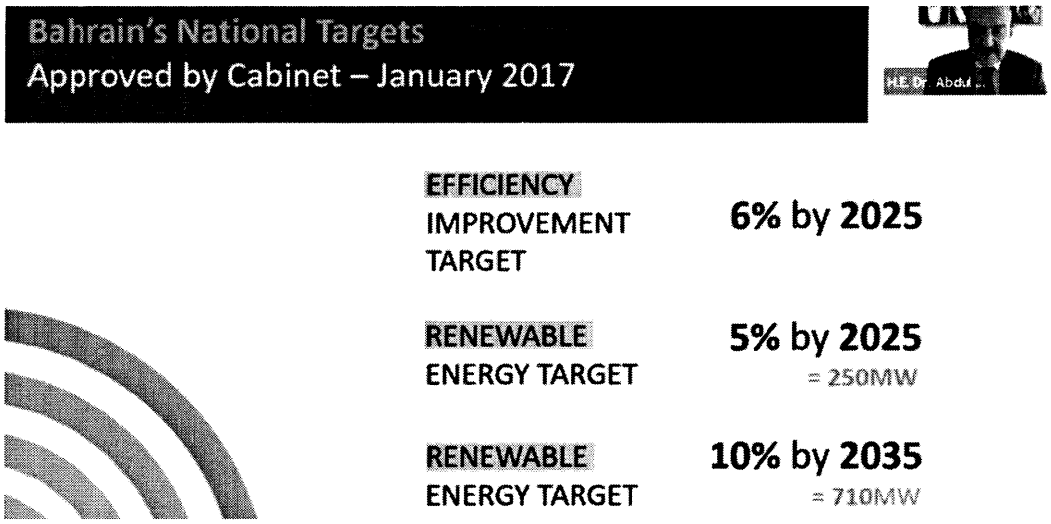
- Carbon Dioxide – Which manifests the global warming.
- Nitrogen Oxides and Hydrocarbons – Resulting in smog.
- Carbon Monoxide – Results in the emission of toxic gas.
- Particulate Matter – Resulting in adverse health effects on respiratory system.
- Sulphur Dioxide – Causing acid rain effect.

There are 2 main methods to tackle the adverse effects caused by usage of non-renewable energy sources and also their possible depletion as a part of the sustainable development goals (SDG's):

Method 1 - Implementing Energy Efficiency Practices - in all aspects of energy distribution, production and consumption to use less fuel and obtain the same useful output. Such energy Efficiency (EE) practice is rather a new method that is highly considered nowadays and greatly discussed. The Sustainable Energy Authority (SEA) has created an official National Energy Efficiency Action Plan (NEEAP) to achieve such a tactic (SEA, 2017). The main target set was to reach a 6% energy efficiency goal by 2025 which will ultimately lead to 5,800GWh of energy savings, government saving of 82 million BHD, reduce 3.4 million tonnes of CO_2 emissions and many more.

Method 2 - Adapt to Renewable Energy Sources for Energy - this can be from the various types of renewable energy (RE) sources. The Sustainable Energy Authority (SEA) has made a similar action plan to that of NEEAP but targets renewable energy which is called the National Renewable Energy Action Plan (NREAP) (SEA, 2017). The summary was setting a goal to reach 5% and 10% RE adaptation by the years 2025 and 2035 respectively. Achieving 5% would lead to clean energy generation of approx. 480GWh/yr, an annual saving of 1.6 million BHD, reduce greenhouse gas emissions by 392,000 tons of CO_2/yr., attract 140 million BHD of investments etc. Main RE source studied to reach target are PV and wind energies.

Fig. 23: Bahrain National EE and RE Targets – 2nd Annual International Sustainable



Energy Event (iSEE) (H.E Dr. Mirza, 2021).

To clarify, RE sources are the opposite of conventional energy sources that are fossil fuels as RE sources are a form of clean energy that does not have direct impacts on the environment and are considered sustainable sources of energy meaning they will keep replenishing and existing unlike fossil fuels will eventually deplete and cause adverse effects. RE sources are also called

green energy sources, alternative energy sources, and sustainable energy sources. The 5 types of RE sources as seen below in Fig. 24:

- Solar Energy: can be either solar thermal or photovoltaic energy systems (PV). Solar thermal systems operate via harnessing solar radiation in form of thermal energy whereas PV energy systems harness the actual electromagnetic radiation in the form of waves.
- Wind Energy: conversion of kinetic energy of wind into electricity via use of wind turbines.
- Hydro Energy: conversion of potential energy to kinetic energy and finally to electrical energy as a permitted downstream flow of water that was collected water in large dam at higher elevation above ground.
- Biomass Energy: Biomass is an organic RE source which can be formed via variety of sources such as agriculture, forests, residues, crops etc.
- Geothermal Energy: As discussed earlier, it is thermal energy generated and/or stored within the Earth's core (beneath crust/land).

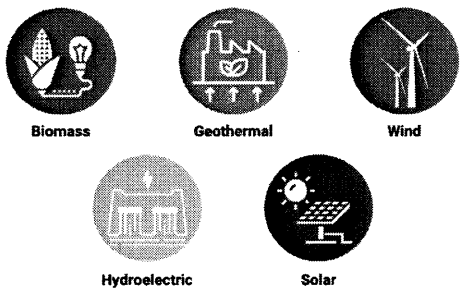


Fig. 24: Renewable Energy (RE) Sources

Considering Fig. 25 below, more than 27% of the global electricity is renewable at the end of 2019 where hydropower is leading the way at 15.9% followed by wind and solar PV.

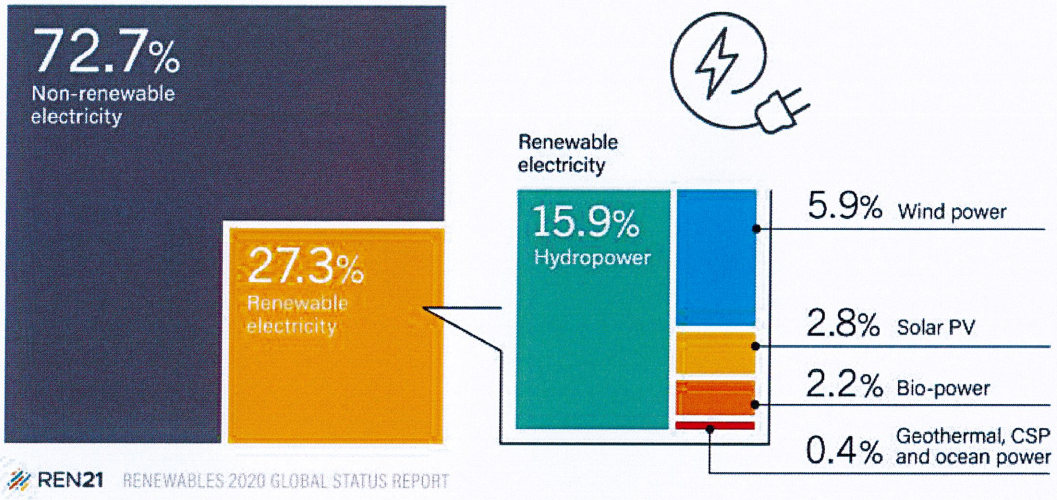


Fig. 25: Estimated Renewable Energy Share of Global Electricity Production at End of 2019 (IRENA, 2020)

RE capacity is increasing rapidly as seen in Fig. 26. More than 200GW added in 2019, most from solar PV (115GW) as it is now very cheap.

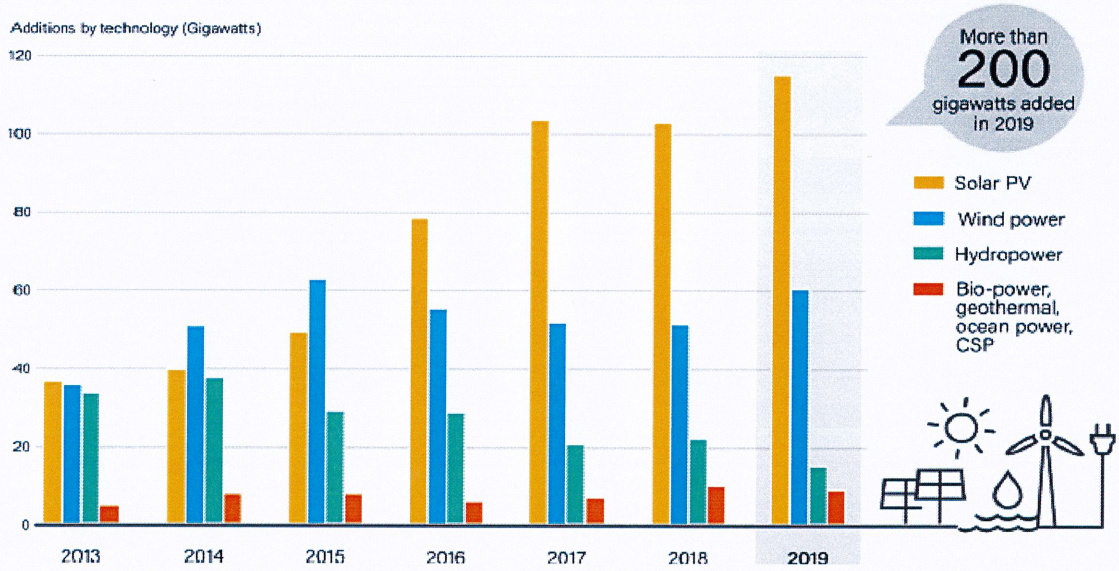


Fig. 26: Annual Additions of Renewable Power Capacity 2013-2019 (IRENA, 2020)

Considering Fig. 27 representation below, costs of all forms of RE technologies are decreasing except geothermal power. To add, costs for solar PV and concentrated solar thermal power (CSP) and both onshore and

offshore wind have all drastically increased within 9-year time frame as well as solar PV technology is slowly reaching a stage in becoming the cheapest.

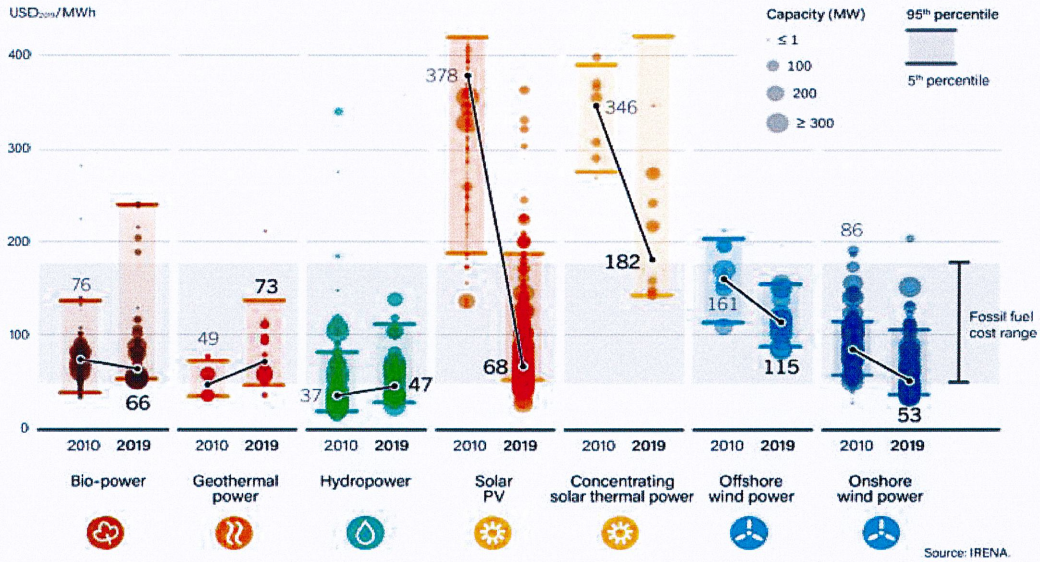


Fig. 27: Global Levelized Cost of Electricity of Electricity from Newley Commissioned, Utility-scale Renewable Power Generation Technologies (IRENA, 2020)

2.4.1 Reason for Selecting Solar PV RE Source

Upon the various points discussed in the previous section, PV energy system is to be considered for our application due to its low cost especially for small-scale applications, easily applicable at any location where solar radiation is available, low complexity, low maintenance cost compared to other sources of RE, material easily sources and many more reasons which will be clarified more as we progress. To add, solar energy availability in Bahrain is far more superior than available wind energy as well as that geothermal energy analysis is not fully developed locally (SEA, 2017).

2.4.2 Classification of Solar PV Systems

Solar PV Systems are classified into 2 main types that being off-grid and on-grid systems of which the difference being the following:

- On-Grid Solar PV Systems: on-grid type PV systems mean that system is connected to the grid as described by the name. Such type of PV system type can only generate and store additional energy when grid connection is available. Excess electricity generated from PV during daytime and not consumed directly by loads can be channeled to the government grid to obtain positive energy credit for later use like nighttime without additional cost instead of being stored in a battery. Thus, such type of PV systems are cheaper compared to off-grid type due to not requiring batteries however, they obviously require nearby grid access which could sometimes be unavailable see Fig. 28.

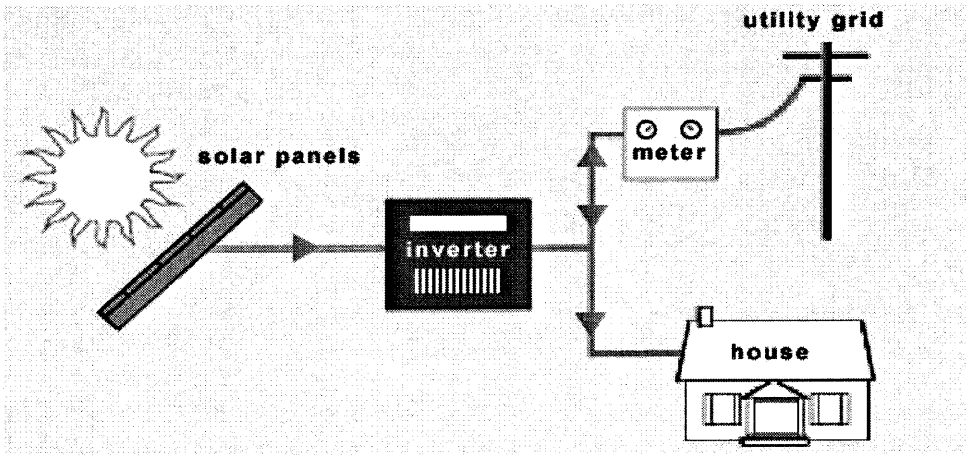


Fig. 28: On-Grid PV Solar Systems (Mepcell, 2018)

- Off-Grid Solar PV Systems: latter type of PV systems in comparison to on-grid type do not require grid connection due to that excess produced electricity from PV panels throughout the day are stored in batteries for

later intended use. Off-grid PV solar systems are more expensive to that of on-grid type due to the harsh cost of batteries especially since multiple ones are usually required to store sufficient amount of energy as per PV size. Yet, a major advantage of off-grid PV systems is that it is applicable in any remote location where sun is available, but no electricity grid lines available as it is a fully independent system (Fig. 29).

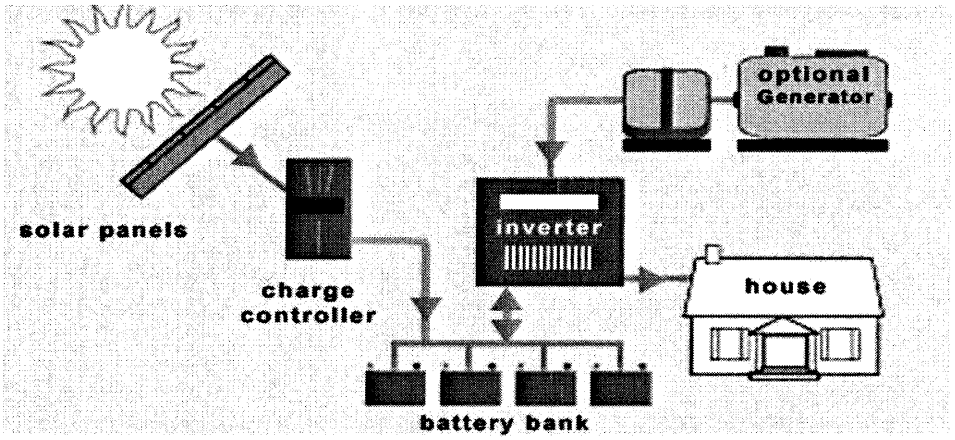


Fig. 29: Off-Grid PV Solar Systems (Mepcell, 2018)

There is a third type of solar PV system known as hybrid solar PV systems, but it essentially combines on-grid and off-grid types. They are just like hybrid vehicles trying to operate on two different principles for higher adaptability and yield the best of both ways. Nevertheless, grid access is assumed to be unavailable for our application, so utilizing hybrid-type PV systems is not optional.

2.4.3 Off-Grid PV System Components and Details

Upon discussing the two types of PV solar systems, this thesis will focus on the utilization of the off-grid type of which main reason is that such a system is intended for worst case remote use whether if applied and piloted in

Bahrain or externally in extreme water scare regions of the world. That said, the section is dedicated to discuss the four main necessary components required for off-grid PV systems that being the Photovoltaic Panels (PV), Solar Charge Controller (SCC), Battery and lastly the Inverter (Fig. 30):

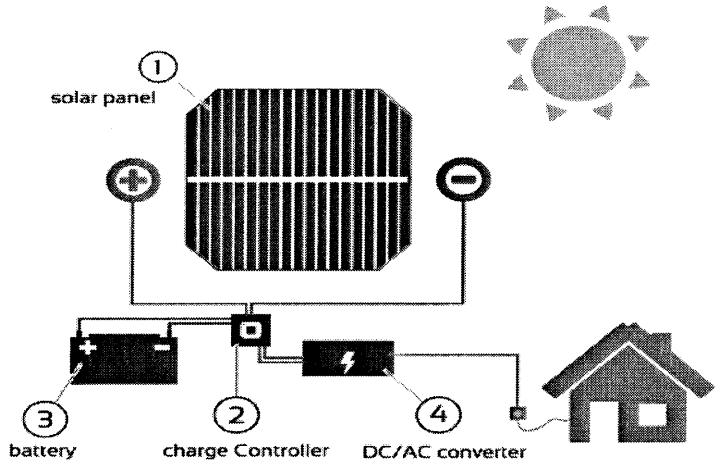


Fig. 30: Diagram Showing Main Components for Off-Grid PV System (BhgPower, 2020)

1. Photovoltaic Panels – PV panels are the first part of the solar PV system which initiate the process of electricity production. They function by means of absorbing the electromagnetic energy waves radiated from the sun via the photovoltaic cells thus, converting into DC electric power. PV Panels are available in various types, specifications and sizes classified in Wattage (W) and they are selected based on solar system sizing calculations which will be looked at later stage. They are the second most expensive component in an off-grid type system of which the first being the batteries. Simply said, here are 3 main types of PV panels that being monocrystalline, polycrystalline, and thin film (KiwiEnergy, 2021). As seen in Table 1, selection is to be prioritized for monocrystalline

type as it has highest Effiency and longevity. Moreover, honestly, most of the PV Panels in market now are monocrystalline type as price difference between it and polycrystalline reduced due to increase in production.

Table 1, Types of Solar Panels (Description, Pros and Cons) – (Taleb, 2020).

Type of PV Panel	Monocrystalline	Polycrystalline	Thin Film
Description	Cells made from Pure single silicon ingot.	Cells made from several silicon pieces melted and moulded together.	Made from amorphous silicon thin films allowing it to have flexible structure.
Pros	• Highest longevity • Highest η of all types ≅ 20% • Widely Available	• Economical • Widely Available	• Flexible Structure – can be used for complex shapes. • Cheap.
Cons	Most Expensive.	Medium η of all types ≅ 13-16%.	Lowest η of all types ≅ 13-16%.

2. Solar Charge Controller (SCC) – Second part of off-grid PV system and is installed between the PV panel and the batteries. It permits the DC generated power produces from the PV panels to flow through the battery allowing it to charge safely. The SCC is very crucial safety component as it maintains electrical cells of battery from overcharging to avoid damage. They are generally not expensive; however, they must be properly sized and selected based on battery and PV panel sizing as they come in various specifications that being voltage V and ampere A.

3. Battery: The battery/battery bank within an off-grid type PV system is known as the heart of the system where it stores the electricity generated from the panels after passing through the SCC. It is the most expensive part within the system and can be sized in various required capacities based on what is required (loads, day of autonomy etc). Additionally, there is an important parameter to consider when selecting batteries and that is the depth of discharge (DoD). It defines the amount of power that can be extracted from the batteries upon being fully charged. A battery with 80% DoD battery implies that you are only be able to extract and take use of 80% of the electrical power stored within the battery each cycle or else it will fail and deteriorate rapidly. There are many types of batteries available on the market especially with new developments in the field however, we can summarize 2 main common types below in Table 2 of which being worst and best them lead acid and lithium-Ion type batteries respectively. Note that Lead Acid batteries are to be selected for our simple application to minimize cost.

Table 2, Types Batteries (Description, Pros and Cons) – (UnboundSolar, 2020).

Battery	Some Pros	Some Cons
Lead Acid Batteries	• Very cheap compared to lithium-ion batteries. • Extremely easy to source.	• Approx. 50% safe DoD. • Low Charging Rate. • Low Energy Density - Heavy. • Contains Acid = dangerous. • Low expected lifetime performance.

Lithium-Ion Batteries	• Higher DoD - Some can safely reach 80-100% DoD. • High quality and performance. • Fast charging rate. • Light = higher energy density.	• Expensive compared to lead type batteries – 5 to 6 times more. • Hard to easily source. • Not safe in areas of high temperature.

4. Inverter – Final main component in off-grid type PV system is the inverter also known as a DC/AC converter. It is essentially used to convert the direct current (DC) power from battery whether 12V, 24V, 36V, 48V etc. to alternating current (AC) type voltage whether 110 or 220V etc. so that it can be used to power various appliances that require AC type power. If we were to use an inverter, we would select one that coverts from DC voltage depending on battery series arrangement and/or battery voltage to 220V AC. However, that will not be necessary as we aim to select appliances that utilized similar voltage of the battery arrangement to minimize system cost.

2.4.4 Off-Grid Solar PV System Sizing Equations

In the following section, we will discuss how to size an off-grid PV system focusing on load, battery, PV Panels and finally SCC based on (M. Taleb, 2020). As disclosed earlier, due to the usage of DC equipment that can harness power directly from battery inverter sizing will not be necessary.

2.4.4.1 Load Estimate Including Wiring Efficiency

Load is estimated based on appliances power requirement to be operated via such system in relation to operation time per day as seen in equation (2-26) below:

$$Load = P_{Appliance} * t_{Operation} \quad (2\text{-}26)$$

where Load is the load required for the utilized appliance in Watt hour per day (Wh/day), $P_{Appliance}$ is power specification required by the appliance to operate in Watt (W) and finally $t_{Operation}$ is the total time of operation of the appliance in hours (h). Nevertheless, the total load required (Wh/day) is a sum of all loads of appliances per day seen in eq (2-*27*) below:

$$Total\ Load = \Sigma Load \quad (2\text{-}27)$$

But, equation (2-*27*) above does not consider wiring Effiency and thus, equation (2-*28*) is developed:

$$Total\ Max\ Load = \frac{Total\ Load}{\eta_{Wiring}} \quad (2\text{-}28)$$

where total max load (Wh/day) is the total load per day divided by the wiring efficiency η_{Wiring} (%). Wiring efficiency is usually neglected in calculation due to making a minor change however, for the sake of additional details and accuracy, we disclosed it above in equation (2-28). The value of the wiring efficiency varies depending on manufacturer but usually 95-97% is the value used in calculations (Taleb, 2020).

2.4.4.2 Battery Sizing

Battery sizing calculations include the following:

$$Capacity\ Required = \left(\frac{Total\ Max\ Load}{V_{Appliances} * \eta_{battery} * DoD}\right) * Autonomy \quad (2\text{-}29)$$

Considering (2-29), Capacity required is the minimum required capacity of battery for the PV system utilization in Ampere Hour (Ah), $V_{Appliances}$ is the voltage (V) of appliances utilized based on operated DC voltage, $\eta_{battery}$ is the efficiency of the battery based on type selected and provided by manufacturer, however a common value of 90% is typically used for calculations (M. Taleb, 2020).

50% DoD commonly utilized for lead acid batteries for safe usage. Finally, autonomy is the days of autonomy in days considering a safety margin used to approximate maximum No of days that sunshine might not be available to allow PV panels to generate electricity. Since we are in Bahrain only 2 days of autonomy will be considered as chances to not have sunshine is very low especially within the operational time of the AWG system.

Before progressing to next set of equations, it is important to understand that there exists series and parallel strings in electrical engineering in general of which series arrangement increases the total voltages of the appliances by summing it whether batteries or PV Panels etc., whereas parallel connection increases the current of the appliances via summing it as seen in Fig. 31 below.

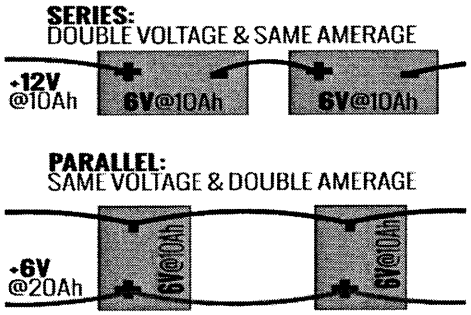


Fig. 31: Series vs Parallel String Arrangement (Minder, 2022)

(2-30)

$$No\ of\ Batteries\ in\ Series\ = \left(\frac{V_{Appliances}}{V_{Battery}}\right)$$

$$No\ of\ Batteries\ in\ Parallel\ = \left(\frac{Capacity\ Required}{Battery\ Capacity\ Selected}\right) \quad (2\text{-}31)$$

$$Total\ Batteries\ = No\ in\ Series * No\ in\ Parallel \quad (2\text{-}32)$$

Considering Equations (2-30), (2-31) and (2-32) above, Batteries in series is the No of required string of batteries in series were it depends on the voltage of appliances utilized in DC $V_{Appliances}$(V) as mentioned earlier divided by the selected battery voltage $V_{Battery}$(V). Moreover, batteries in parallel is the No of required string of batteries in parallel where it is the capacity required as shown above in (2-29) divided by the battery capacity selected in (Ah). Finally, the total amount of batteries required is the product of the number of batteries in series and parallel strings.

2.4.4.3 PV Panel Sizing

PV Panel sizing consists initially of estimating necessary output current of PV panel required and then to select a PV panel model to access the specifications to finally determine No of panels required in both series, parallel and total. Consider equations (2-33), (2-34), (2-35) and (2-36):

$$Required\ PV\ Panel\ Current = \left(\frac{Total\ Max\ Load}{V_{sys} * \eta_{PV} * Peak\ Sun\ Hrs}\right) \quad (2\text{-}33)$$

where required PV Panel current is the minimum required current of the PV panels to be selected. it should be < short circuit current Isc_{Panel} of panel

selected (A) where value can be found on technical data sheet of considered panel. To clarify, short circuit current refers to current through the solar cell when voltage across the cell is 0V (PVEdu, 2021).

V_{sys} is considered as the system voltage as per design = battery series voltage = appliances DC Voltage. η_{PV} is the efficiency of the PV panel, it is based on the manufacturer of which commonly being 85-90% and finally, $Peak\ Sun\ Hr$ is the total No of hours of which that solar radiation intensity is highest per day (Palmetto, 2022). A total of 6 hours of peak sun hrs is common is Bahrain (SEA, 2017).

$$No\ of\ Panels\ in\ Series = \left(\frac{V_{sys}}{VOC_{Panel}}\right) \quad (2\text{-}34)$$

where panels in series are the No of required string of PV panels selected in series, VOC_{Panel} is open circuit voltage (V) of selected PV Panel of which value can be found of technical data sheet of panel. To elaborate, VOC is the maximum voltage available from a solar cell which occurs when current is 0 A (PVEdu, 2021).

$$No\ of\ Panels\ in\ Parallel = \left(\frac{Required\ PV\ Panel\ Current}{Isc_{Panel}}\right) \quad (2\text{-}35)$$

$$Total\ Panels = No\ PV\ Panels\ in\ Series * No\ PV\ Panels\ in\ Parallel \quad (2\text{-}36)$$

Finally, the total amount of PV panels required is the product of panels in series and parallel strings.

2.4.4.4 SCC Sizing

Equations (2-*37*) and (2-*38*) below describe how the solar charge controller is properly sized for the off-grid PV system:

$$SCC\ Current\ = Panels\ in\ Parallel * Isc_{Panel} * Limit\ margin \quad (2\text{-}37)$$

$$SCC\ Voltage\ = Voltage\ of\ Batteries\ Series\ String \quad (2\text{-}38)$$

where SCC current is the minimum required current specification for the selection of the SCC (A), limit margin is the additional safety margin placed to make SCC withstand additionally to that of the Isc_{Panel} of which 125% is a reasonable margin. Moreover, SCC voltage is the required voltage specification for SCC selection of which it basically is the voltage of batteries in series string. If there exists only a single 12V battery, then SCC voltage required would be also 12V. On the other hand, if there are two 12V batteries connected in series, SCC voltage required would be 24V.

2.4.5 Estimating Payback Period of PV Systems

It is important to estimate the payback period (PBP) of a solar system irrelevant of type as it aids in analyzing feasibility in relation to cost.

$$Annual\ Grid\ Energy\ = Total\ Max\ Load\ (day) * 365 \quad (2\text{-}39)$$

$$Cost\ Annual\ Grid\ Energy\ = Annual\ Grid\ Energy * E_{Rate} \quad (2\text{-}40)$$

$$PBP\ = \frac{Total\ PV\ System\ Cost}{Cost\ Annual\ Grid\ Energy} \quad (2\text{-}41)$$

Considering equations (2-39), (2-40) and (2-41), Annual grid energy is the total required grid energy per year (Wh/yr). Cost Annual grid energy is the

total cost of energy utilized in a single year (BHD), E_{Rate} is the electricity rate in Bahrain of which is 0.029BHD/kWh for commercial use (Bahrain, 2021). PBP is the payback period of the PV system (yrs), Total PV System cost (BHD) is the sum of the cost of all PV components considered that being PV Panels, batteries, SCC and inverter if considered.

2.5 Additional Equations

2.5.1 Helical Coil Pipe Length Formula

The reason why this section is relevant is because to estimate the water production/generation, the variable of the pipe length is crucially important as it plays an important role in the estimation. To add, as seen in equations (2-17) and (2-18), an increase in pipe length would result in an overall increase in heat transfer rate occurring thus, ultimately resulting to an increase of water generation as discussed above making it a direct relationship.

To clarify, the reason why helical coil pipe design is utilized is because it increases the total length of the pipe without necessarily requiring large vertical dimension just as seen in Fig. 6 being slinky loop design but vertical which is crucially practical if project to be piloted on real life basic as underground drilling is expensive and required a lot of labor. That said, doing so, higher amount of water can be produced per unit length of underground burial as it is requiring lower vertical burial.

That said, to estimate the pipe length based on helical coil design utilized, equation (2-*42*) from (S. Markings, 2013) can be utilized:

$$L_{Total\ Coil} = (p^2 + (2\pi r)^2)^{0.5} N + L_{Excess} \quad (2\text{-}42)$$

where $L_{Total\ Coil}$ is total length of the helical coil design (m), N is Number of coil revolutions (unitless), L_{Excess} is coil excess length (m) which accounts for any additional pipe length utilized in overall design but not apart of helical coil design such as inlet and outlet extensions, p is coil pitch (m) and finally r = radius of coil design (m).

Chapter 3 Methodology and Procedure

3.1 Methodology and Procedural 62

3.2 Mathematical Model 64

3.2.1 Heat Transfer in Solids 64

3.2.2 Surface to Surface Radiation 65

3.2.3 Fluid Flow 66

3.2.4 Moisture Transport in Air – Diluted Species 68

3.3 Parameters and Component Definition 69

3.3.1 Building the 3D Geomtery 70

3.3.2 Mesh Creation 71

3.4 Transient Study 72

3.5 AWG Simplified Model 72

3.1 Methodology and Procedural

As discussed throughout the thesis, the methodology for obtaining results for the investigated thesis topic is to solve the coupled nonlinear set of equations that governs the physical behavior of the current study. The set of the nonlinear equations was solved using COMSOL Multiphysics (COMSOL, 2022) as it can integrate and simulate a variety of theoretical Multiphysics. Moreover, once COMSOL is utilized for modeling the temperature profile of shallow subsurface as well as simulating how much water can be generated via AWG design considered, the underground temperature profile and atmospheric weather readings generated from COMSOL can be utilized directly to attempt simplified model calculations to compare with the results obtained from COMSOL. The procedure summary can be seen in the flowchart diagram shown in Fig. 32. Notice that PV calculations to size off-grid system are not mentioned as it is a direct procedure via calculations as per theory based on load estimation clearly explained earlier in subsection 2.4.4 above.

Nevertheless, the subsections below will provide clear procedures for reaching the above objectives to attain the necessary results for analysis through utilizing COMSOL in subsections 3.2 and 3.5 below to attempt ground temperature profiling at shallow depths and estimate water production. Moreover, the procedure for simplified model calculations is presented in subsection 3.1.2 below. All necessary justifications will be made to provide clarification, and any additional information will be linked to the appendix.

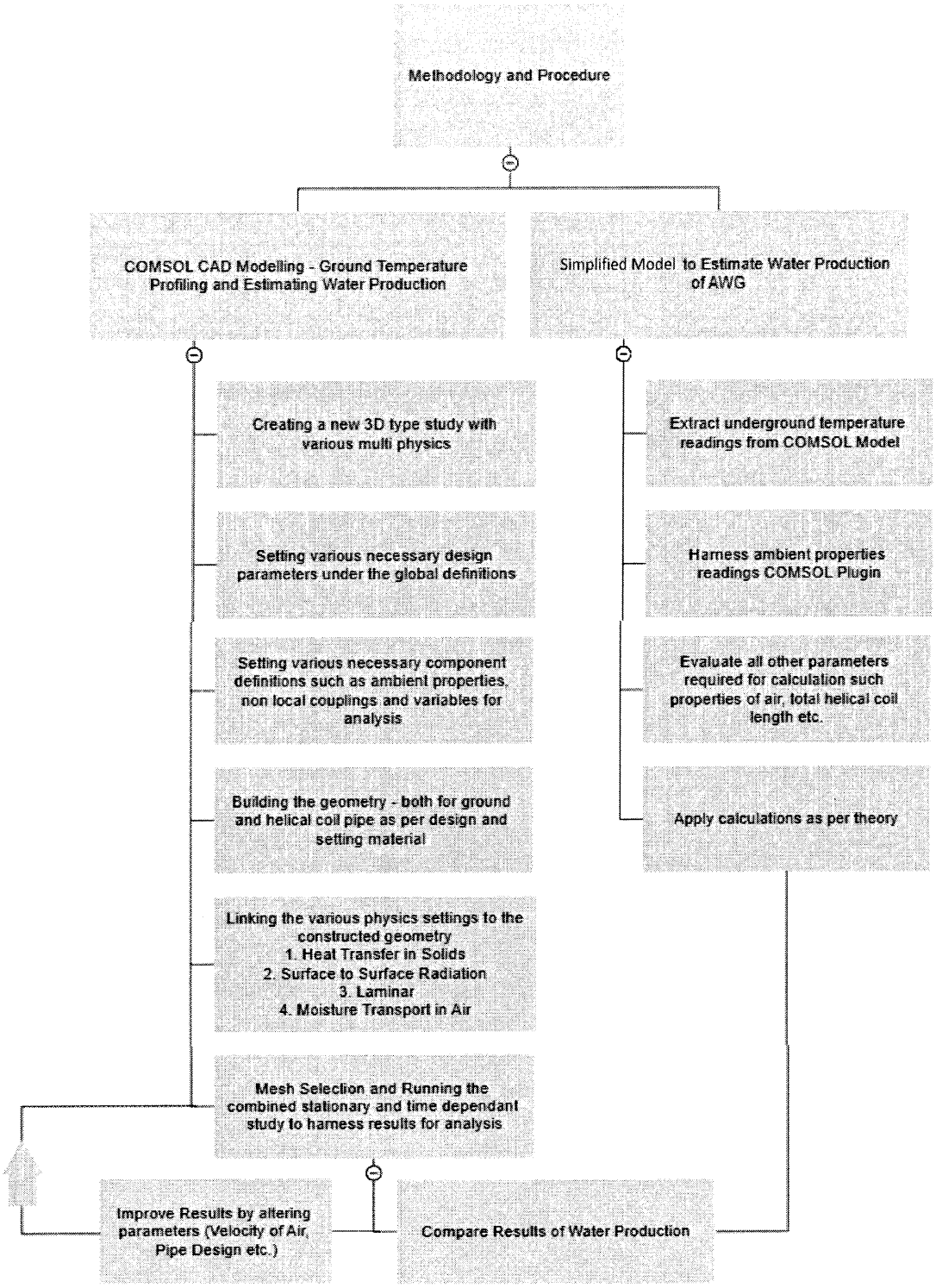


Fig. 32: Summarized Diagram of Thesis Methodology and Procedural.

3.2 Mathematical Model

As mentioned, COMSOL software is used for modeling due to the wide variety of Multiphysics available for analysis. For the topic examined being shallow subsurface temperature profiling and estimating water production via considered AWG, a stationery and time dependent study is created by creating a 3D model with both Heat Transfer Surface to Surface Radiation Multiphysics and Laminar Flow Heat, and Moisture Transport Multiphysics as seen in Fig. 42 in the appendix.

3.2.1 Heat Transfer in Solids

The governing time dependent equation for the heat transfer model is based on the differential form of Fourier equation as seen in equation (2-*43*):

$$\rho C_p \frac{\partial T}{\partial t} + \left(\rho C_p \mathrm{u} * \nabla T\right) + \nabla q = Q$$

$$q = -k\nabla T \tag{2-43}$$

where ρ is density of solid material (kg/m^3), C_p being the specific heat capacity at constant pressure for the solid material (J/kgK), k as the solid material's thermal conductivity (W/mK), u being the velocity (m/s), T is the temperature and finally Q as the heat source or sink (W/m^3).

There are two solid domains considered within that being the ground/soil model and the copper pipe shell/thickness as seen in

Fig. 33 in the appendix section. Nevertheless, the settings for heat transfer in solids physics on COMSOL with all of its main fields is explained below while linked in the appendix section similarly:

- Solid Ground – Responsible for conduction heat transfer for soil/Ground domain where material properties k, C_p and ρ for computation directly taken from soil material library see Fig. 53 in the appendix.
- Initial Values – 25 °C as mentioned in 2.1.3.1. It is the initial model temperature to assess heat transfer occurring see Fig. 54 in the appendix.
- Heat Flux – Included for convection heat transfer via wind effect on the surface of ground, heat transfer coefficient to be external forced convection with the averaged transfer as the width of surface etc. see Fig. 56 and Fig. 57 in the appendix.
- Moist Air – Ambient air passes through the inner pipe walls hence, radial conduction and forced convection heat transfer occur to pipe shell and soil. The air properties are based on the ambient properties plugin Fig. 58 in the appendix.
- Inflow – Ambient air inlet to copper pipe Fig. 60 in the appendix.
- Outflow – Cooled air outlet from copper pipe Fig. 61 in the appendix.

3.2.2 Surface to Surface Radiation

Surface to Surface Radiation Physics is the name of a Heat Transfer Multiphysics in COMSOL of which is a feature that accounts for the heat transfer due to short-wave solar radiation as well as longwave radiation (COMSOL, 2022). The governing equation is as seen in equation (2-*44*):

$$q = \varepsilon(G - e_b(T)) \tag{2-44}$$

where ε is surface emissivity also known as epsilon, G is the solar irradiation based on geographical location, which is directly considered from the ambient properties plugin, $e_b(T)$ is the blackbody hemispherical total emissive power. The main selection considered for the analysis is the upper surface of the ground domain as seem in Fig. 62 in the appendix. Nevertheless, some of the settings for the physics are explained below and linked in the appendix:

- Surface to Surface Radiation – Selection of the top surface of soil block geometry as mentioned for both solar radiation and longwave radiation through selecting solar and ambient wavelength dependency seen in Fig. 62 in the appendix.
- Diffuse Surface – Ambient Temperature to be as per ambient plugin and emissivity to be epsilon value defined earlier in parameters being 0.9 which is common for soil/sand (EngTbx, 2004) as seen in Fig. 63 in the appendix.
- Opacity – Selection Opaque as soil/sand is not transparent as seen in Fig. 65 in the appendix.
- External Radiation Source – Solar Position type of source and both location and Solar Irradiance as per ambient properties as seen in Fig. 66 in the appendix.

3.2.3 Fluid Flow

Two types exist in COMSOL laminar or turbulent. However, our analysis considers laminar flow. Laminar Flow physics/interface allows the computation of both velocity and pressure fields for a flow of single-phase fluid.

The laminar flow type is considered due to the low inlet velocity of the system especially with the pressure increase due to thermodynamic property change caused throughout the pocess which should further reduce the velocity as the relationship is inversely proportional. Additionally, theoretically laminar type flow has less heat transfer rate compared to turbulent thus results are not biasly amplified. moving forward with the laminar model on COMSOL does not.The other option would be to include RANS as a turbulence model type where it considers Reynolds average Navier stokes, but results are minorly effected while increasing simulation time significantly.

Nonetheless, the governing equation for laminar flow physics is the Navier stokes equation for conservation of momentum (2-*45*) and continuity equation (2-*46*) as seen:

$$\rho(\mathrm{u} * \nabla)\mathrm{u} = \nabla[-p\mathrm{I} + k] + \mathrm{F} \tag{2-45}$$

$$\rho\nabla\mathrm{u} = 0 \tag{2-46}$$

where ρ is the density of the fluid (kg/m^3), u is the fluid velocity (m/s), p is the fluid pressure (Pa), k is the kinetic energy (J) and F is external forces applied to the fluid (N). That said, considering equation (2-*45*), the first, second and third terms represent the internal forces, pressure and viscous forces and external forces acting on the fluid, respectively.

The main settings for the laminar flow interface on COMSOL are explained below and linked in the appendix:

- Laminar Flow – The selection to be the inner section of the pipe representing the air domain, as seen in Fig. 67 in the appendix.
- Fluid Properties – Fluid considered is atmospheric air and hence all of its thermodynamic properties, that being temperature, density and dynamic viscosity considering Newtonian fluid, are based on atmospheric data framework as seen in Fig. 69 in the appendix.
- Wall – This feature automatically considers the interior boundary of the pipe to assess wall condition, as seen in Fig. 71 in the appendix.
- Inlet – Set based on the inlet velocity considered or assessed in parameters, as seen in Fig. 72 in the appendix.
- Outlet - The pressure boundary condition is used to assess static pressure seen in the appendix in Fig. 73.

The general system layout can be seen in Figure 68 in the appendix.

3.2.4 Moisture Transport in Air – Diluted Species

The moisture transport in air physics/interface is utilized in COMSOL to simulate moisture transport as a result of convection heat transfer and diffusion in moist air (COMSOL, 2022). Nonetheless, low vapor concentration conditions are assumed to be similar to atmospheric air. The density is constant with moisture content variation. Thus, time dependant diluted species formulation considered is as seen below in equation (2-*47*):

$$M_v \frac{\partial c_v}{\partial t} + (M_v \mathrm{u} * \nabla c_v) + \nabla g_w = G \qquad (2\text{-}47)$$

$$g_w = -M_v D \nabla c_v$$

$$c_v = \varphi_w c_{sat}$$

where M_v represents the molar mass of water vapor (kg/mol), c_v is the vapor concentration (mol/m^3), u is the air velocity (m/s), φ is the RH, c_{sat} is vapor saturation concentration (mol/m^3), D represents the vapor diffusion coefficient in air, and G is the moisture source (kg/m^{3}s).

That said, the main settings for moisture transport in air physics are explained below while linked in the reference section:

- Moisture Transport in Air – The selection to be the inner section of the pipe representing moist atmospheric air domain as seen in the appendix in Fig. 74 .
- Most Air – Pressure, velocity and temperature of moist air to be as linked with other added physics as seen in the appendix in Fig. 75.
- Inflow – Selection of pipe inlet where RH is specified based on upstream temperature and RH, as seen in the appendix in Fig. 78.

3.3 Parameters and Component Definitions

System design variables are automatically inputted as seen in the appendix in Fig. 45 this includes pipe length, inner diameter and outer diameter of pipe etc. Other vital inputs are to be defined as ambient properties under component definitions seen in Fig. 46 in the appendix. It accesses all necessary weather properties of ambient air necessary for ground simulation and AWG like solar irradiance, wind speed, temperature, dew point temperature, etc. COMSOL allows selection of various ranges: Lowest, Low, Average, High and Highest values. Considered properties as seen were all selected as average values except DWPNT which was high.

The ambient properties setting is clearly seen in Fig. 46 of the appendix, where it is set under Bahrain weather station, starting from 1st of January as day 01 to 31st of Dec as day 365.

3.3.1 Building the 3D Geometry

3D block geometry of soil domain and pipe design was made as seen in Fig. 33. The dimensions settings of the constructed 3D model are seen in Fig. 48 and Fig. 49 in the appendix. To clarify, 3D type model is considered in COMSOL is to utilize surface to surface radiation Multiphysics to account for the whole surface of the ground aswell as so that the pipe could be modeled and account for all 3 coordinates x, y and z.

The ground solid is constructed via block geometry, whereas the pipe design is constructed via helix coil geometry to increase heat transfer as a result of increase surface area due to increase of length. The dimensions are based on the parameters depicted in Fig. 45 in the appendix. The pipe design is considered as a U shape to replicate inlet and return sections where the middle point of the U shape design is where condensation data is extracted to estimate the water production rate.

Additionally, the material for ground, pipe shell and fluid domains in which inner pipe space is to be defined for the computation domain of which copper material is selected for the pipe shell. The soil is selected for the ground domain and atmospheric air for the fluid domain. The properties are shared in the appendix in Fig. 50, Fig. 51 and Fig. 52, respectively.

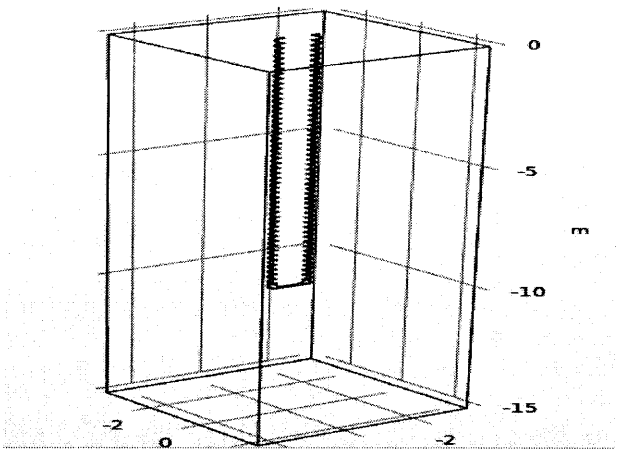


Fig. 33: Illustration of the 3D domain configuration – Ground and Pipe Profile

3.3.2 Mesh Generation

Mesh is applied once physics settings are set and before running the simulation shown in Fig. 34. To reduce computation time, normal element size mesh is to used for the full system instead of the finer tiers as just normal mesh type takes around 20 hrs depending on steps considered. The normal element size mesh is selected instead of the lower tier versions, such as coarse, coarser, extra coarse and extremely coarse to accurately estimate results. To add, mesh independency has been considered to assure that there are no siginicant deviations between results of higher tier meshes.

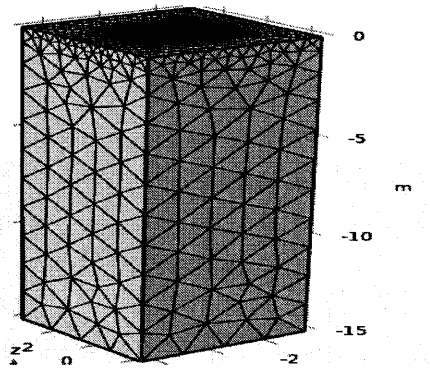


Fig. 34: Mesh Settings in COMSOL.

3.4 Transient Study

Results of modeled design on COMSOL are obtained after considering all of the above settings mentioned above. The physics and variables are computed on combined stationery and time-dependent study. The time-dependent study setting is seen in Fig. 44 in the appendix, where the time unit is in days (d) and the output times start from day 0 up to day 365 with 8-hour steps. Smaller steps allow the differentiation of a single day into 3 sections for a more accurate analysis of AWG water production rate throughout the day.

3.5 AWG Simplified Model

The procedure for the simplified model that estimates the amount of water generated via considered AWG to compare with results obtained from COMSOL is carried out by the following steps in Table 3 below of which correlates to what was shown in the diagram of Fig. 32 earlier in the chapter:

Table 3, Procedural for Simplified Model.

Phase and Step	Obtaining Necessary Data
1	Shallow Subsurface Temperature Profile – To harness and use data obtained from COMSOL Simulation results in Excel as boundary conditions for the temperature at various depths are collected.
2	Weather Data – To extract daily step of atmospheric weather data properties of air through utilizing COMSOL Ambient Weather Properties global definitions plugin in Excel as they are necessary for calculations. This includes DBT, DWPNT, RH and SH.

	To clarify, the ambient weather properties plugin/feature on COMSOL is interlinked from ASHRAE that is respectively linked to the Bahrain weather station.
3	Pipe Variables Related to Calculation – Pipe Coil Length being as Calculated Total Length of Pipe used per helical coil designed in COMSOL, ID and OD as designed in COMSOL are gathered.
4	Determining Air Properties for Calculation - Thermal conductivity, density, dynamic viscosity, specific heat capacity etc all to be considered at average temperature between DBT and underground (EngTbx, 2004).
Phase and Step No	Estimation of Water Production Rate
1	Stating all Assumptions and utilized Variables – To highlight and mention any other data utilized or assumptions made to simply calculation.
2	Consider a small sample to study out of the total variables at 3 various steps in the same day. This is applied on steps where water is produced. This is simplified by ignoring steps that condensation is not possible where DWPNT<Temperature @10m depth. Also, there are going to be a total of more than 200 steps where calculating each is unnecessary.
2	Applying all defined formulas – To Estimate the amount of water to be produced via such a system on a daily basis considering equations (2-15), (2-16) and (2-25) respectively using Excel.
3	Comparison – Compare simplified model sample results with COMSOL mathematically modelled results to verify results or notice any deviation while commentating on reasoning. Comparison is to be made at based step to step as well as average.

Chapter 4 Results, Discussion and Recommendations

4.1 Shallow Underground Temperature Profile Modelling 75

4.2 Intial Analysis of AWG Feasibility 78

4.3 Annual Water Production Rate 79

4.3.1 Assumptions and Variables Utilized 79

4.3.2 Water Production Rate - COMSOL 80

4.3.3 Design Modification to Increase Yield 82

4.3.4 Water Production Rate - Simplified Model 85

4.3.5 Comparison of Water Production Rates 87

4.4 Off-Grid PV System Sizing 89

4.4.1 Assumptions and Variables Utilized 89

4.4.2 Load Estimate 90

4.4.3 Sizing of Components 90

4.4.4 PBP Period 92

4.6 Conclusion 94

4.6 Recommendations and Future Work 96

This chapter is related to discussing the thesis topic results based on the set objectives. The results of the mathematical model of the underground shallow temperature profile will be presented to investigate temperature variation throughout the year with depth change as well as the estimated annual water production rate based on ambient properties. The simplified model results for the water production rate of a similarly designed system will also be compared with that of the COMSOL results. Finally, the results of the off-grid solar system sized for the application will also be demonstrated, along with mentioning the payback period (PBP). Nevertheless, once results have been shown and discussed, the chapter will discuss recommendations for future work and conclusion.

4.1 Shallow Underground Temperature Profile

Upon considering the procedure and methodology mentioned in section 3.1, the results of the shallow ground temperature profile simulation were as the following after utilizing the latter inputs variables seen in Table 4 via considering literature as mentioned and discussed earlier:

Table 4, Considered Variables Used for Ground Simulation

Variable	Value
Sand/Soil Surface Emissivity – ε_{sand}	0.9
Soil Thermal Conductivity - k_{sand}	1.15 (W/m K)
Soil Density – ρ_{sand}	2050 (kg/m^3)
Soil Specific Heat Capacity at Constant Pressure - c_p	1843 (J/kg K)
Soil Width	6 m
Soil Height	6 m
Soil Depth	15 m
Initial Domain Temperature	25 °C

Fig. 35 shows a single timestep 3D result for how the ground/soil domain was modeled in COMSOL. The result shows the temperature change throughout the ground model's various shallow depths on day #226 of the year (mid-august). As depicted the temperature on the surface at 0 m depth, reaching approx. 50 °C, whereas it decreases with an increase in depth up to the initial boundary temperature of 25 °C.

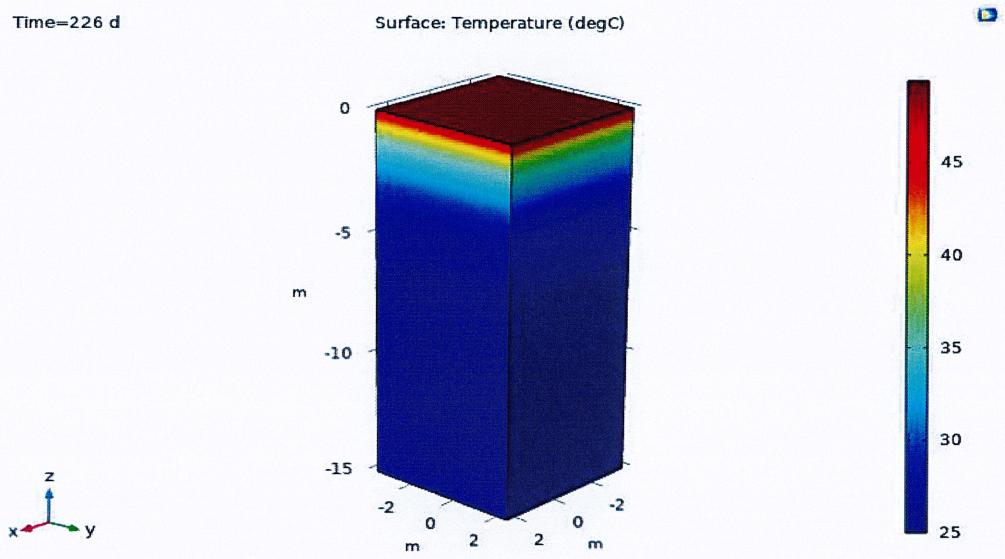


Fig. 35: COMSOL Shallow Underground Temperature Profile Sample Result Day 226.

The ground temperature profile is better depecited and interpreted in Fig. 36 below. The graph represents the results for the shallow subsurface modeling of temperature profile vs depth throughout the year in Bahrain as simulated in COMSOL. As seen, the maximum and minimum surface temperatures (0m depth) can each 58 and 17 °C through the hottest and coldest seasons in Bahrain respectively making it approx. 40 °C fluctuation at same surface level throught the seasons. Nonetheless, as seen in the graph, with the increase in depth, the fluctuation of the temperature through the year decreases significantly whereas an example there's only 10 °C fluctuation through the

year considering -2m depth. Finally, we can see that the temperature fluctuation is almost insignificant and stays constant throughout the year starting from -7m depth just as the initial set boundary temperature of 25 °C. As mentioned earlier, the decision of considering 25 °C as boundary condition can be verified actual experiment are taken as real data.

The results in Fig. 36 confirm with the literature as described earlier in Fig. 11 and Fig. 12 by (NIT, 2017) and (S. Sofyan, 2020) respectively which highlighted that the temperature starts to be greatly stable at depths starting from 6-7m while almost stay stable at 10m depth

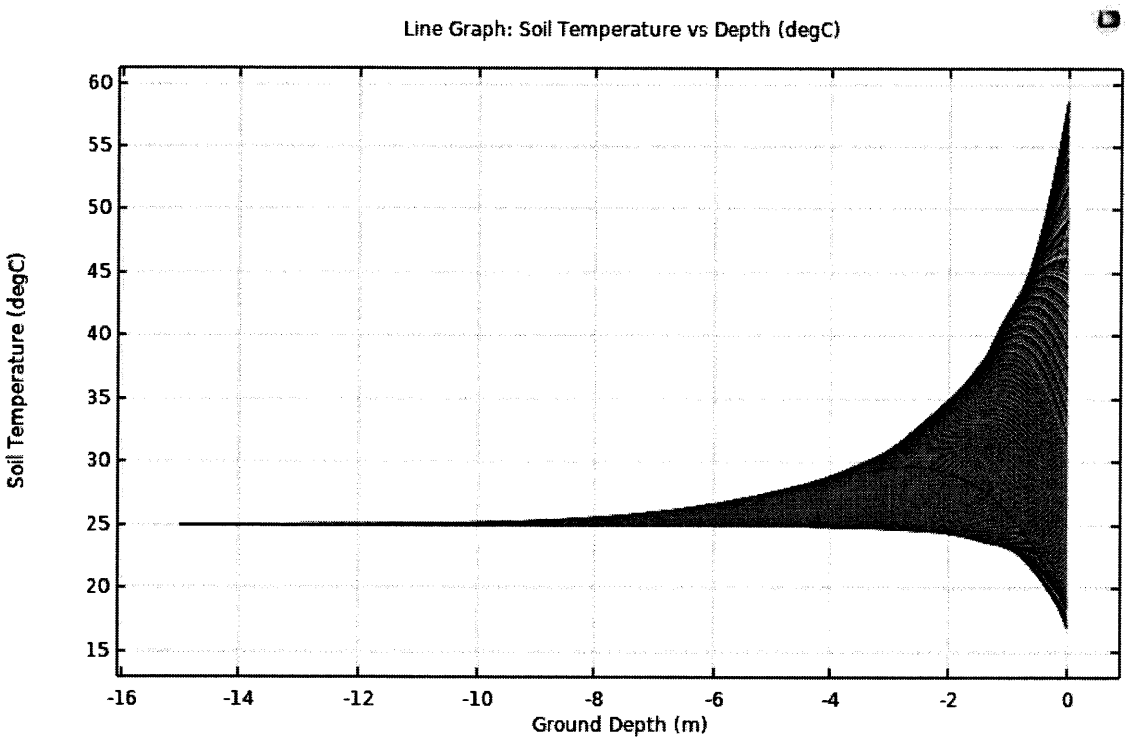


Fig. 36: COMSOL Shallow Underground Temperature Profile Result (Temp vs Depth)

4.2 Initial Analysis of AWG Feasibility

As mentioned in the objectives, modeling the shallow subsurface temperature profile can aid in initial estimates if water can be collected by analyzing the ambient air properties along with the underground temperature. That said, Fig. 37 below shows the DBT, DWPNT and RH of ambient air from COMSOL ambient properties plugin for Bahrain weather station along with the stabilized underground boundary temperature being 25 deg C.

Considering Fig. 37, the DBT and RH relationship are opposite of each other, i.e., the higher the DBT, the lower the RH and vice versa. Nevertheless, we can mainly depict that DWPNT is above min underground temperature from approximately days #175 to 280 of the year (end of June to end of Sep). This means that the underground temperature during the latter days is less than the required DWPNT. Hence, water can be theoretically produced if sufficient heat transfer is achieved. Moreover, note that the underground temperature is 25 °C and stays constant annually at around 7-10m depth so pipe design should reach further depths to pass the required DWPNT. Such result verification is essential as it initially aids AWG functionality to produce water for approx. 100 days. As mentioned earlier, DBT, RH are all set as averages whereas DWPNT is set to high.

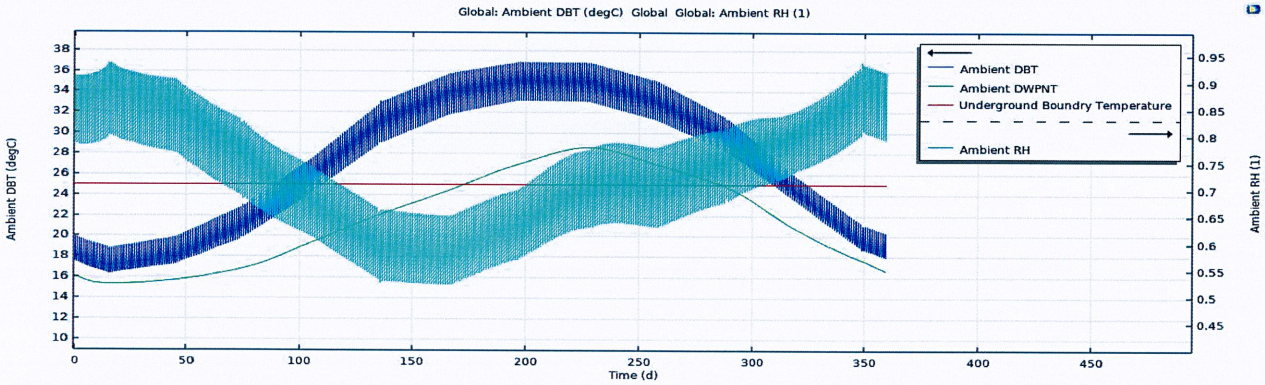


Fig. 37: Initial AWG Analysis - Ambient Properties & Ground Temp (High DWPNT).

4.3 Annual Water Production Rate

Upon considering the procedural and methodology mentioned in section 3.1 via utilizing four physics on COMSOL, the other assumptions and variables utilized for system design are considered in section 4.3.1. Moreover, the final results are included in subsection 4.3.2 where the annual water condensation rate is highlighted. Finally, subsection 4.3.3 will highlight the various design modifications considered to increase yield.

4.3.1 Assumptions and Variables Utilized

As discussed previously in chapter 2, the functionality of the AWG depends mainly on the airflow within the pipe and the rate of heat rejection at the underground level. The table shows the utilized variables and assumptions for obtaining the water condensation rate on COMSOL. Note that the design modification of these variables is to be discussed in subsection 4.3.3.

Table 5, Considered Variables Used for AWG Simulation

Assumptions and Parameters Placed with Description and Justification	
Air Inlet Pipe Design	Material: Copper because of its high thermal conductivity and corrosion resistivity. Dimensions: Standard K Type OD 41.3mm, ID 37.6mm, 1.85mm Gauge (CopperKType, 2004). Coil Design: Single Coil, 0.2m Pitch, 51 Rev, 0.1m Radius, 0m excess. $L_{Total\ Coil} = (0.2^2 + (2\pi * 0.1)^2)^{0.5} * 51 + 0 = 33.63m.$ Rejecting heat from 0m-10m underground vertical depth to reach constant boundary temperature at min significant fluctuation noted in Fig. 36.
Soil is Thermal Sink	Soil is considered as thermal energy reservoir (sink) meaning it can replenish and its thermodynamic properties are constant.
Velocity Air	$v_{air} = 4.25m/s.$

4.3.2 Water Production Rate – COMSOL

Firstly, Fig. 38 represents the condensation indicator graph showcasing when condensation occurs as a result of the air flowing underground achieving 100% RH. As seen, condensation starts to occur from day #198 to 267 of the year, considering 8-hour steps, which makes it a total of around 69 days (Mid Jul to Start of Oct). As seen in Fig. 37, the feasible theoretical amount based on underground temperature profile modeling was approximately 100 days ≅ from day 175 to 280. However, that is the ideal case with sufficient heat transfer rate occurring to the system. To clarify, 100 day condensation would be possible by reducing velocity to increase the heat transfer rate to reach DWPNT of air flow entering system as air is allowed more time to cool but this would reduce the amount of condensed water. Hence, as a result of increasing the velocity up to optimized level = 4.25m/s to focus on increasing yield rather than days of water generation, only 69/100 days are operative. Additionally, looking at Fig. 38 below, it can be seen that at the beginning and end of the condensation cycle, the condensation indicator fluctuates to positive and zero. The reason is due ambient properties are not initially sufficient for reaching condensation based on system design in the first and final days of the cycle but instead get stable from days #209-259.

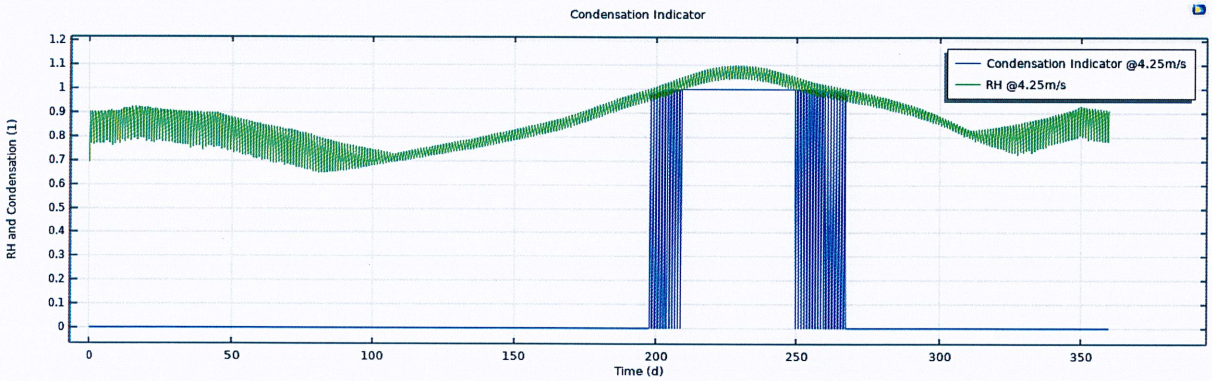


Fig. 38: Condensation Indicator @4.25m/s.

Upon consideration and analysis of curve behavior shown in Fig. 38 above, Fig. 39 below shows the condensation rate during the annual cycle, which is seen as 0 kg/s when the condensation indicator is 0 and positive when condensation occurs. Nonetheless, the min and max range of condensation rate varies from around $25*10^{-7}$ kg/s up to $87*10^{-7}$ kg/s of water.

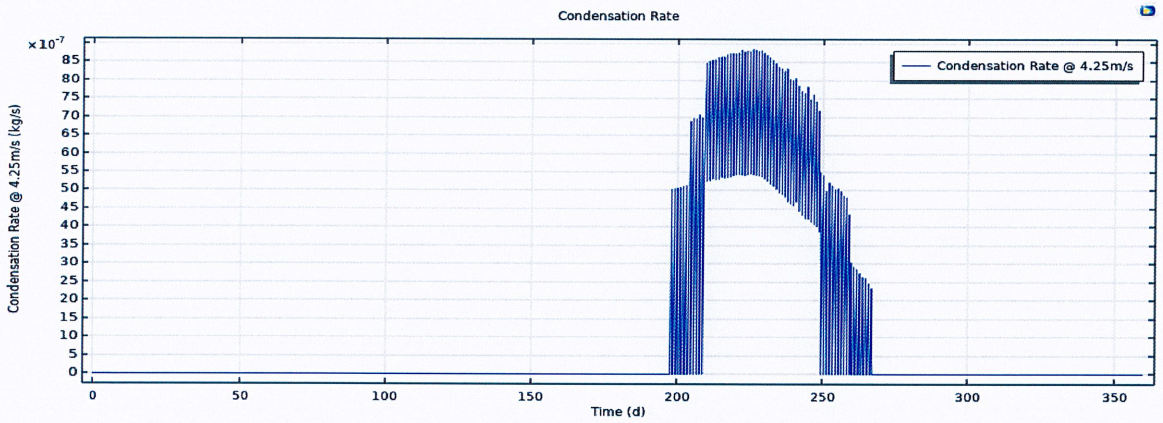


Fig. 39: Condensation Rate @4.25m/s.

Nonetheless, the breakdown of the condensation rate for the daily steps in which condensation occurs is mentioned in Table 14 in the appendix after being extracted from COMSOL simulation. Hence, the total amount of water generated annually via this designed system is 29.22 kg/yr with a maximum of ≅ 0.65 l/day and at an avg of 0.423 l/day considering the total 69-day cycle. Such results as mentioned in Table 6 below. The amount of water production is low compared to other water production methods however, the focus is to check if such system can/is able of producing water or not especially considering regions/countries where no water source is available nearby to consider other systems (RO or thermal driven). Thus, due to such system being capable of producing water, as an option, multiple systems can be installed at the same time in countries with similar climate to Bahrain (high DBT and RH) to increase water production.

Table 6, Water Condensed/Produced at a velocity of 4.25 m/s – COMSOL Result.

Estimation of Water Condensed/Produced via COMSOL Simulation @4.25m/s
Annual Total m_{WG} = 29.22 kg/yr
Max Daily m_{WG} = 0.65 kg/day
Average Daily m_{WG} = 0.423 kg/day

4.3.3 Design Modification to Increase Yield

As discussed in chapter 2, water production/condensation is due to parameters like pipe length, helical coil pipe design, vertical underground depth and underground boundary temperature, and volumetric air flow rate. Thus, comments on each parameter will be provided below on how they were considered or neglected with justification to improve yield

1. Pipe Length – Pipe length has a direct relationship to improving yield of which the longer the pipe, the higher the surface area hence the higher heat transfer rate thus, more water particles present in ambient air can be condensed if the volumetric flow rate increases. As mentioned, the straight vertical pipe was not selected for the design but rather a helical coil design to increase length, whereas if a straight pipe was used, $L_{Total\ Coil}$= 10m would be considered instead of 33.63m for the coil.
2. Helical Coil Pipe Design – No of rotations with pitch was selected to allow for a total of 10m vertical depth. However, the pitch could have been decreased with an increase in turns. Moreover, the radius of the coil could have also been increased to eventually increase the heat transfer rate, which results in condensing more water if the volumetric flow rate increased, but our justification is that firstly, we are mainly

considering if such a system can function and be feasible. Moreover, an increase in turns and coil radius causes gravity to be ineffective, causing condensed water to stagnate and an increase in material usage, respectively.

3. Vertical Underground Depth – The considered depth for rejection heat from atmospheric air underground is from 0-10m. The reason only 10m was considered, as mentioned earlier, is that the soil temperature is almost constant throughout the year, thus allowing for consistent results and uses of parameters accordingly. Although increasing depth after 10m can increase water production, it is firstly unnecessary due to not adding anything additionally and significantly as the main deliverable of assuring AWG feasibility was attained. Secondly, material usage is increased at a cost. Finally excavation of underground holes is challenging, which could complicate practical installation; hence, the lowest depth necessary is ideal.

4. Volumetric Flow Rate – The volumetric flow rate of air entering the system is crucial to optimize in order to yield maximum water and hence it depends on two parameters which are the ID of the pipe and v_{air} were pipe ID and air velocity utilized were a 37.6mm and 4.25 m/s, respectively. Changing the ID of the pipe at the same velocity would increase the volumetric flow rate but not necessarily heat transfer, as it is mainly limited to the surface area. Therefore, the volumetric flow rate must be constant. That said, its preferable to increase air velocity instead of increasing pipe size as an increase in pipe size would result in an increase in material = price increase and an increase in air velocity is easier to accomplish. Moreover, increasing airflow velocity in a small pipe overcomes stagnation and

pressure drop compared to a bigger pipe with a slower velocity. That said, realistically, only the velocity parameter was considered to modify the results.

The airflow velocity, which is a design parameter investigated in this work, was altered to search for the optimum conditions that results in maximizing the water production rate. Hence, it is found that setting this parameter to 4.25m/s resulted in maximizing this rate, as depicted in Fig. 40. As seen below, at the lowest velocity of 2.5 m/s the generated water is approximately 23 kg/yr. However, the highest water generation is not at a higher velocity, i.e., 5.5m/s, but rather at 4.25 m/s, which is the optimized velocity. The reason is that with increasing the velocity, the volumetric flow rate increases, but heat transfer occurring is only sufficient to a certain amount of the volumetric flow occurring to achieve condensation. Thus, at specific high velocities, the heat transfer taking place is insufficient to allow full condensation of airflow, which equals a reduction in the condensation rate.

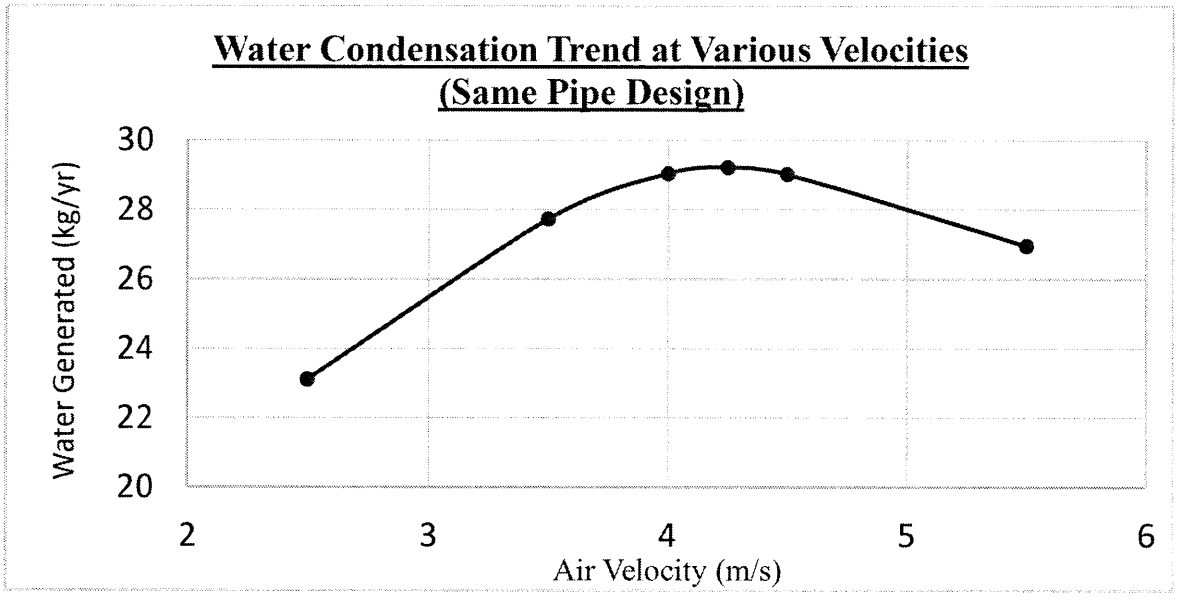


Fig. 40: Condensation Trend at Various Velocities for similar pipe design.

4.3.4 Water Production Rate – Simplified Model

As mentioned in section 3.5, for simplified model estimation of water production rate, a small sample is going be considered to obtain the results to have an average estimate. This is due to that as analyzed in Fig. 38, there are around more than 200 steps which equates to 200 calculations where water is produced via the system and estimating for each is unnecessary and a lengthy process as defined by the procedural steps in section 3.5. That said, the considered steps are for day 210, 210.333 and 210.667. That said, assumptions and initial variables utilized are as seen in Table 7:

Table 7, Considered Variables Used for AWG Simplified Model

Assumptions and Parameters Placed with Description and Justification				
Pipe Design (Similar to COMSOL)	Material: Copper/ Dimensions: OD 41.3mm, ID 37.6mm, 1.85mm Gauge. $L_{Total\ Coil} = 33.63m.$ Rejecting heat from 0m-10m.			
Velocity Air (Similar to COMSOL)	$v_{air} = 4.25m/s.$ Volumetric flow rate of air assumed constant flowing in and out of system is assumed constant.			
Pipe Outer Surface Temperature T_3	T_3 = 30 °C (Average 1-10m refer to Fig. 36).			
Temperature @10m depth $T_{@10m}$	$T_{@10m}$ = 25 °C			
Ambient Properties (COMSOL)	Day/Step	210	210.333	210.667
	DBT (°C)	33.13	35.06	36.84
	RH (%)	74.1%	66.7%	60.5%

	DWPNT (°C)	27.85	27.92	27.94
	SH_{in} (g/kg)	0.02197	0.0221	0.02204
	SH_{out} (g/kg)	0.0203	0.0198	0.0193

Considering Table 8 below, the estimated water condensation quantity for a system design is similar to COMSOL but via a simplified calculation. As seen, the water generated per 8 hours (each step) is 0.2677, 0.3624 and 0.4325 for day 210, 210.33 and 210.667. The calculation was all done automatically in Excel, as attached in Fig. 80 in the appendix.

The main element to assess in Table 8 is that $\dot{Q}_{Actual} > \dot{Q}_{Required}$ for all steps/days. This is crucial as mentioned in chapter 2, where condensation can only occur if such a rule applies. Nevertheless, it can be seen that Q_{Actual} in day 210.333 and 210.667 are significantly higher than the required. This is due to the selection of a velocity of 4.25 m/s, which satisfies all the conditions/days/steps and not only some segregated days. Otherwise, the velocity has to continuously change with respect to ambient properties etc., to yield the highest results. However, our analysis is on a fixed constant velocity that has been modified to yield the highest results while being stable.

Table 8, Water Condensed/Produced @4.25 m/s – Simplified Model Sample Result

Day	**210**	**210.333**	**210.667**
v_{air} **(m/s)**	4.25	4.25	4.25
T (Hrs)	8	8	8

$\dot{m}_A$ (kg/s)	$5.513*10^{-3}$	$5.494*10^{-3}$	$24.134*10^{-3}$
$T_{Avg\ Atm\text{-}10m}$ (°C) – Prop of Air & Water	29.1	30.03	30.9
R_{RC} (°C/W)	$1.145*10^{-6}$	$1.144*10^{-6}$	$1.145*10^{-6}$
R_{FC} (°C/W)	0.0092	0.01123	0.0112
Q_{Actual} (W)	340.363	450.24	608.27
Q_{SA} (W)	29.064	39.468	49.094
$\dot{m}_{Win}$ (kg/s)	$121.1128*10^{-6}$	$121.295*10^{-6}$	$120.777*10^{-6}$
$\dot{m}_{Wout}$ (kg/s)	$111.832*10^{-6}$	$108.711*10^{-6}$	$105.761*10^{-6}$
Q_{SW} (W)	2.657	3.626	4.503
Q_{LW} (W)	302.82	303.24	301.943
$Q_{Required}$ (W)	334.542	346.33	355.54
m_{WG} (kg)	**0.2677**	**0.3624**	**0.4325**

4.3.5 Comparison of Water Production Rates

Considering Table 9 and Fig. 41 below showcasing deviation between Simplified Model and COMSOL results to that of the water condensation amount for days 210, 210.333 and 210.667 that were considered as samples, the minimum deviation is 43.3% for day 210.667 and a maximum of 43.6% for day 210. Nonetheless, the average deviation is 43.4%.

The main element of the depicted deviation is due to COMSOL variable estimation when considering the volumetric flow rate of the air. The meaning of this is that once we assess the simplified model calculations, we consider the governing rule to be $\dot{Q}_{Actual} > \dot{Q}_{Required}$ at which the volumetric flow rate is fixed based on fixed inlet air velocity and

temperature. COMSOL on the other hand can be more accurate; hence, the volumetric flow rate was estimated based on velocity and temperature parameter change while considering integration variable estimation. The deviation is high, so COMSOL software is an ideal means to be considered for more accurate results, as the simplified model can be extremely complicated if you need to assess every variable change with respect to velocity and thermodynamic properties. To add, as seen in Fig. 41, the trend of both set of results are identical.

Table 9, Comparison of Water Condensation Results.

$m_{WG}(kg)$ Day/Step	Simplified Model Results	COMSOL Results	Deviation (%)
210	0.2677	0.151	**43.6**
210.333	0.3624	0.2051	**43.4**
210.667	0.4325	0.2454	**43.3**
Average Deviation			**43.4**

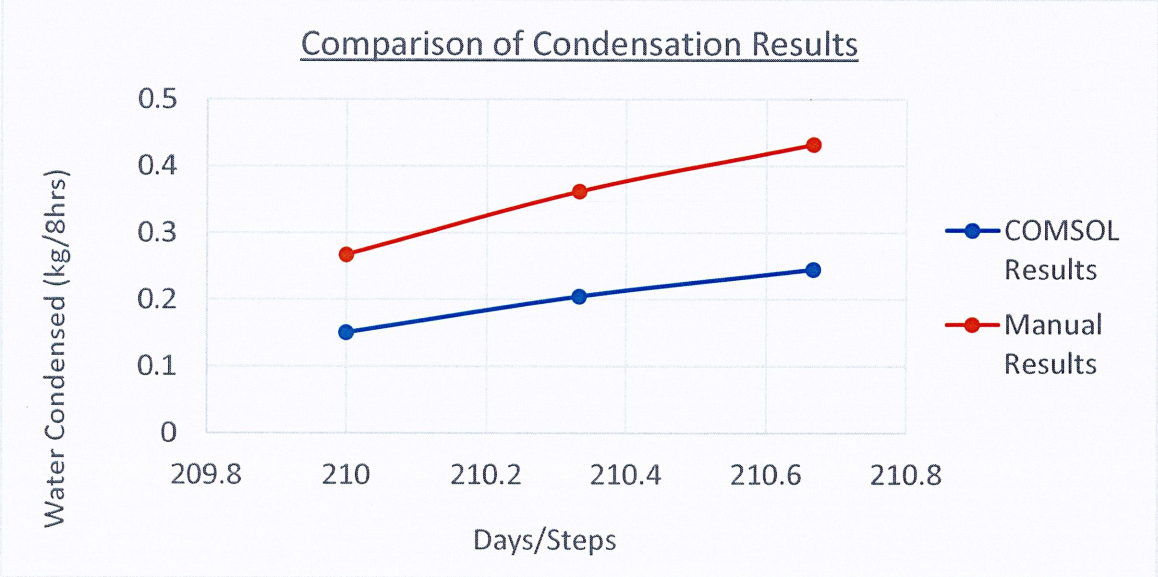


Fig. 41: Comparison of Water Condensation Results.

4.4 Off-Grid PV System Sizing

As mentioned, the AWG is designed to operate in worst case scenario that being in regions where there isn't any grid electricity available hence off grid solar PV system is sized considering PV panels, batteries, solar charge controller (SCC) are all required. To add, as mentioned alternating current (AC) to direct current (DC) inverter will not be utilized because were are considering DC appliances only. PBP results will also be shared.

4.4.1 Assumptions and Variables Utilized

As discussed earlier, Table 10 below highlights the utilized variables necessary for calculation based on AWG system design and PV Solar system sizing common variables:

Table 10, Off-Grid PV System Sizing Variables

Variable	Value
Wiring Effiency – η_{Wiring}	97%
Peak Sun Hours	6 Hrs
PV Panel Efficiency - η_{PV}	85%
Days of Autonomy	2 Days
Battery Efficiency - $\eta_{battery}$	90%
DoD (Lead Acid)	50%
SCC Limit if of I_{SC} - $Limit$	125%
Output Voltage/Appliance Voltage - $V_{Appliances}$	12V DC
Air Inlet Velocity - v_{air}	4.25 (m/s)
Maximum Time of Operation Per Day - $T_{Max\ Operation}$	24 Hrs
Maximum Water Generated Daily	0.65 lt

4.4.2 Load Estimate

The loads considered for the PV System sizing are fans to supply air within the system to maintain consistent air velocity. Moreover, other load is for the water extraction pump that will be utilized to harvest the water condensed at 10m underground up to ground surface level. Nonetheless, the results are shared in Table 11 whereas the detailed calculation is mentioned in Table 15 in the appendix.

As seen, based on the selected appliances the total maximum load with 97% η_{Wiring} is 127 Wh of which the total load prior to considering η_{Wiring} is 123Wh. Nonetheless, 120Wh is the daily load by 2x fans to supply air flow to the AWG system design as they operate for 24Hrs whereas only 3Wh is required for the water extraction pump as it only operates for less than 1 minute per day to extract the accumulated maximum water produced per day being 0.65lt at the end of the day.

Table 11, PV System Load Estimate.

$Total\ Load = \Sigma Load$	**123 *Wh***
$Total\ Max\ Load$ (with η_{Wiring})	**127 *Wh***

4.4.3 Sizing of Components

As seen below in Table 12, all of the off-grid solar PV components required to operate AWG have been determined. As a summary, the battery capacity required is 50Ah hence a 12V 50A sealed maintenance-free lead acid battery is selected making the total required batteries 1 Nos. The reason why SMF Lead acid batteries were selected instead of flooded type is due to not

requiring any maintenance. Additionally, as mentioned earlier, Gel Deep Cycle or Li-Ion batteries are not selected due to being very expensive, that being 3x and 6x Price, respectively. Furthermore, the required PV panel current is 2.1A; hence a 40W 2.56A Isc current monocrystalline PV panel is selected with 21.7V Voc. That said, only a total of 1 PV Panel will be required. Finally, based on the voltage of the battery series string = 12V and SCC current sizing based on the limit, Isc and panels in parallel, the selected SCC is a waterproof IP67 12V 5A SCC.

Table 12, Results of Off-Grid Solar PV Component Sizing

Off-Grid Solar PV Component Sizing		
Battery	Capacity Required	$\left(\frac{Total\ Max\ Load}{V_{Appliances} * \eta_{battery} * DoD}\right) * Autonomy$ $\left(\frac{127}{12 * 0.9 * 0.5}\right) * 2 = \mathbf{50Ah}$
	Selected Battery	**12V 50Ah** Lead Acid Sealed Maintenance Free (SMF) Batteries available in Bahrain from Arabian Parts Company = 22BHD.
	No of Batteries in Series	$\left(\frac{V_{Appliances}}{V_{Battery}}\right) = \left(\frac{12}{12}\right) = \mathbf{1}$
	No of Batteries in Parallel	$\left(\frac{Capacity\ Required}{Battery\ Capacity\ Selected}\right) = \left(\frac{50}{50}\right) = \mathbf{1}$
	Total Batteries	$No\ in\ Series * No\ in\ Parallel = 1 * 1 = \mathbf{1}$
PV Panel	Required PV Panel Current	$\left(\frac{Total\ Max\ Load}{V_{sys} * \eta_{PV} * Peak\ Sun\ Hrs}\right) = \left(\frac{127}{12 * 0.85 * 6}\right) = \mathbf{2.1A}$

	Selected PV Panel	Selected PV Panel Specification = 40W Monocrystalline, 21.7 (Voc), 2.56A (Isc), 17.4V (mpp), 2.48A (Impp) (Ivensun, 2022) = approx. 50$ = 19BHD
	No of Panels in Series	$\left(\frac{V_{sys}}{VOC_{Panel}}\right) = \left(\frac{12}{21.7}\right) = \mathbf{1}$
	No of Panels in Parallel	$\left(\frac{Required\ PV\ Panel\ Current}{Isc_{Panel}}\right) = \left(\frac{2.1}{2.56}\right) = \mathbf{1}$
	Total Panels	$No\ PV\ Panels\ in\ Series * No\ of\ PV\ Panels\ in\ Parallel = 1 * 1 = \mathbf{1}$
SCC	SCC Current	$PV\ Parallel * Isc_{Panel} * Limit = 1 * 1.25 * 2.56 = \mathbf{3.2A}$
	SCC Voltage	$Voltage\ of\ Batteries\ Series\ String = \mathbf{12V\ DC}\ like\ Battery$
	Selected SCC	Selected SCC = 5A, 12V SCC for 15$ = 6BHD (Amazon, 2022). Additionally, it is IP67 Rating waterproof and suitable for safely charging lead acid batteries.

4.4.4 Payback Period

Examining the content of Table 13 below, the total cost of the off-grid PV system is 47BHD, where the battery, panel and SCC are approx. 47%, 40% and 13%, respectively, of the total cost. As estimated, the PBP is high because the life expectancy of batteries is approximately 3-5 years approximately and PV panels 20-25 years, which means by the time pack back period comes, batteries were changed seven times (min) and PV panels changed again once. However, keep in mind that the above 47BHD solar

system with 36 years of PBP is relatively cheap when you gain 29.2 L of water free per year in a remote area. Although, ideally, if there is a grid nearby, it would be better to utilize it in order to reduce AWG system's total price as PV solar system will not be required, which also means no maintenance is required of batteries/panels, appliances must be changed to AC instead of DC.

Typically, the PBP off-grid systems are high in general due to mainly battery price. However, it can be utilized in any remote area. Nevertheless, the system is proven feasible in constructing with an off-grid solar system for that low amount of 47BHD, as you get 29.2Lt of water per year.

Table 13, Estimating the PV System Pay Back Period (PBP).

PBP Estimation of the Sized Off-Grid PV System		
Cost	Battery	Selected Battery = 1x12V 50Ah SMF = **22 BHD**
	PV Panels	Selected PV Panel = 40W, 21.7 (Voc), 2.56A (Isc), 17.4V (mpp), 2.48A (Impp) = approx. 50$ = **19BHD**
	SCC	Selected SCC = 5A, 12V SCC for 15$ = **6BHD**
	Total Cost	Battery Price + Panel Price + SCC = 22+19+6 = **47BHD**
PBP	Annual Grid Energy	$Total\ Max\ Load\ (day) * 365 = 127Wh * 365 = 45.625kW/year$
	Cost Annual Grid Energy	$Annual\ Grid\ Energy * E_{Rate} = 45.625 * \left(\frac{0.029BHD}{kW}\right) = 1.323\ BHD\ per\ year$
	Pay Back Period	$\frac{Total\ PV\ System\ Cost}{Cost\ Annual\ Grid\ Energy} = \frac{47}{1.323} = 36\ Years$

4.5 Conclusion

In Conclusion, all thesis topic objectives were attained successfully, and the concerns were answered as a part of obtaining the necessary results. Nevertheless, the main motivation of the research was due to water scarcity; hence, an attempt to mitigate the issue is by studying the feasibility of off-grid solar-powered AWG, which functions via underground heat rejection. The system's functionality was based on designing a system where ambient humid, warm air is forced to follow underground at shallow depths up to 10m to reject its thermal energy causing it to condense upon reaching desired DWPNT. The main study focused on assessing feasibility of such system in the sense of whether such principle is capable of producing water.

Four steps were erected. Firstly 3D model temperature profile of shallow underground temperature in Bahrain via COMSOL Software. Secondly, design, and integrate AWG pipe design into modeled ground in COMSOL to simulate condensation results. Thirdly, attempt simplified model calculations and compare its result with COMSOL simulation results. Lastly, utilize AWG in clean & remote applications, off-grid solar PV system sized if the system is deemed feasible and estimate its PBP.

Considering results, firstly, upon simulating the shallow underground soil temperature in Bahrain via COMSOL software through considering ambient properties, heat transfer in solids and solar radiation physics was that surface temperature ranged between 58 and 18 °C during the hottest and coldest intervals of the year while being fully stable with minor annual fluctuation at set temperature boundary condition of 25 °C @9-10m depth. The latter results served as initial assessments for the feasibility of condensation of ambient air to produce water being possible where DWPNT

is greater than boundary temperature during the year's hot season, days #175 to 280 (corresponding to end of June to end of Sep).

Consecutively, a coil copper pipe was 3D modeled and integrated into the soil domain to study diluted species and fluid flow physics to estimate water condensation. Pipe design being 41.3mm OD, 37.6mm ID with a coil design equation to $L_{Total\ Coil} = 33$, the optimum velocity of air to yield the highest output was found to be $v_{air} = 4.25$ m/s, where a total yield of 29.2kg water can be produced for 69 days/yr, considering 8-hour step simulations.

Thirdly, a small sample for simplified model calculations was attempted to be compared with COMSOL results by extracting ambient properties directly from COMSOL. The sample was for 3 days/steps being 210, 210.333 and 210.667 where average deviation between results was noted to be 43.4%. The reasoning for deviation was due to COMSOL integration of volumetric flow rate as a function of velocity and temperature change, whereas simplified model considered only fixed variables.

Finally, since the system was deemed feasible, the off-grid PV system was sized based on the estimated based on load estimated $Total\ Max\ Load$ 127Wh, required components included a 50 Ah battery, 40W Panel and 5A SCC with an estimated PBP of 36 years. The inverter was not sized, as the appliances used were of a Direct current (DC).

Based on what was learned, recommendations are suggested for future work below, mainly to attempt harnessing actual underground temperature readings, constructing a real-life model to experiment with AWG and considering additional software to compare or validate results of which details can be seen provided below.

4.6 Recommendations and Future Work

Upon reaching this thesis topic objectives, work include:

1. Harnessing Actual Underground Data – An important variable was approximated and used that being the undergoing boundary temperature = 25 deg C. As mentioned, value cannot be 100% proven unless if actual real life measured data of temperature at various shallow depths is taken and then compared with model to reassess.
2. Experimenting – Simulation and calculations help initial exploration to approximate outcomes; actual experimental data is concrete as it considers complex real-life physics without polishing results. Attempting the AWG experiment as per design after endeavoring and passing recommendation 1 to assess outcome is recommended. This is due to the limitation of calculations and control of COMSOL settings such as ambient properties etc. whereas in real life, it would continuously change; hence, results can be better or worse. COMSOL steps can be increased, but computation time increases drastically.
3. Copper Metal Mesh – As a recommendation to increase the amount of water generated, metal copper wire mesh/sponge can be added to the pipe. This will increase surface area, increasing heat transfer rejection rate to allow for more air flow.
4. Utilization of Other Software – COMSOL Software was utilized for modeling. However, if an additional/new set of analysis was attempted, considering a second credible software to utilize hand in hand with COMSOL to compare is recommended. Such software might include Ansys, MATLAB etc.

References

[DIY Solar Power with Will Prowse]. (2019, Oct 4). How to Size your Solar Power System [YouTube Video]. Retrieved From www.youtube.com/watch

[Technion]. (2020, Feb 17). Producing Water from Air New Technion Moisture Harvesting System [YouTube Video]. Retrieved from https://www.youtube.com/watch?v=8fQRnM4-4W4

[TEDx Talks]. (2016, Feb 17). How to Turn Thin Air into Water l Konstantin Avdienko l TEDxTeen [YouTube Video]. Retrieved from https://www.youtube.com/watch?v=o68leKAf-Gk

[UC Berkeley]. (2018, Jun 8). This water harvester can turn desert air into drinkable water [YouTube Video]. Retrieved from https://www.youtube.com/watch?v=-6T3ICXWqjc

A History of Geothermal Energy in America. (2020, April). Retrieved from https://www.energy.gov/eere/geothermal/history-geothermal-energy-america.

Air - Specific Heat at Constant Pressure and Varying Temperature. (2022, June). Retrieved from https://www.engineeringtoolbox.com/air-specific-heat-capacity-d_705.html

Bahrain Economic Vision 2030. (2008). Retrieved from https://www.bahrain.bh/.

Bahrain Sustainable Development Goals. (2000). Retrieved from https://www.sdgs.gov.bh/

Bensebaa, F. (2013). Water Purification. Retrieved from www.sciencedirect.com/water-purification

Tong, Li, Duanmu and Wang, (2020, Nov 27). Prediction of the temperature profiles for shallow ground in cold region and cold winter hot summer region of China. Retrieved

from
https://www.sciencedirect.com/science/article/abs/pii/S0378778821002309?via%3Dihub

Compared: Grid-Tied, Off-Grid, and Hybrid Solar Systems. (2022, April). Retrieved from https://www.solarreviews.com/blog/grid-tied-off-grid-and-hybrid-solar-systems

COMSOL Heat Transfer in Solids Physics Document. (2022, April). Retrieved from https://doc.comsol.com/5.5

COMSOL Laminar Flow Physics Document. (2022, June). Retrieved from https://doc.comsol.com/6.5

COMSOL Surface to Surface Radiation Physics Document. (2022, June). Retrieved from https://doc.comsol.com/5.5/doc/com.comsol.help.heat/heat_ug_multiphysics_features.12.15.html

COMSOL The Moisture Transport in Air Interface Document. (2021, August). Retrieved from
https://doc.comsol.com/5.5/doc/com.comsol.help.heat/heat_ug_interfaces.08.52.html

Convection Heat Transfer, (2020). Retrieved May 19, 2020, from http://www.mhhe.com/engcs/mech/cengel

Copper Tubes Type K - Dimensions and Physical Characteristics. (2019, October). Retrieved from https://www.engineeringtoolbox.com/copper-tubes-dimensions-d_357.html

Chehab (2019). Energy, Environment and Sustainability, EN8905 Course Notes, EnergyEnv Chris Hamper 8-1 to 8-3 [PDF File]. Isa Town, Bahrain: Bahrain Polytechnic.

Chehab (2019). Energy, Environment and Sustainability, EN8905 Course Notes, Energy Future lll (130-141) [PDF File]. Isa Town, Bahrain: Bahrain Polytechnic.

Chehab (2019). Energy, Environment and Sustainability, EN8905 Course Notes, --Types of Renewable Clean Energy (2) [Word File]. Isa Town, Bahrain: Bahrain Polytechnic.

Chehab (2019). Energy, Environment and Sustainability, EN8905 Course Notes, --World energy consumption = [PDF File]. Isa Town, Bahrain: Bahrain Polytechnic.

Chehab (2019). Energy, Environment and Sustainability, EN8905 Course Notes, --World_energy_resources-ResearchGate [PDF File]. Isa Town, Bahrain: Bahrain Polytechnic.

Chehab (2019). Energy, Environment and Sustainability, EN8905 Course Notes, --World energy resources – Wikipedia [PDF File]. Isa Town, Bahrain: Bahrain Polytechnic.

Dry Bulb, Wet Bulb and Dew Point Temperatures. (2022, June). Retrieved from https://www.engineeringtoolbox.com/dry-wet-bulb-dew-point-air-d_682.html

Electricity Generation. (2022, June). Retrieved from https://www.energy.gov/eere/geothermal/electricity-generation

Emissivity Coefficient of common Products. (2022, June). Retrieved from https://www.engineeringtoolbox.com/emissivity-coefficients-d_447.html

Energy.org. (2022, June). Retrieved from http://www.geo-energy.org/geo_basics_plant_cost.aspx

Engineering Design Process. (2017, May). Retrieved from http://www.teachengineering.org/k12engineering/designprocess

Free Online Interactive Psychrometric Chart. (2022, June). Retrieved May 19, 2020, from http://www.flycarpet.net/en/PsyOnline

Geothermal Energy Pros and Cons. (2018, February). Retrieved from https://energyinformative.org/geothermal-energy-pros-and-cons/

Geothermal Energy. (2018, February). Retrieved from https://www.mpoweruk.com/geothermal_energy.htm

Geothermal Power. (2019, December 12). Retrieved from https://en.wikipedia.org/wiki/Geothermal_power

Geothermal. (2018, February). Retrieved from http://www.darvill.clara.net/altenerg/geothermal.htm.

Gido, Friedler, Broday (2016, July 26). Assessment of Atmospheric Moisture Harvesting by Direct Cooling. Retrieved from https://cee.faculty-ms.technion.ac.il

Grid-Tied, Off-Grid and Hybrid Solar Systems. (2021, April). Retrieved from https://www.mepcell.com/grid-tied-off-grid-and-hybrid-solar-systems/?lang=en

Jameel (2022, June). How Wet and Dry Bulb Temperatures work. Retrieved from https://alj.com/en/

Jamil (2020). Renewable Energy System Fundamentals, REE601 Course Notes, Questions [PDF File]. Isa Town, Bahrain: University of Bahrain.

Jamil (2020). Renewable Energy System Fundamentals, REE601 Course Notes, Questions [PDF File]. Isa Town, Bahrain: University of Bahrain.

Kanoglu, Cengrel and Cimbala (2020, Nov 27). Fundamentals and Applications of Renewable Energy. McGrawHill.

Know Your Solar Panels: 3 Types of Solar Panels (2022). Retrieved from https://kiwienergy.us/know-your-solar-panels-3-types-of-solar-panels/

Latent and Sensible Heat. (2018, March). Retrieved from https://legacy.climate.ncsu.edu/edu/Heat

Latent heat of condensation of water: Socratic. (2017, July 22). Retrieved from https://socratic.org/questions/

Lead-Acid vs. Lithium Batteries: Which Are Best for Solar (2022). Retrieved from https://unboundsolar.com/blog/lead-acid-vs-lithium-batteries.

Links (2014, March 22). Geothermal Power. Retrieved from https://www.slideshare.net/asertseminar/geothermal-power-32613981.

Markings (2019, March 2). How to Calculate Helical Length. Retrieved from https://sciencing.com/calculate-helical-length

Ministry of Transportation and Telecommunications (2022, June). Retrieved from https://mtt.gov.bh/

Modi (2019). Applied and Process Heat Transfer, EN8918 Course Notes, Conduction in Details [PPT File]. Isa Town, Bahrain: Bahrain Polytechnic.

Modi (2019). Applied and Process Heat Transfer, EN8918 Course Notes, Dimensionless Numbers [PPT File]. Isa Town, Bahrain: Bahrain Polytechnic.

Modi (2019). Applied and Process Heat Transfer, EN8918 Course Notes, Presentation on Conduction, Convection, Radiation - Principles [PPT File]. Isa Town, Bahrain: Bahrain Polytechnic.

National Geographic Society. (2012, November 16). geothermal energy. Retrieved from https://www.nationalgeographic.org/encyclopedia/geothermal-energy/.

Nemali (2019, Feb). History of Controlled Environment Horticulture: Greenhouses. Retrieved from https://www.researchgate.net/figure/Psychrometric-chart

Office of EE and RE. Geothermal Heat Pumps. (2021). Retrieved from https://www.energy.gov/eere/ghp.

Open-Circuit Voltage (2020, October). Retrieved from https://www.pveducation.org

Purushothama, B. (2009). Definitions of terms used in humidification engineering. Retrieved from https://www.sciencedirect.com/psychrometrics

Radial Conduction. (2019, Oct). Retrieved from www.researchgate.net/figure/Definition-of-a-cylindrical-system-with-radial-heat-conduction_fig4_224600441

Relative Humidity in Air. (2022, June). Retrieved from www.engineeringtoolbox.com/relative-humidity-air-d_687.html

Rinkesh (2016, December 25). Geothermal Energy History. Retrieved from https://www.conserve-energy-future.com/geothermalenergyhistory.php.

Short-Circuit Current (2020, October). Retrieved from https://www.pveducation.org

Singh and Sharma (2017). Numerical Analysis for Ground Temperature Variation. Retrieved from https://geothermal-energy-journal.springeropen.com

Sofyan, Hu , Kotousov, Riayatsyah, Khairil and Hamdani (2020). A New approach to modelling of seasonal soil temperature fluctuations and their impact on the performance of a shallow borehole heat exchanger. Retrieved from https://www.sciencedirect.com/science/article

Solar PV System Components (2020). Retrieved from https://bhgpower.co.za/what-equipment-do-you-need-for-a-solar-power-system/

Surface Emissivity Table. (2022). Retrieved from https://www.thermoworks.com

Taleb (2020). Photovoltaic Energy Systems, REE602 Course Notes, Lecture 1 [PDF File]. Isa Town, Bahrain: University of Bahrain.

The Kingdom of Bahrain National Energy Effiency Action Plan (NEEAP) (2017, Jan). Retrieved from https://www.sea.gov.bh

The Kingdom of Bahrain National Renewable Energy Action Plan (NREAP) (2017, Jan). Retrieved from https://www.sea.gov.bh

Water - Specific Heat. (2022, June). Retrieved from https://www.engineeringtoolbox.com/specific-heat-capacity-water-d_660.html

Water Scarcity. (2010). Retrieved from https://www.unicef.org/wash/water-scarcity

Water Scarcity. (2018). Retrieved from www.sciencedaily.com/terms/water_scarcity.htm

Xu, W and Yaghi (2020, July 21). Metal-Organic Frameworks for Water Harvesting from Air, Anywhere, anytime. Retrieved from http://yaghi.berkeley.edu

Zehar (2021). Special Topic in Renewable Energy Engineering, REE605, Introduction to Renewable Energy Part 1 [PDF File]. Isa Town, Bahrain: University of Bahrain.

Zehar (2021). Special Topic in Renewable Energy Engineering, REE605, Introduction to Renewable Energy Part 2 [PDF File]. Isa Town, Bahrain: University of Bahrain.

APPENDICES

APPENDIX A. Mathematical Modelling (COMSOL)

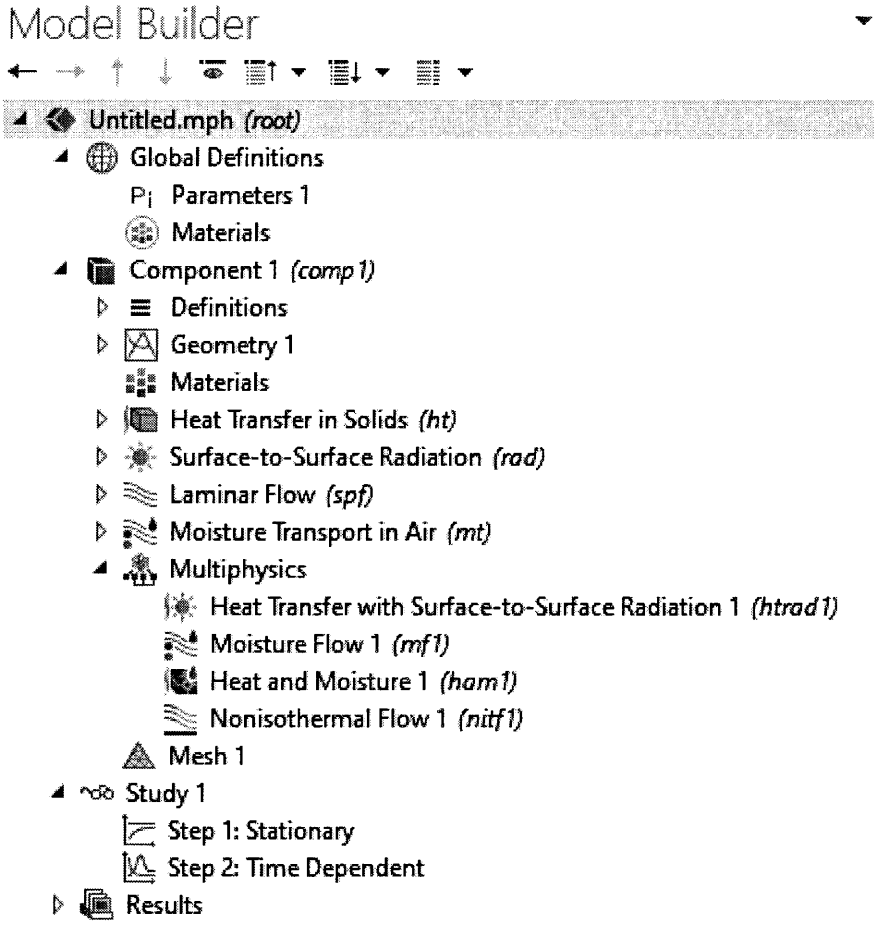


Fig. 42: COMSOL Study Settings (Multiphysics Model Builder).

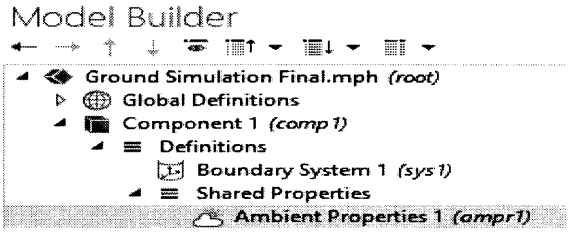


Fig. 43: Component Definitions – Ambient Properties.

Settings

Time Dependent

= Compute

Label: Time Dependent

Study Settings

Time unit: d

Output times: range(0,8[h],360) d

Tolerance: Physics controlled

Results While Solving

Physics and Variables Selection

Modify model configuration for study step

Physics interface	Solve for	Equation form
Heat Transfer in Solids (ht)	☑	Automatic (Time dependent)
Surface-to-Surface Radiation (rad)	☑	Automatic (Time dependent)
Laminar Flow (spf)	☐	Automatic (Stationary)
Moisture Transport in Air (mt)	☑	Automatic (Time dependent)

Multiphysics couplings	Solve for	Equation form
Heat Transfer with Surface-to-Surface R...	☑	Automatic (Time dependent)
Moisture Flow 1 (mf1)	☑	Automatic (Time dependent)
Heat and Moisture 1 (ham1)	☑	Automatic (Time dependent)
Nonisothermal Flow 1 (nitf1)	☑	Automatic (Time dependent)

Fig. 44: COMSOL Time Dependant Study Settings.

Settings

Parameters

Label: Parameters 1

Parameters

Name	Expression	Value	Description
dT	3[K]	3 K	Half diurnal temperature...
depth	15[m]	15 m	Soil/Sand/Ground Depth
alpha	0.65	0.65	Surface Absorptivity of S...
epsilon	0.9	0.9	Surface Emissivity of Sand
p_d	37.6[mm]	0.0376 m	Inner pipe diameter
p_T	1.85[mm]	0.00185 m	Pipe Thickness
vin	4.25[m/s]	4.25 m/s	Inlet Velocity
Ain	pi/4*p_d^2	0.0011104 m^2	Pipe Inlet Area
pipedepth	-10[m]	-10 m	Pipe Length

Fig. 45: Utilized Parameters Settings in COMSOL

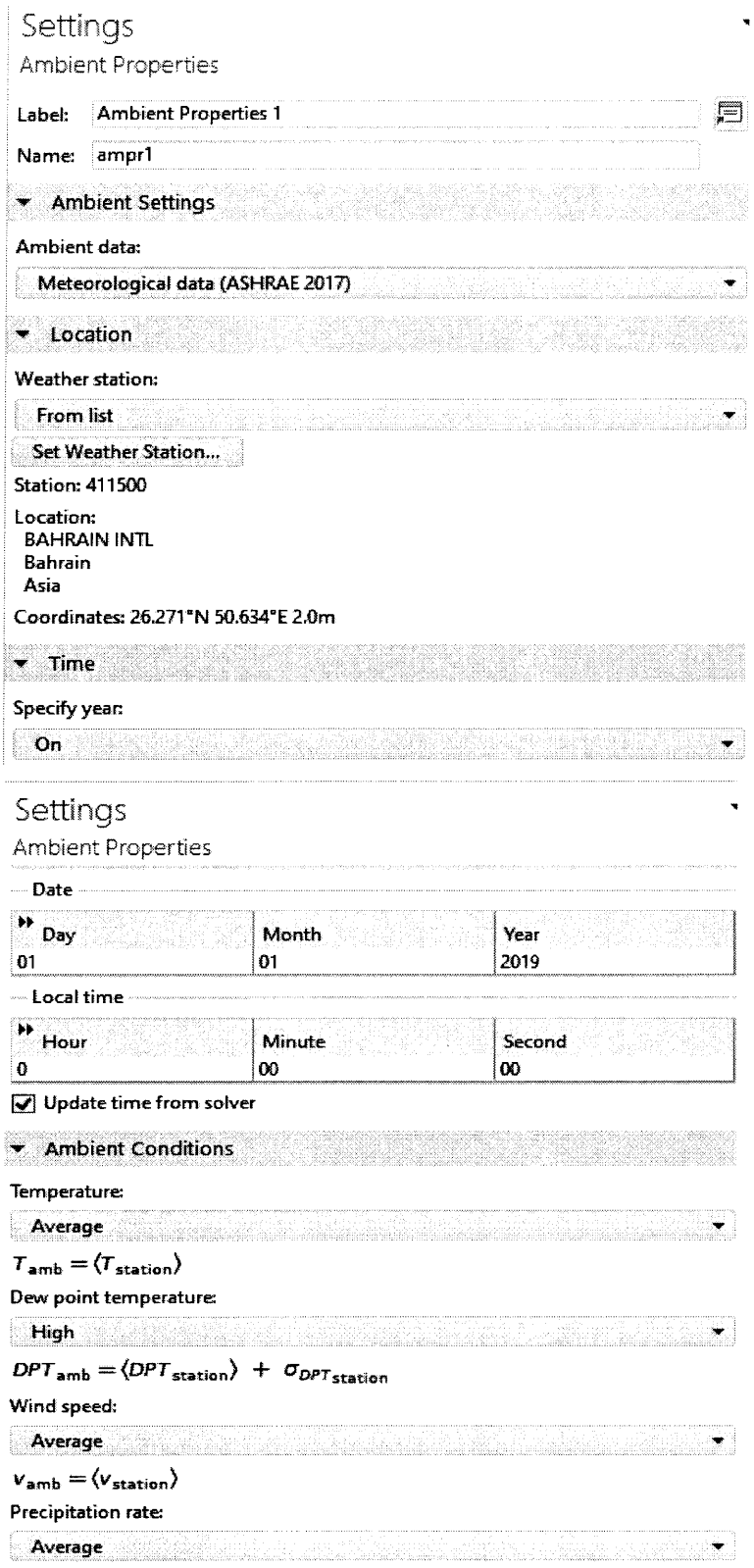


Fig. 46: Ambient Properties Settings in COMSOL.

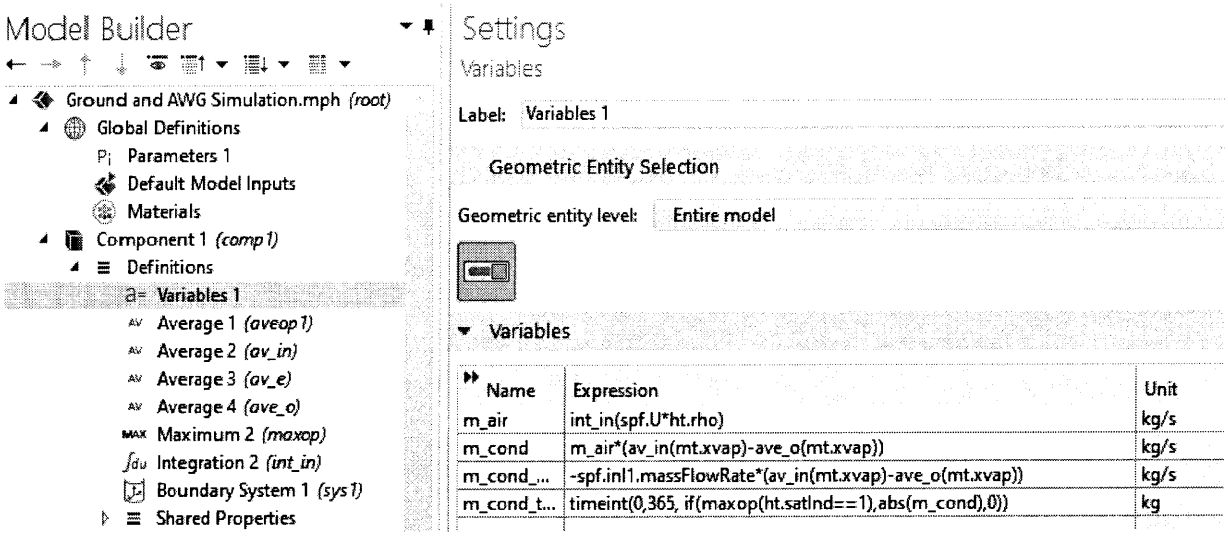


Fig. 47: Nonlocal couplings and Properties Settings in COMSOL.

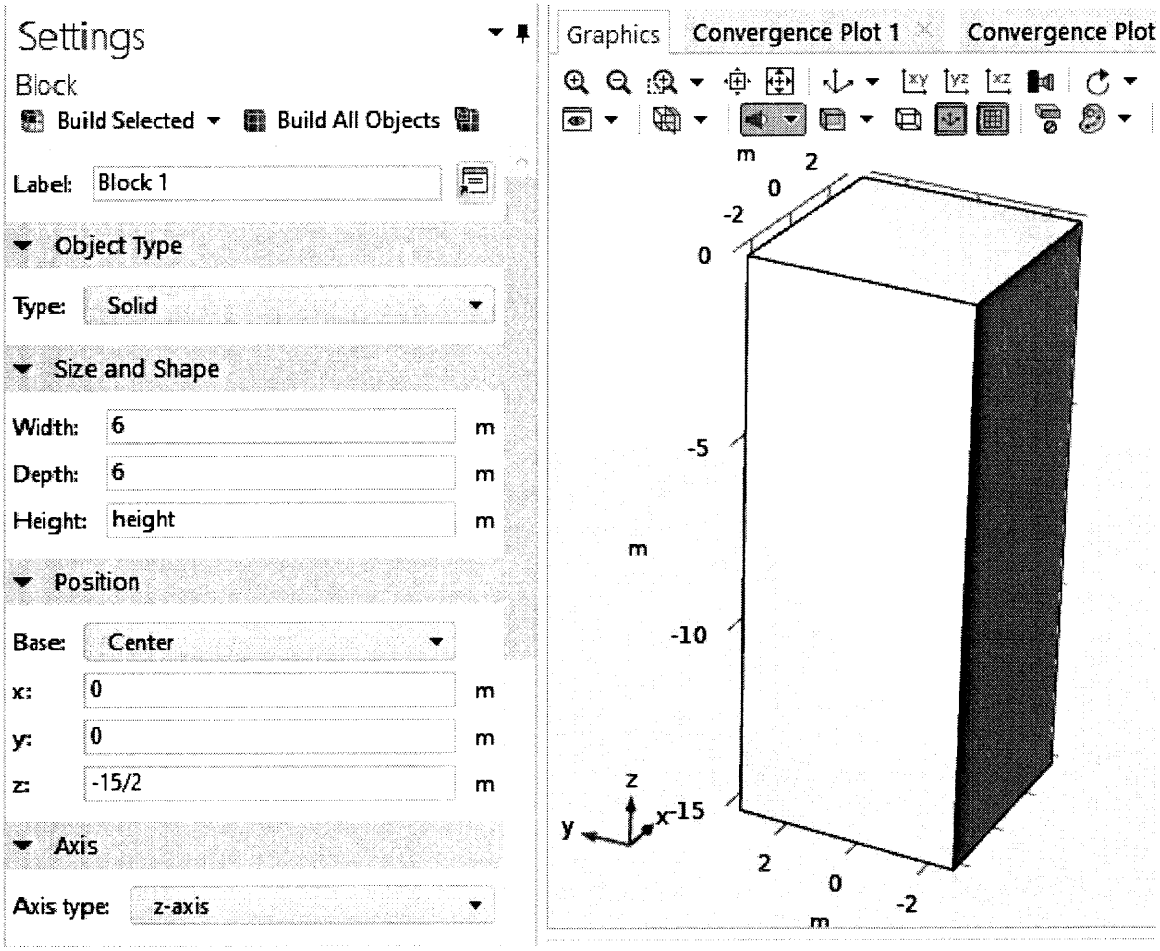


Fig. 48: Building Geometry in COMSOL – Ground Block Settings

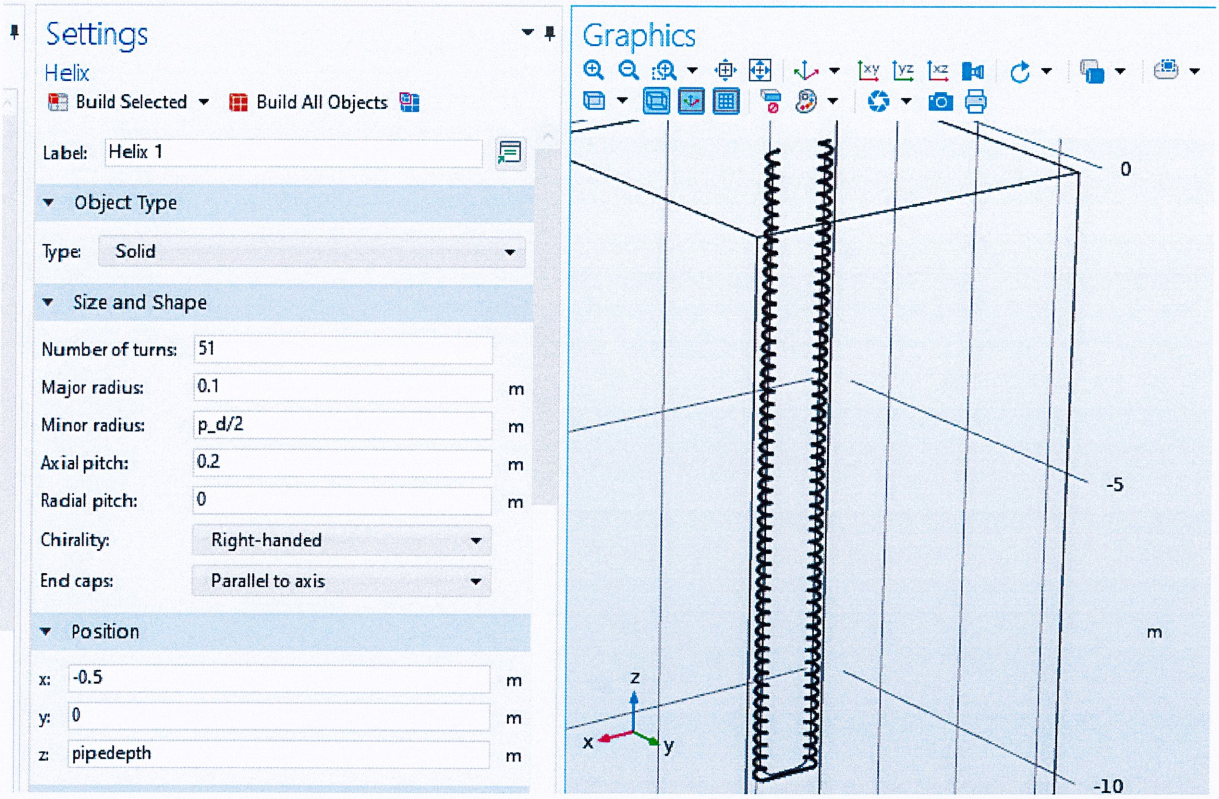


Fig. 49: Building Geometry in COMSOL – Pipe Design Helix Settings.

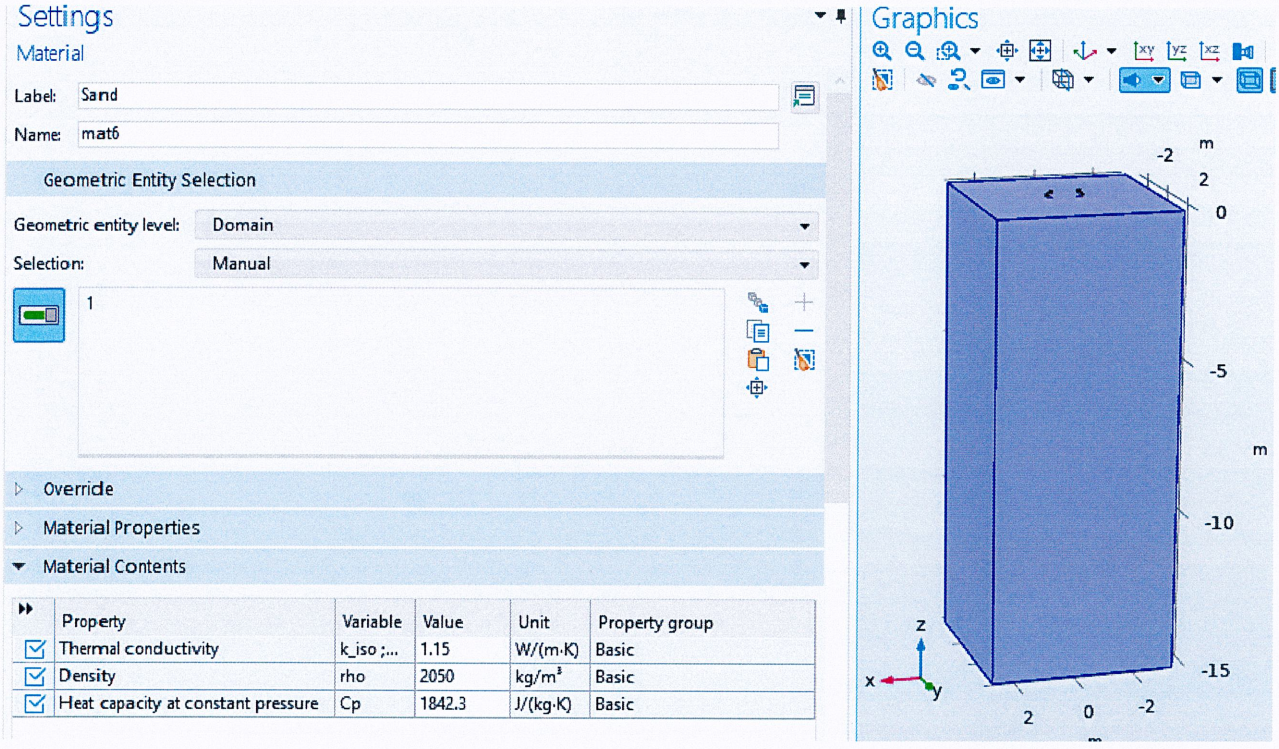


Fig. 50: Setting Soil Material for Ground Domain - COMSOL

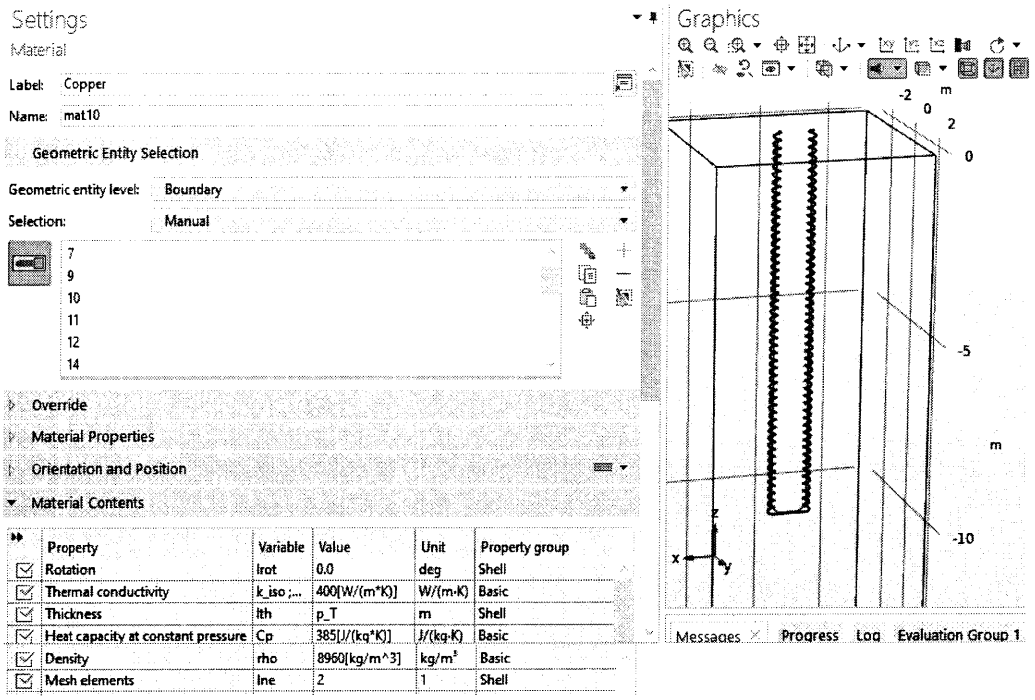


Fig. 51: Setting Copper Material for Pipe Domain - COMSOL

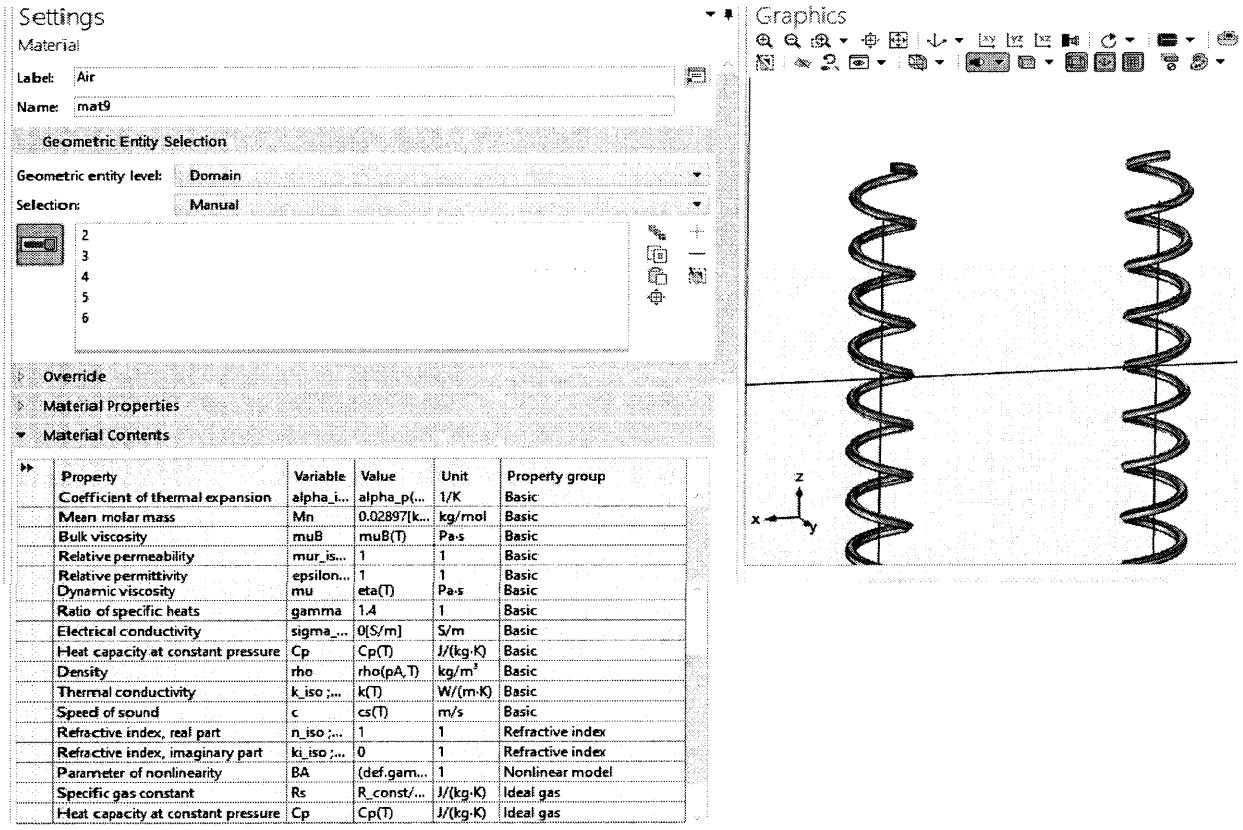


Fig. 52: Setting Copper Material for Air Domain – COMSOL

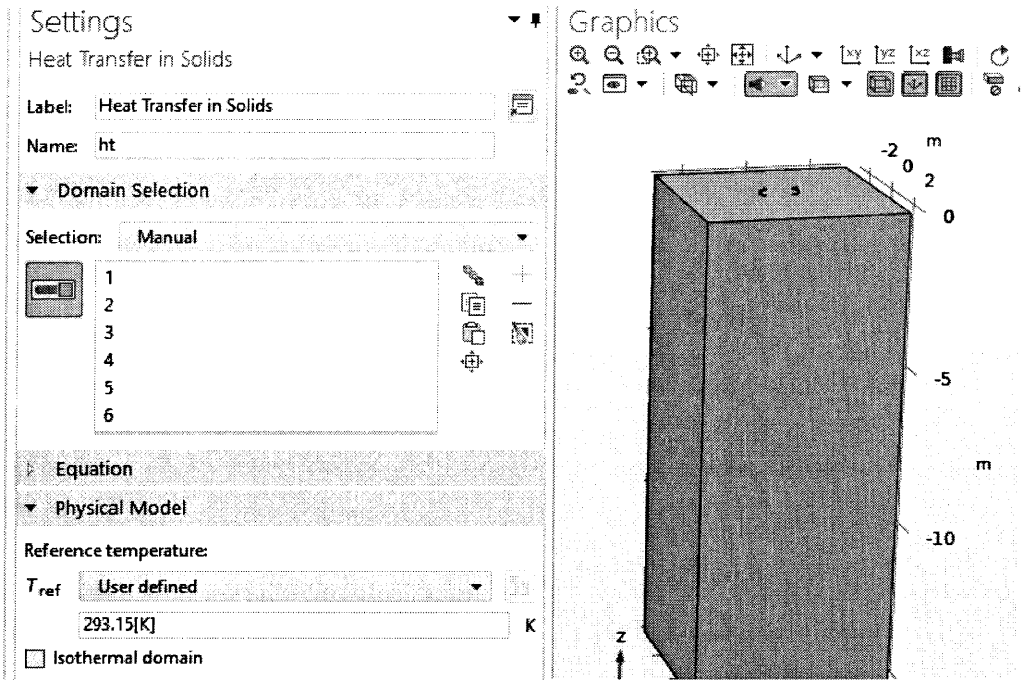


Fig. 53: COMSOL Heat Transfer in Solids Physics Settings

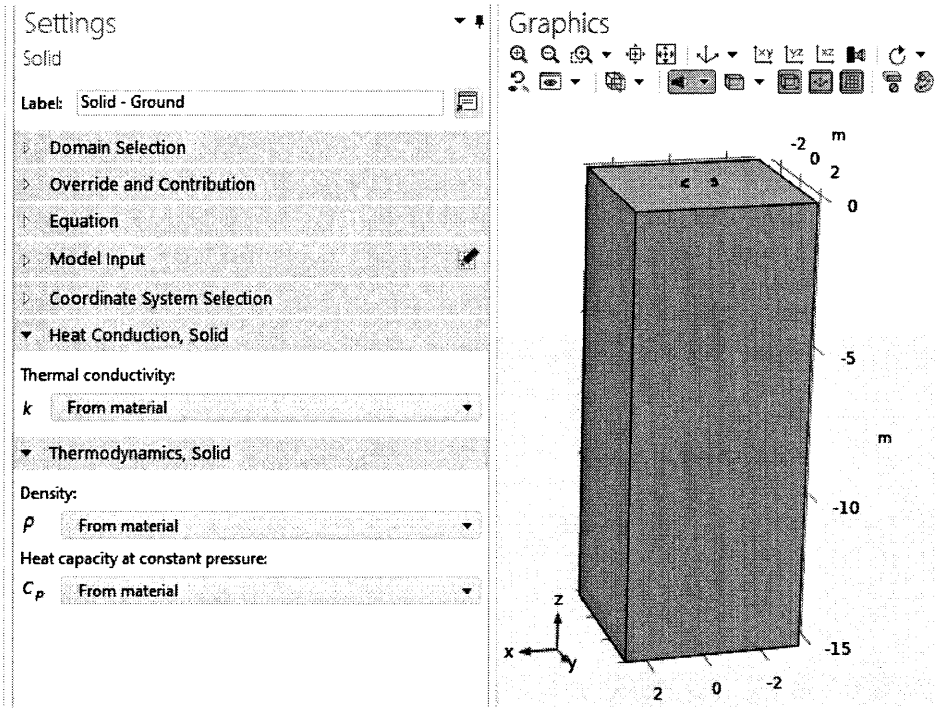


Fig. 54: COMSOL Heat Transfer in Solids Physics – Solid Ground Settings

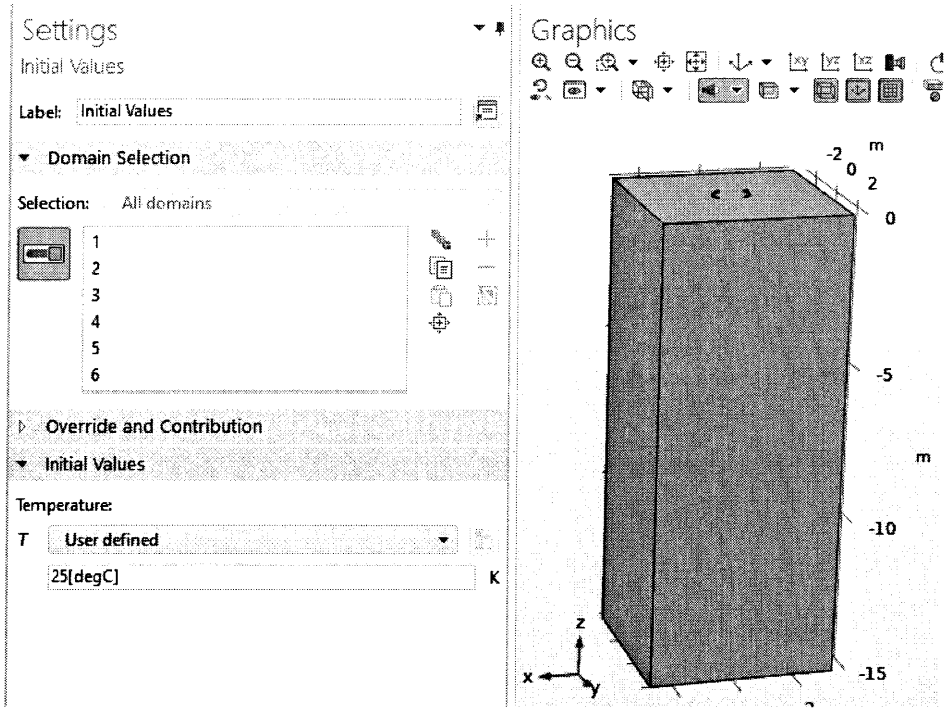


Fig. 55: COMSOL Heat Transfer in Solids Physics – Initial Values Settings

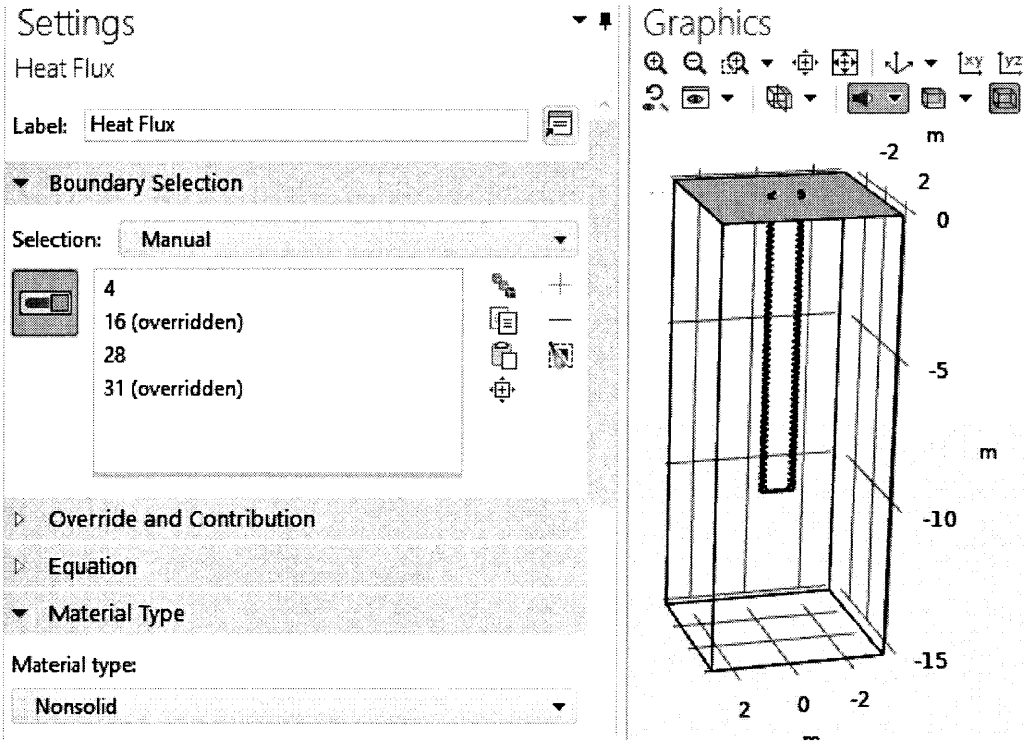


Fig. 56: COMSOL Heat Transfer in Solids Physics – Heat Flux Settings Part 1

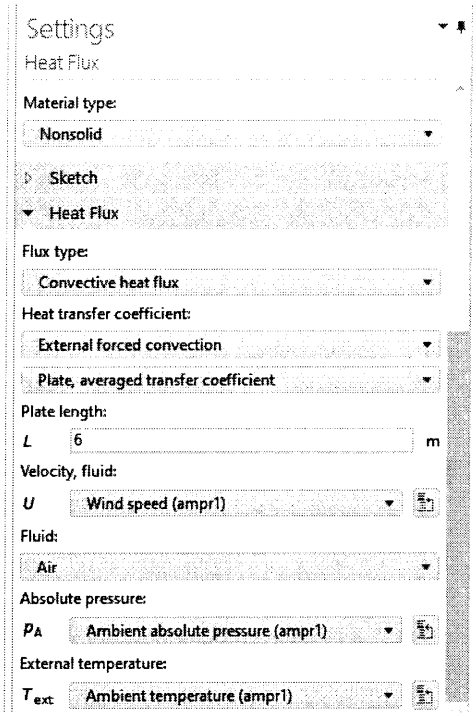


Fig. 57: COMSOL Heat Transfer in Solids Physics – Heat Flux Settings Part 2

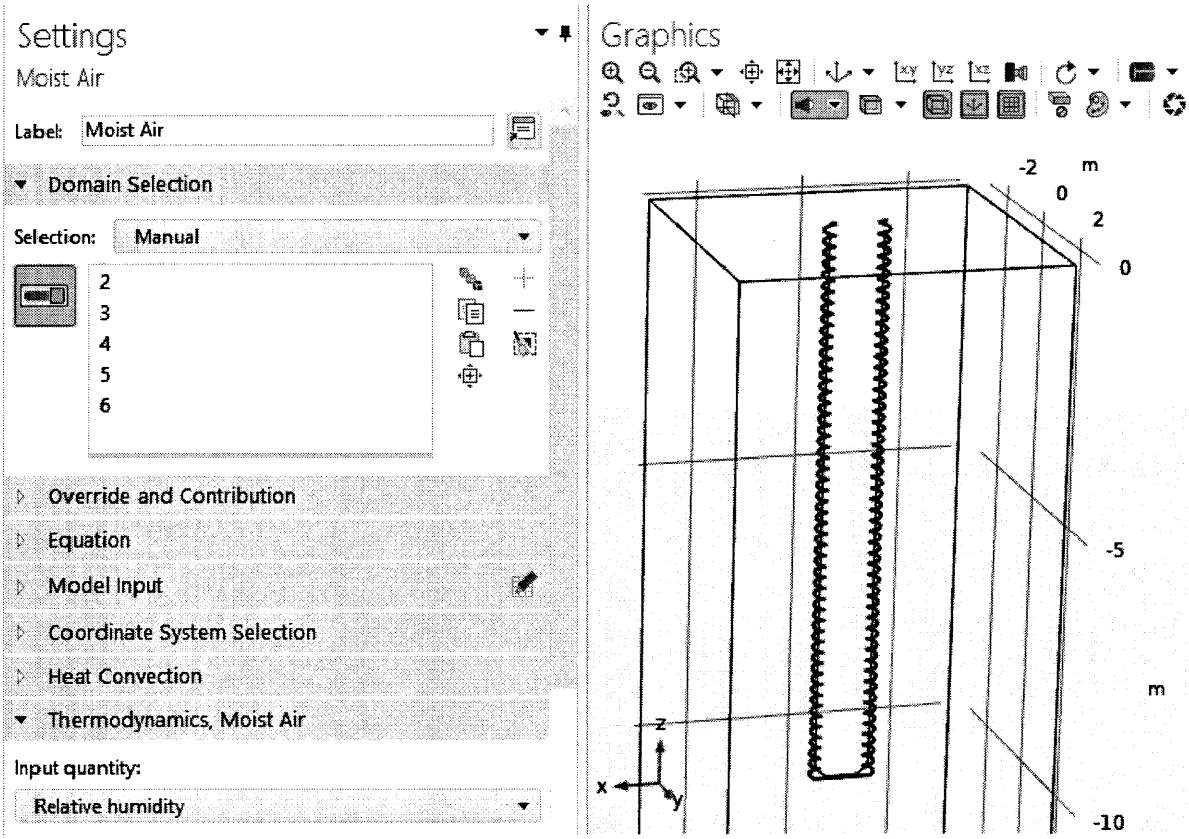


Fig. 58: COMSOL Heat Transfer in Solids Physics – Moist Air Settings

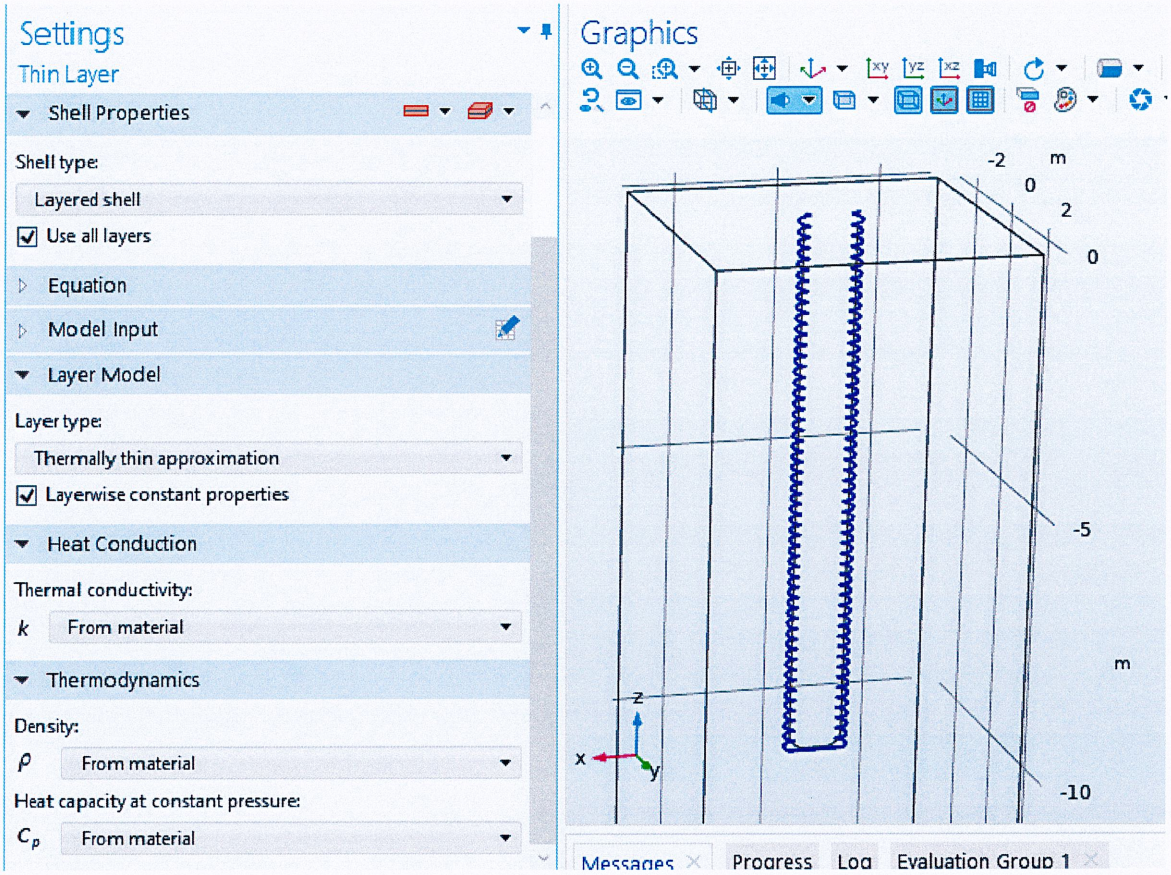


Fig. 59: COMSOL Heat Transfer in Solids Physics – Thin Layer Pipe Shell Settings

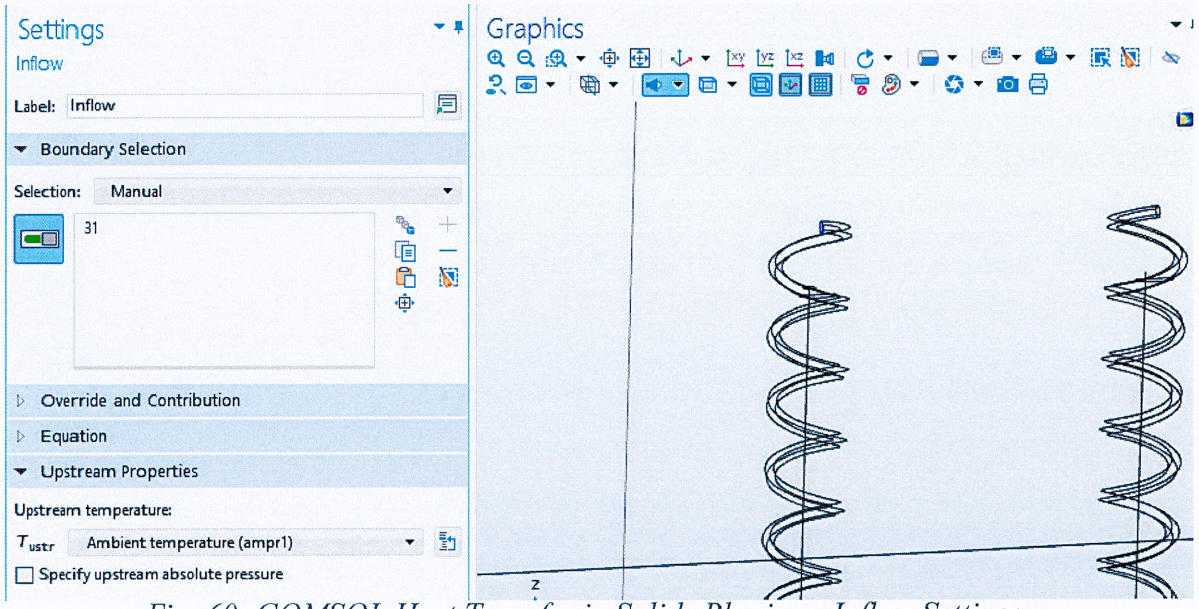


Fig. 60: COMSOL Heat Transfer in Solids Physics – Inflow Settings

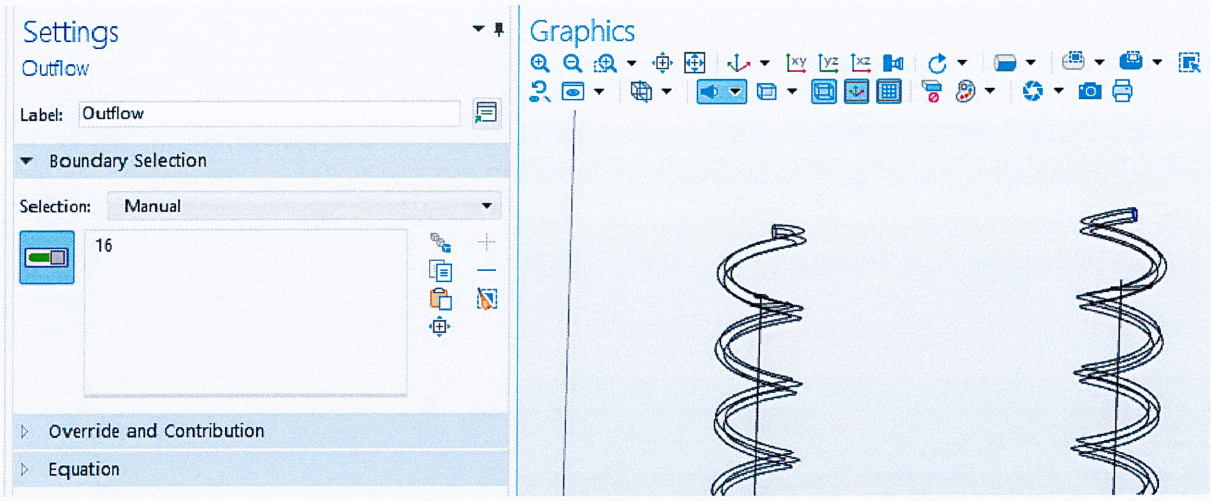


Fig. 61: COMSOL Heat Transfer in Solids Physics – Outflow Settings

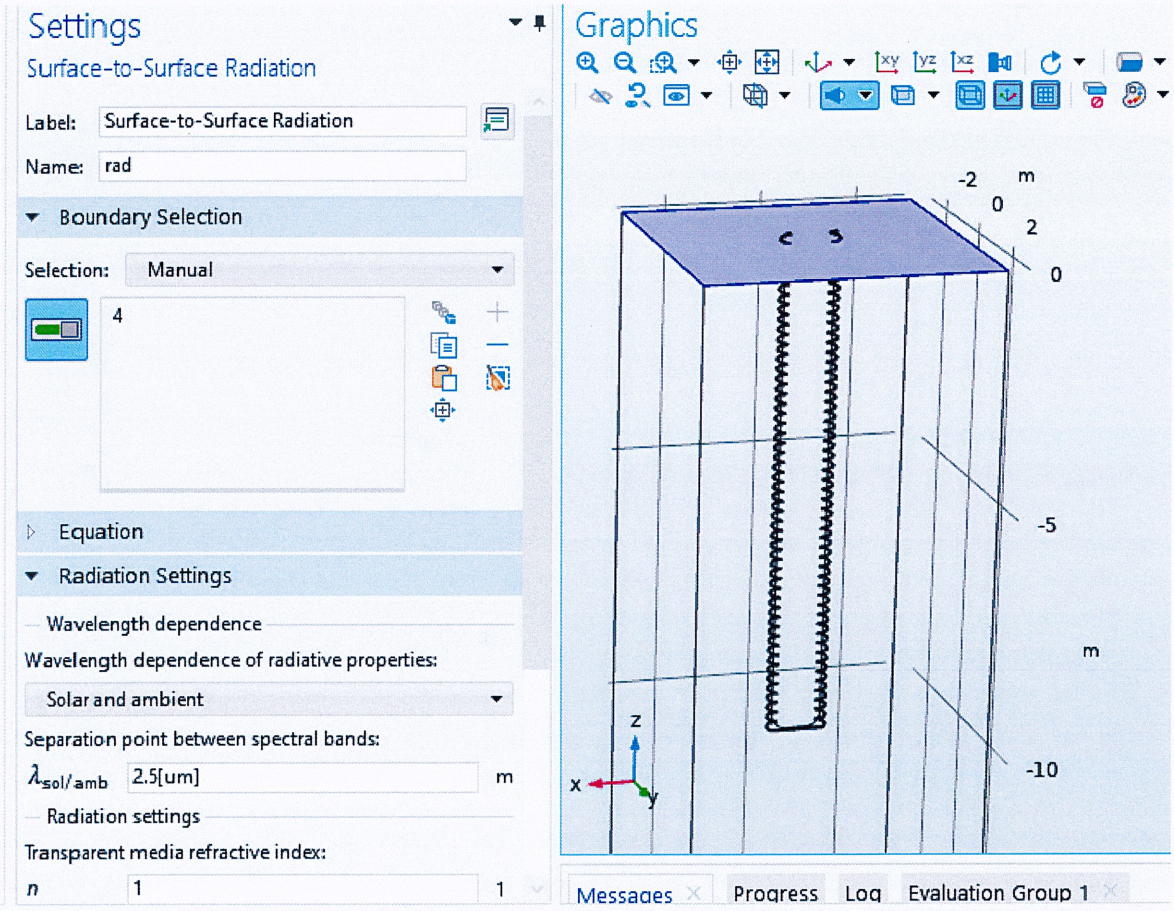


Fig. 62: COMSOL Surface to Surface Radiation Settings

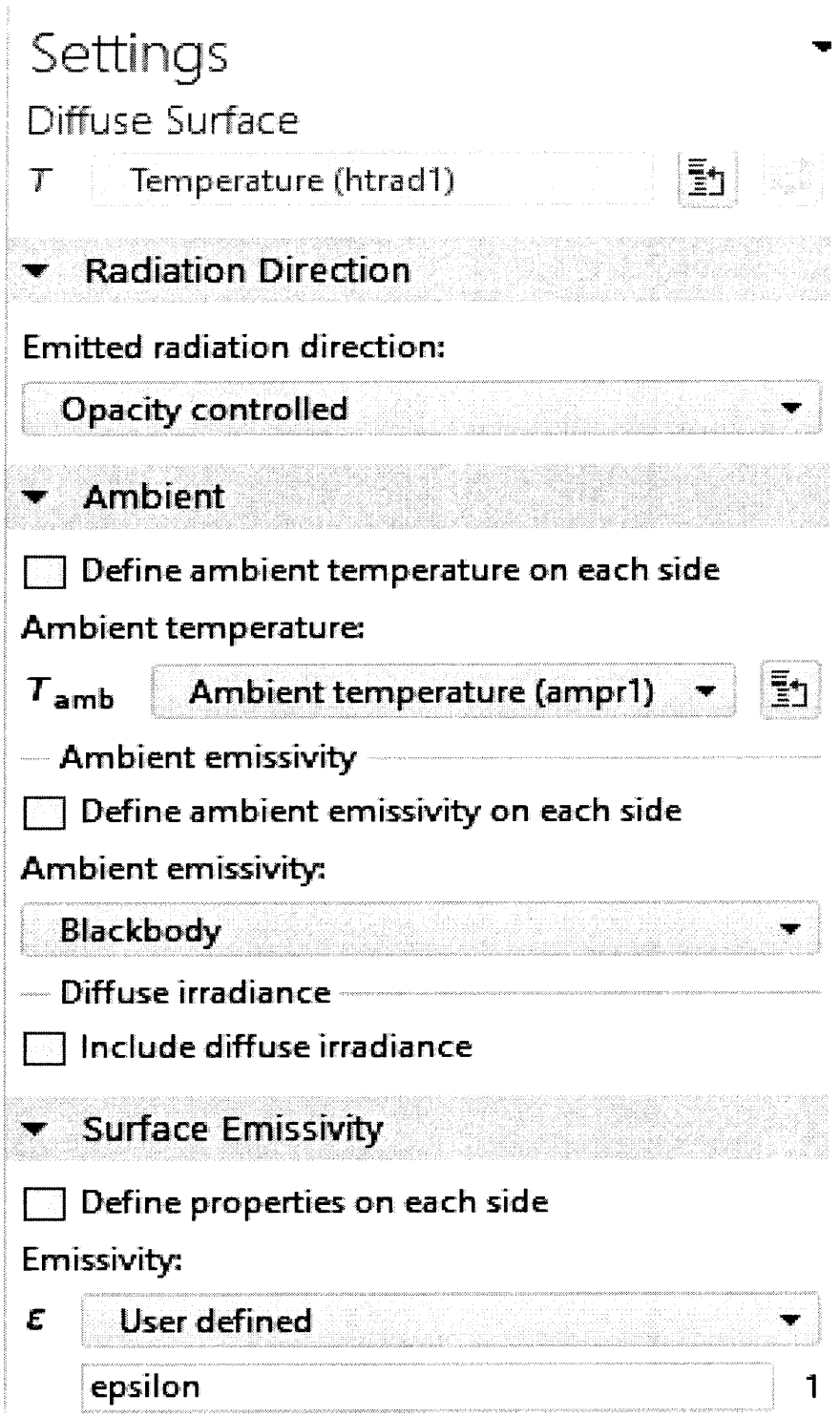


Fig. 63: COMSOL Surface to Surface Radiation – Diffuse Surface Settings

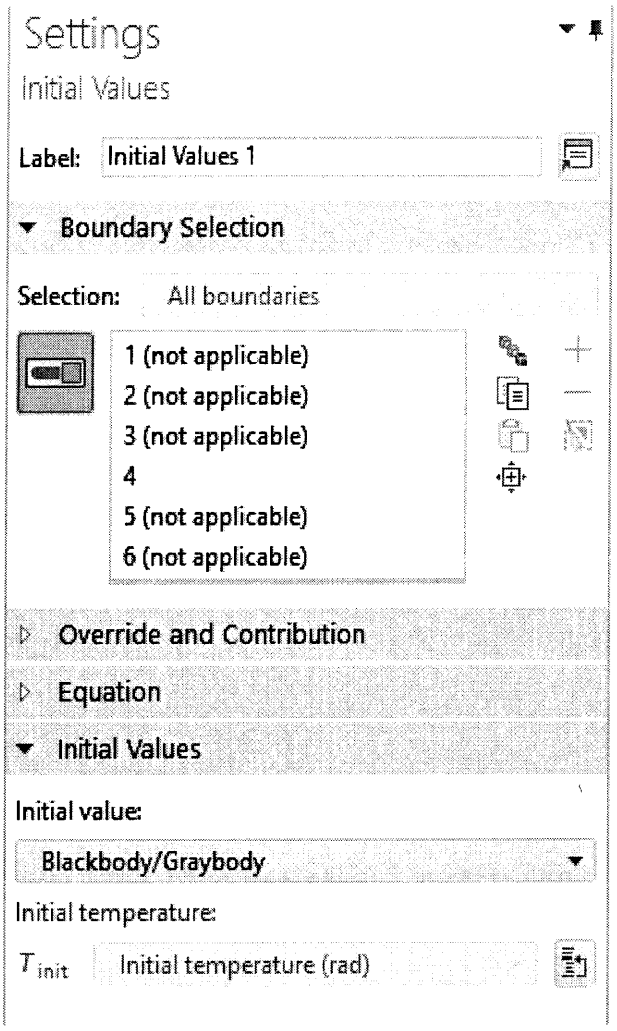


Fig. 64: COMSOL Surface to Surface Radiation – Initial Values Settings

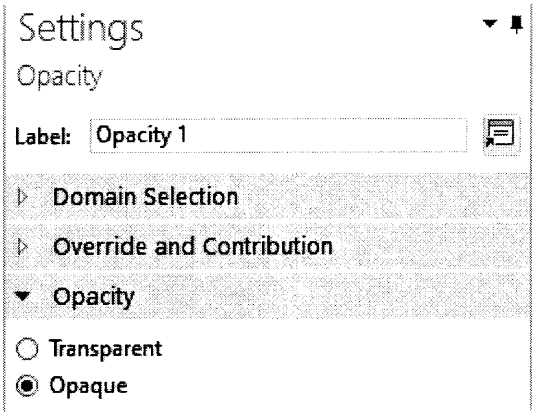


Fig. 65: COMSOL Surface to Surface Radiation – Opacity Settings

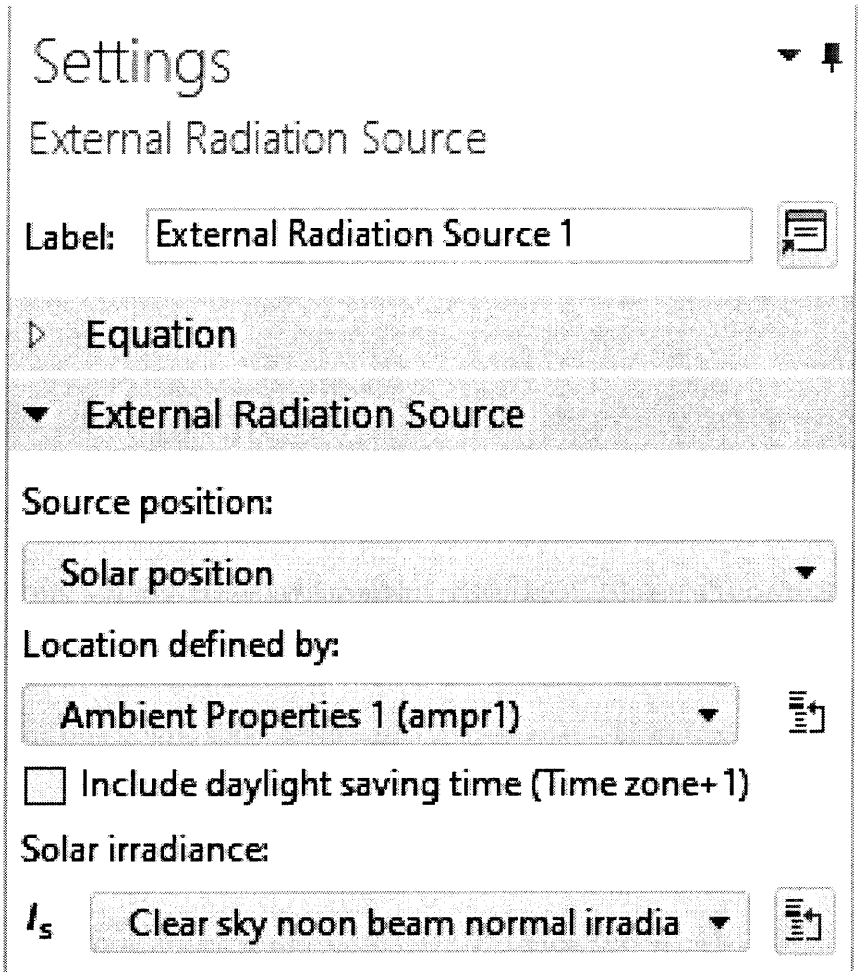


Fig. 66: COMSOL Surface to Surface Radiation – External Radiation Source Settings

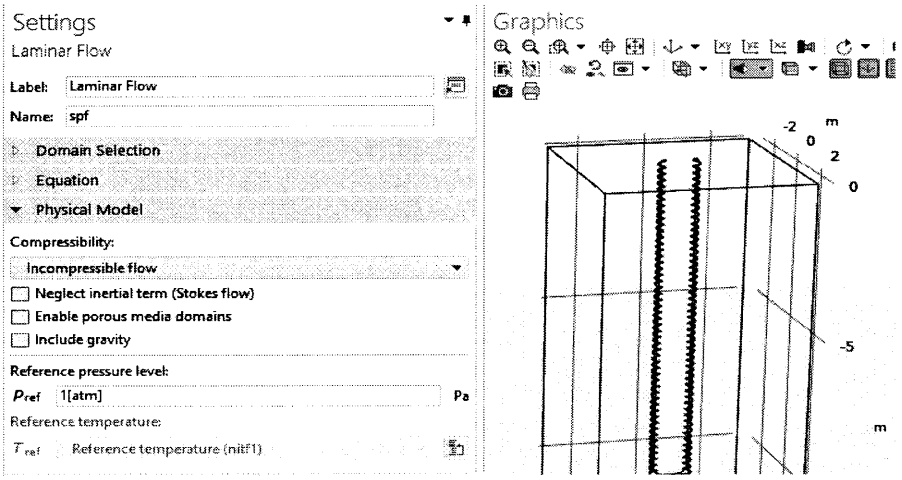


Fig. 67: COMSOL Laminar Flow Physics Settings.

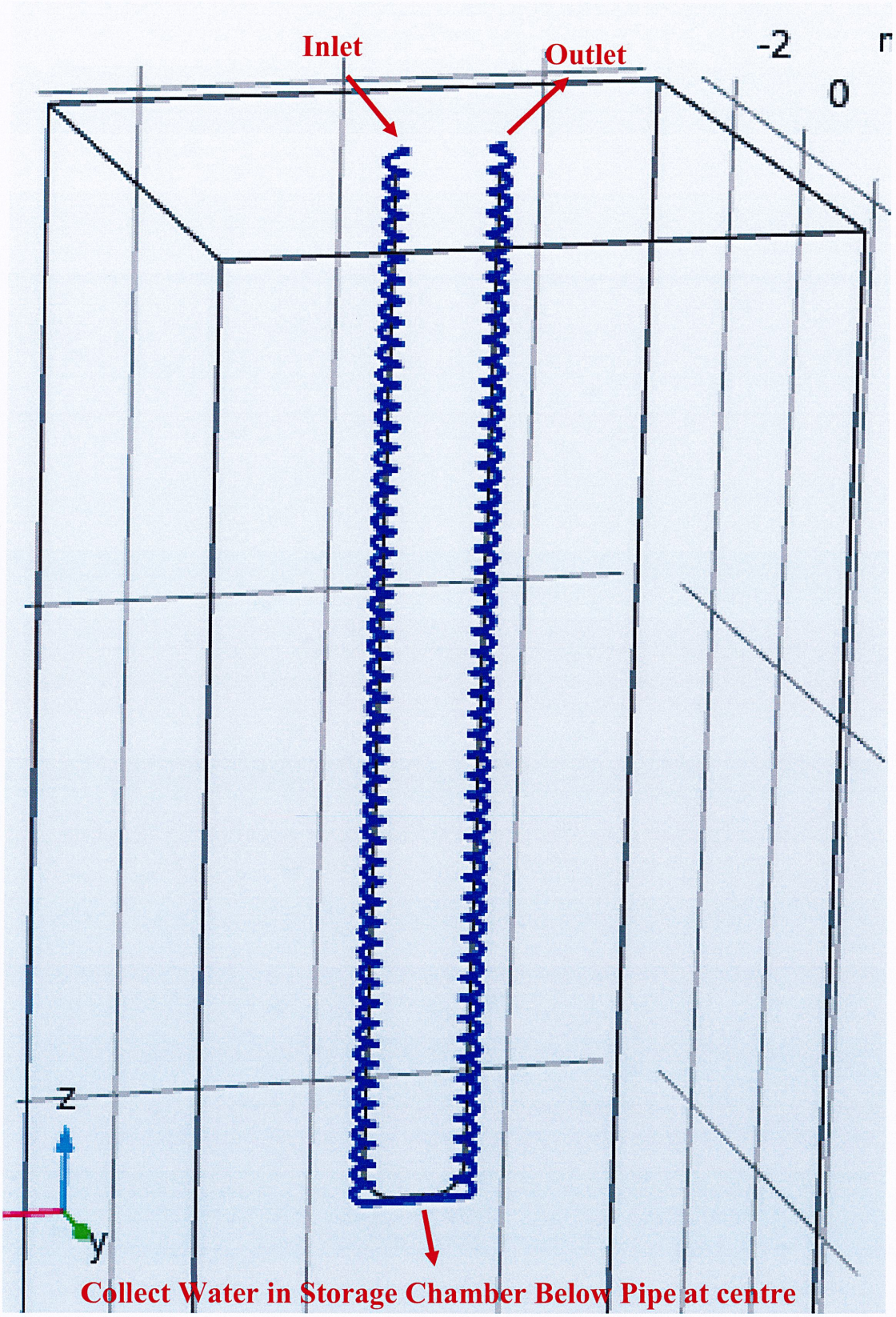


Figure 68, Diagram Showing Inlet Air Flow and Collect Condensed Water Region

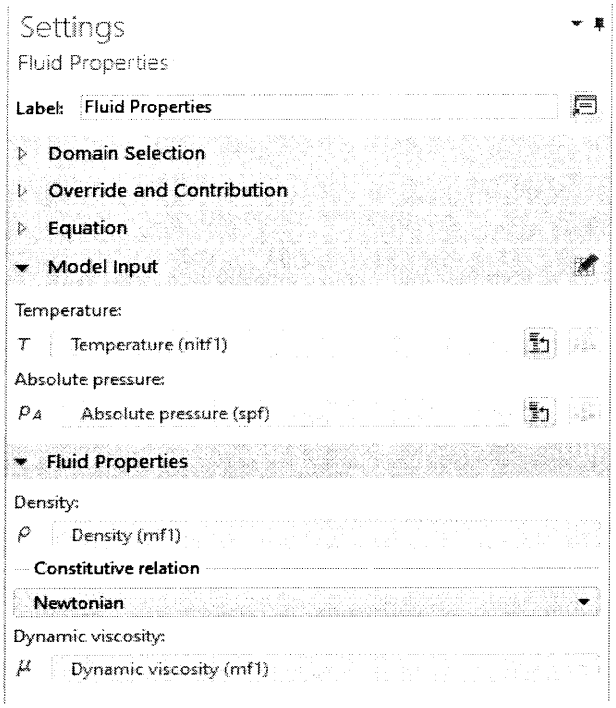


Fig. 69: COMSOL Laminar Flow Physics – Fluid Properties Settings.

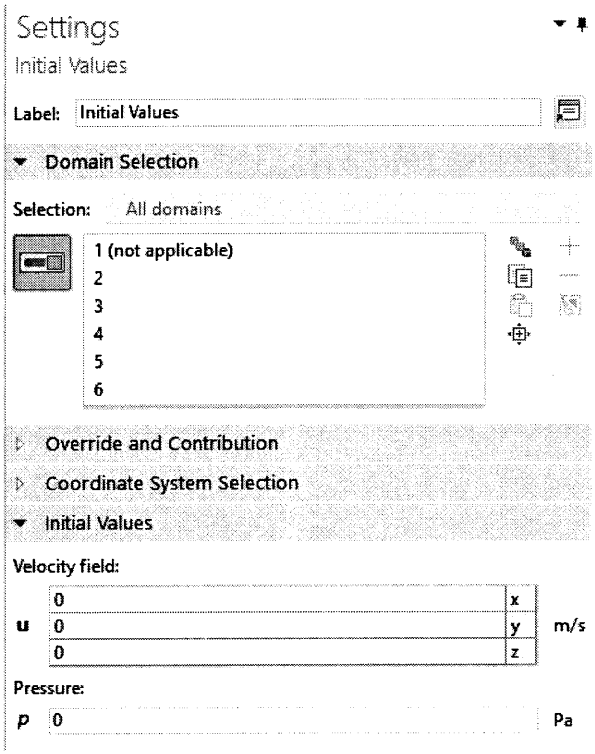


Fig. 70: COMSOL Laminar Flow Physics – Initial Values Settings.

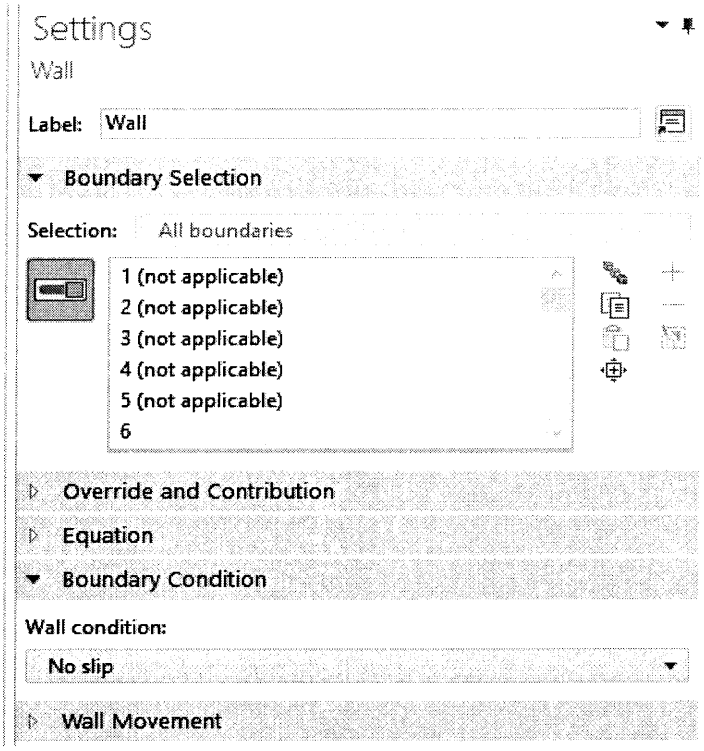


Fig. 71: COMSOL Laminar Flow Physics – Wall Settings.

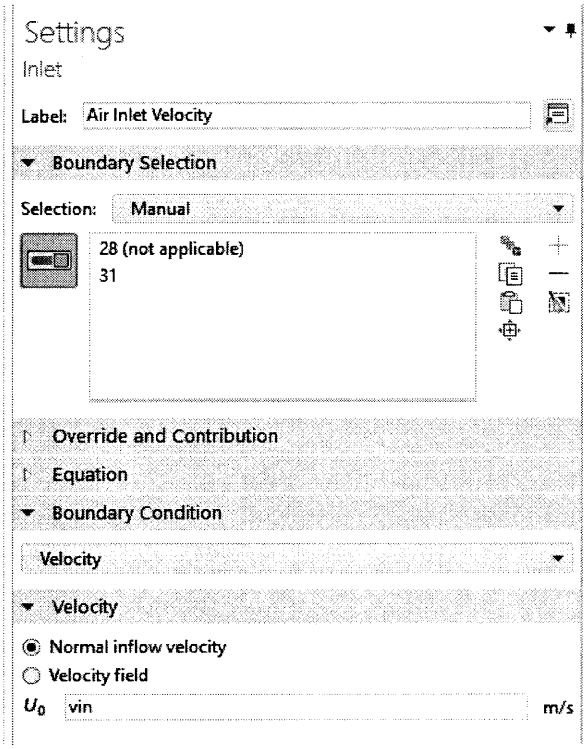


Fig. 72: COMSOL Laminar Flow Physics – Inlet Settings.

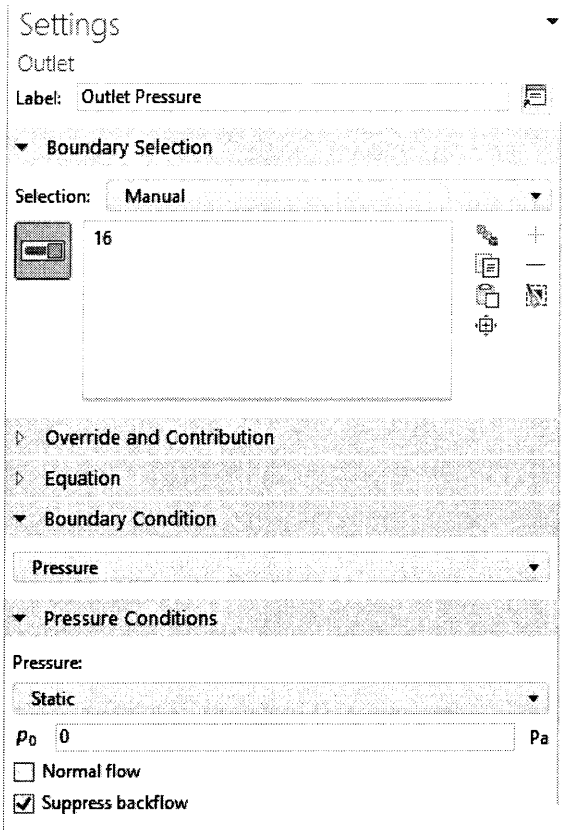


Fig. 73: COMSOL Laminar Flow Physics – Outlet Settings.

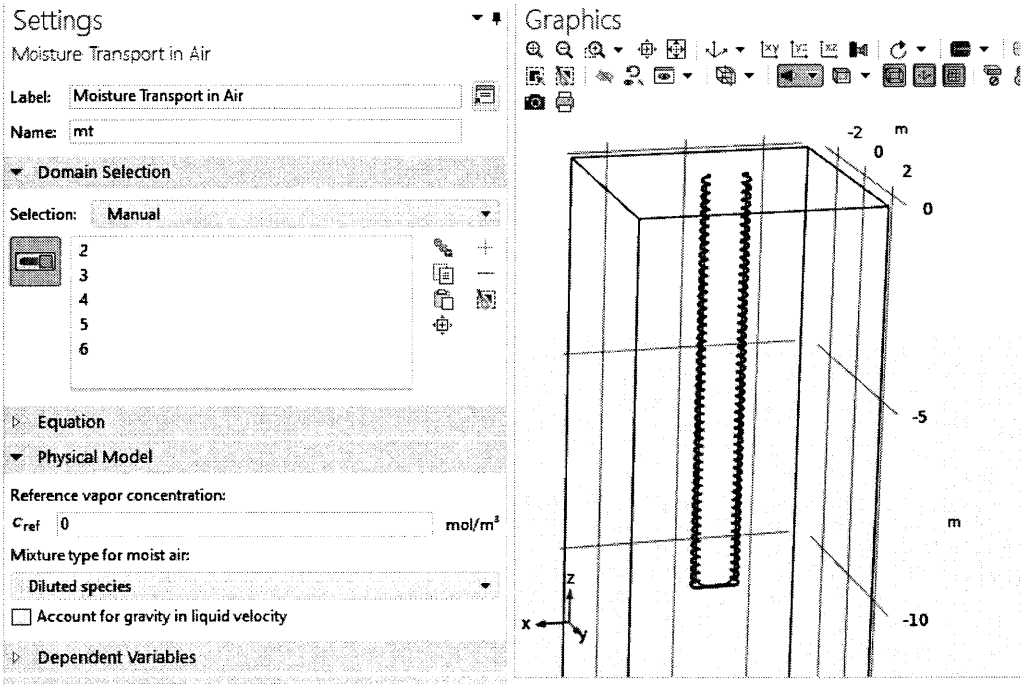


Fig. 74: COMSOL Moisture Transport in Air Physics Settings.

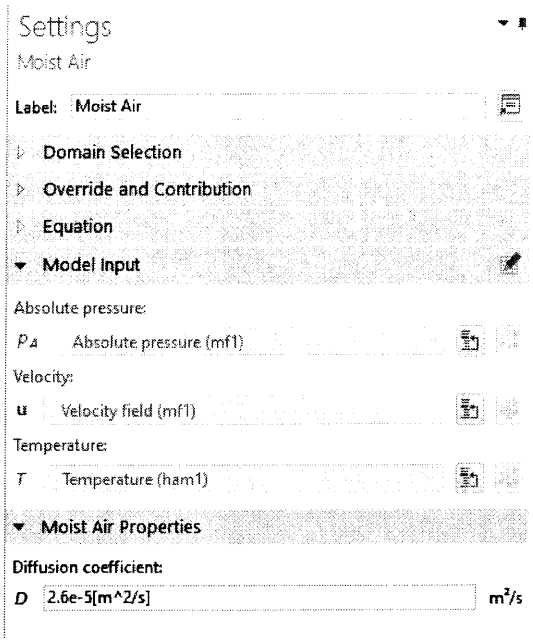


Fig. 75: COMSOL Moisture Transport in Air Physics – Moist Air Settings.

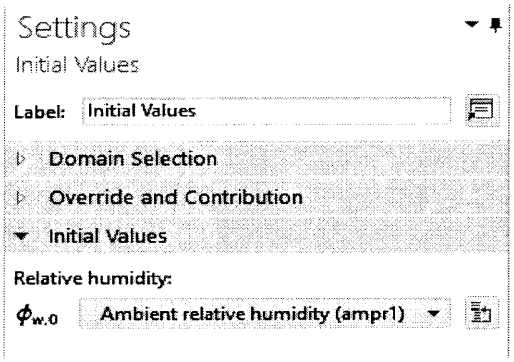


Fig. 76: COMSOL Moisture Transport in Air Physics – Initial Values Settings.

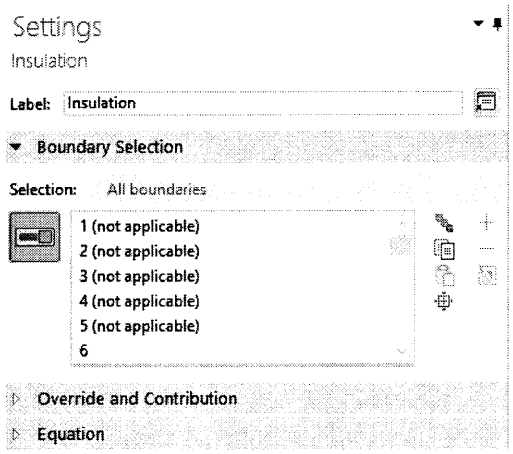


Fig. 77: COMSOL Moisture Transport in Air Physics – Insulation Settings.

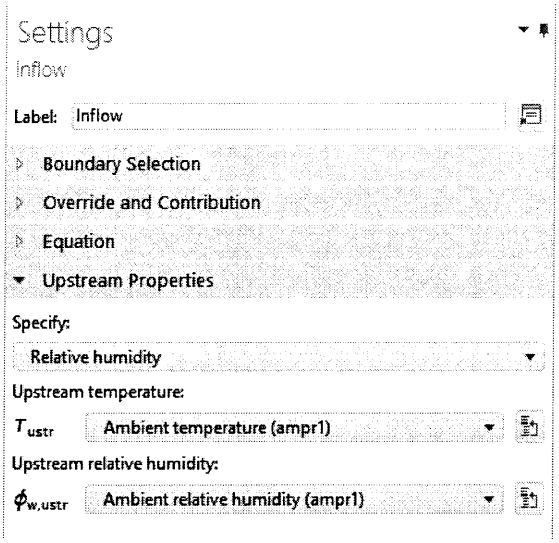


Fig. 78: COMSOL Moisture Transport in Air Physics – Inflow Settings.

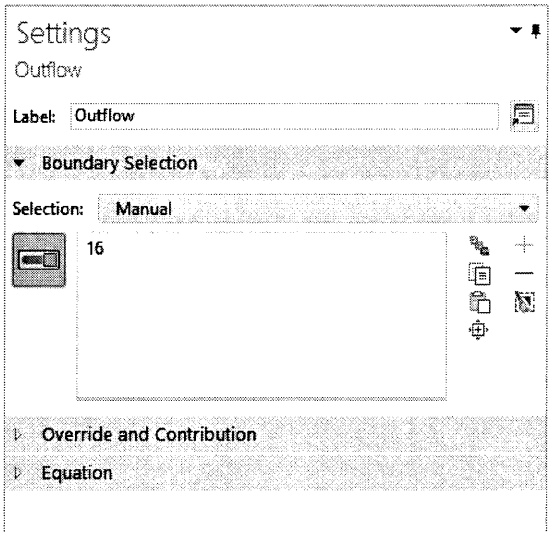


Fig. 79: COMSOL Moisture Transport in Air Physics – Outflow Settings.

APPENDIX B. COMSOL Condensation Result

Table 14, COMSOL Condensation Result @4.25 m/s.

Day	Condensation Rate (kg/s)	Condensed Water Per 8 Hrs (Kg or lt)	Day	Condensation Rate (kg/s)	Condensed Water Per 8 Hrs (Kg or lt)
198	5.02E-06	0.144613633	232.6667	8.55E-06	0.246246021
198.3333	0	0	233	5.11E-06	0.147294225
198.6667	0	0	233.3333	6.81E-06	0.196172435
199	5.04E-06	0.145194235	233.6667	8.46E-06	0.243759691
199.3333	0	0	234	5.03E-06	0.144983157
199.6667	0	0	234.3333	6.74E-06	0.194135055
200	5.07E-06	0.145923196	234.6667	8.36E-06	0.240771071
200.3333	0	0	235	4.94E-06	0.142188103
200.6667	0	0	235.3333	6.66E-06	0.191736148
201	5.08E-06	0.146327028	235.6667	8.32E-06	0.23951158
201.3333	0	0	236	4.89E-06	0.140886141
201.6667	0	0	236.3333	6.57E-06	0.189324004
202	5.11E-06	0.147047544	236.6667	8.25E-06	0.237642023
202.3333	0	0	237	4.82E-06	0.138942014
202.6667	0	0	237.3333	6.61E-06	0.190347448
203	5.12E-06	0.147540686	237.6667	8.31E-06	0.239318419
203.3333	0	0	238	4.69E-06	0.135192353
203.6667	0	0	238.3333	6.44E-06	0.185334939
204	5.15E-06	0.148210241	238.6667	8.03E-06	0.231157387
204.3333	6.88E-06	0.198269226	239	4.65E-06	0.133784071
204.6667	0	0	239.3333	6.33E-06	0.182266567
205	5.17E-06	0.148846896	239.6667	8.00E-06	0.230286363
205.3333	6.96E-06	0.200489283	240	4.59E-06	0.132262931
205.6667	0	0	240.3333	6.36E-06	0.18305847
206	5.19E-06	0.149554989	240.6667	8.05E-06	0.231963972
206.3333	6.94E-06	0.199971379	241	4.69E-06	0.135149029
206.6667	0	0	241.3333	6.27E-06	0.180490781
207	5.19E-06	0.14938639	241.6667	7.85E-06	0.225968636
207.3333	7.05E-06	0.203106687	242	4.44E-06	0.127775834
207.6667	0	0	242.3333	6.08E-06	0.175073595
208	5.19E-06	0.149521674	242.6667	7.70E-06	0.221889026
208.3333	6.98E-06	0.201138282	243	4.34E-06	0.124862278
208.6667	0	0	243.3333	6.03E-06	0.173561662
209	5.23E-06	0.150653159	243.6667	7.65E-06	0.220385376

209.3333	7.01E-06	0.201786761	244	4.24E-06	0.122056677
209.6667	8.46E-06	0.24373324	244.3333	5.97E-06	0.172063674
210	5.24E-06	0.151010025	244.6667	7.82E-06	0.225205396
210.3333	7.12E-06	0.205117696	245	4.23E-06	0.121749816
210.6667	8.52E-06	0.245399047	245.3333	5.88E-06	0.169289007
211	5.26E-06	0.151515539	245.6667	7.47E-06	0.21517136
211.3333	7.05E-06	0.203022409	246	4.15E-06	0.119485048
211.6667	8.55E-06	0.24624882	246.3333	5.76E-06	0.16588826
212	5.32E-06	0.153111374	246.6667	7.61E-06	0.219086862
212.3333	7.07E-06	0.203723125	247	4.08E-06	0.117489746
212.6667	8.56E-06	0.2464427	247.3333	5.68E-06	0.163515362
213	5.29E-06	0.15249065	247.6667	7.41E-06	0.213493359
213.3333	7.19E-06	0.207046892	248	4.02E-06	0.11574269
213.6667	8.61E-06	0.247991928	248.3333	5.60E-06	0.16131606
214	5.31E-06	0.152977291	248.6667	7.17E-06	0.206483696
214.3333	7.11E-06	0.204747086	249	3.88E-06	0.111678334
214.6667	8.64E-06	0.248711131	249.3333	5.50E-06	0.158543331
215	5.36E-06	0.154431561	249.6667	0	0
215.3333	7.14E-06	0.20562638	250	3.79E-06	0.109088802
215.6667	8.64E-06	0.248793065	250.3333	5.40E-06	0.155561655
216	5.34E-06	0.153802539	250.6667	0	0
216.3333	7.25E-06	0.208795322	251	3.72E-06	0.107168574
216.6667	8.69E-06	0.250336128	251.3333	4.99E-06	0.143659869
217	5.36E-06	0.154335088	251.6667	0	0
217.3333	7.16E-06	0.20616141	252	3.70E-06	0.106628131
217.6667	8.72E-06	0.25110071	252.3333	5.21E-06	0.149914692
218	5.37E-06	0.15467532	252.6667	0	0
218.3333	7.19E-06	0.20705447	253	3.59E-06	0.103338615
218.6667	8.74E-06	0.251640866	253.3333	5.12E-06	0.14754398
219	5.41E-06	0.155733094	253.6667	0	0
219.3333	7.22E-06	0.207983455	254	3.51E-06	0.101094775
219.6667	8.73E-06	0.251332113	254.3333	5.02E-06	0.14469617
220	5.43E-06	0.156287724	254.6667	0	0
220.3333	7.27E-06	0.209345431	255	3.45E-06	0.099290626
220.6667	8.75E-06	0.251919209	255.3333	5.05E-06	0.145548978
221	5.44E-06	0.15672422	255.6667	0	0
221.3333	7.20E-06	0.207298967	256	3.56E-06	0.102416227
221.6667	8.82E-06	0.254086964	256.3333	4.98E-06	0.143386283
222	5.42E-06	0.156113044	256.6667	0	0
222.3333	7.20E-06	0.207501793	257	3.33E-06	0.096018832
222.6667	8.78E-06	0.252905801	257.3333	4.85E-06	0.139692636

223	5.41E-06	0.155847048	257.6667	0	0
223.3333	7.23E-06	0.20810087	258	3.25E-06	0.093585698
223.6667	8.80E-06	0.253533672	258.3333	4.81E-06	0.138442647
224	5.44E-06	0.156599529	258.6667	0	0
224.3333	7.26E-06	0.209223409	259	3.12E-06	0.089794994
224.6667	8.79E-06	0.253088969	259.3333	4.35E-06	0.125274414
225	5.45E-06	0.156984427	259.6667	0	0
225.3333	7.22E-06	0.207858567	260	3.05E-06	0.087732626
225.6667	8.84E-06	0.254710716	260.3333	0	0
226	5.43E-06	0.156397667	260.6667	0	0
226.3333	7.22E-06	0.20782197	261	2.91E-06	0.083878703
226.6667	8.83E-06	0.254166175	261.3333	0	0
227	5.41E-06	0.155892417	261.6667	0	0
227.3333	7.20E-06	0.207244933	262	2.85E-06	0.082186592
227.6667	8.79E-06	0.253090125	262.3333	0	0
228	5.40E-06	0.155537527	262.6667	0	0
228.3333	7.17E-06	0.206520608	263	2.74E-06	0.079015883
228.6667	8.81E-06	0.253792525	263.3333	0	0
229	5.38E-06	0.154998348	263.6667	0	0
229.3333	7.11E-06	0.204668992	264	2.64E-06	0.07607715
229.6667	8.74E-06	0.251845567	264.3333	0	0
230	5.32E-06	0.153078492	264.6667	0	0
230.3333	7.04E-06	0.20268719	265	2.61E-06	0.075114319
230.6667	8.68E-06	0.2500989	265.3333	0	0
231	5.25E-06	0.151225002	265.6667	0	0
231.3333	6.96E-06	0.200552248	266	2.46E-06	0.070901008
231.6667	8.61E-06	0.248029833	266.3333	0	0
232	5.18E-06	0.149161454	266.6667	0	0
232.3333	6.89E-06	0.198469499	267	2.34E-06	0.067509121
Total Water Produced (kg or lt)					**29.22262309**

APPENDIX C. Sample Simplified Model Calculation Result (Excel)

Normal Calculation before adjusted for comsol comparison (day 210.6667)	
June	
Number of Tubes	1
Copper Tube Length L (m)	33.63
Kcopper (W/mK)	388
V air	4.25
Inner Diamater D1 (m)	0.0376
Outer Diamater D2 (m)	0.0413
Inner Radius R1 (m)	0.0188
Outer Radius R2 (m)	0.02065
Temperature of Air T1 (Celcius)	35.05642
Relative Humidity RH	67%
Dew Point	27.91505
Specific Humidity SH g/kg	22.0789
Specific Humidity SH kg/kg (Air in)	0.022078915
Specific Humidity SH kg/kg (Air out) = T 25C, 100% RH	0.019788266
Temperature of Outer Tube Surface T3 Same as 10m Below	25
Average Temperature Soil Temperature	30
Average Temp Between T1 and T3 (Celcius)	30.02821
Density Air at Avg Temp (kg/m^3)	1.164
Specific Heat Capacity of Air at Avg Temp Cp (J/kgK)	1006
Thermal Conductivity of Air at Avg Temp Kair (W/mK)	0.02662
Dynamics Viscosity of Air at Avg Temp Uair (Pa s)	0.0000186
Resistance Conduction (C/W)	1.14467E-06
Reynold Number Re	10000.3871
Prandtl Number Pr	0.702915101
Nusselt Number Nu	31.6593821
Heat Transfer Coefficient of Air h (W/m^2 K)	22.41416892
Resistance Convection (C/W)	0.011229398
Heat Transfer Occuring Q (W)	450.2382695
Mass Flow Rate of Air per Tube (kg/s)	0.005493685
Mass Flow Rate of Air Per Tube (g/s)	5.493685451
Heat Transfer Required per Tube to reach dew Point Qdew (W	39.46783511
Mass Flow Rate in of Water Per Second (Kg/s)	0.000121295
Mass Flow Rate out of Water Per Second (Kg/s)	0.000108711
Mass Flow Rate of Water Per Second (g/s)	0.121294612
Latent Heat of Condensation (J/g)	2500
Heat Required to Condense Water (W)	303.2365305
Sensible Heat Water (W)	3.625953824
Sum Heat Transfer Required	346.3303195

Fig. 80: Sample Simplified Model Calculation to Estimate Water Condensation in day/step # 210.667 of the year in Excel.

APPENDIX D. Load Estimation - PV System Sizing

Table 15, Load Estimate Formulas used for Sizing PV System (Fans and Pump)

Estimating the Loads for Single Day		
Load of Fans	Specifications of Available Fan (Amazon)	Fan Dimensions: 120mm D – 60mm Radius Fan Fixed Standard RPM: 3500 RPM∓10% Power at Fixed Standard RPM: 10 W Working Voltage: 12V DC Other Specs = IP65 Waterproof Fan
	Determining Fan RPM Rate	$\frac{Fan\ Fixed\ Standard\ RPM}{Power\ at\ Fixed\ RPM} = \frac{3150}{10} = 315$ RPM Per 1 Watt. Reason 3150RPM was used instead of 3500RPM = taking lower end of -10%
	Determining Fan RPM Required Based on Velocity of Air Flow	$N_{req} = \frac{60*vin}{2\pi r}$ $N_{req} = \frac{60*vin}{2\pi r} = \frac{60*4.25}{2\pi*60*10-3} = 676.4\ RPM$
	Determining Power of Fan Required	$P_{Fan\ Req} = P_{Appliance} = \frac{NReq}{Fan\ RPM\ Rate}$ $P_{Fan\ Req} = \frac{676.4}{315} = 2.15\ W \cong to\ 2.5\ W\ as\ tolerance.$
	Max Load Req for 1 Fan Per Day (Wh)	$L_{Max\ Fan\ (WH)} = P_{Fan\ Req} * T_{Max\ Operation}$ $L_{Max\ Fan\ (WH)} = 2.5*24 = \mathbf{60\ Wh}$

	Determining Max Load Required for Both Fans being blowing and axial fans (Wh)	$L_{Max\ Fans\ (WH)} = L_{Max\ Fan\ (WH)} * 2 = 60 * 2 =$ ***120 Wh***
Load of Water Extraction Pump	Specifications of Found of Water Pump (Amazon)	Pressure Head: 14m (our design = 10-11m as miN). Volumetric Flow Rate at 12m (our condition): 0.063lt/s Power: 180W Voltage: 12V DC
	Pump Maximum Operating Time	$T_{operation\ Pump\ Max} = \frac{Max\ Water\ Volume\ Generated\ Daily}{Volume\ Flow\ Rate\ of\ Pump}$ $T_{operation\ Pump\ Max} = \frac{0.65}{0.063} = 11s$ = better round up to **1 min** as worst case scenario to reach head pressure.
	Determining Maximum Load Required for Pump Per Day (Wh)	$L_{Max\ Pump\ (WH)} = W_{pump} * \left(\frac{Toperation\ Pump\ Max}{3600}\right)$ $P_{Max\ Pump\ Daily\ (WH)} = 180*(60/3600) = 3$ Wh
$Total\ Load = \Sigma Load = 120 + 3 =$ ***123 Wh***		
$Total\ Max\ Load = \frac{Total\ Load}{\eta_{Wiring}} = \frac{123}{0.97} =$ ***127 Wh***		

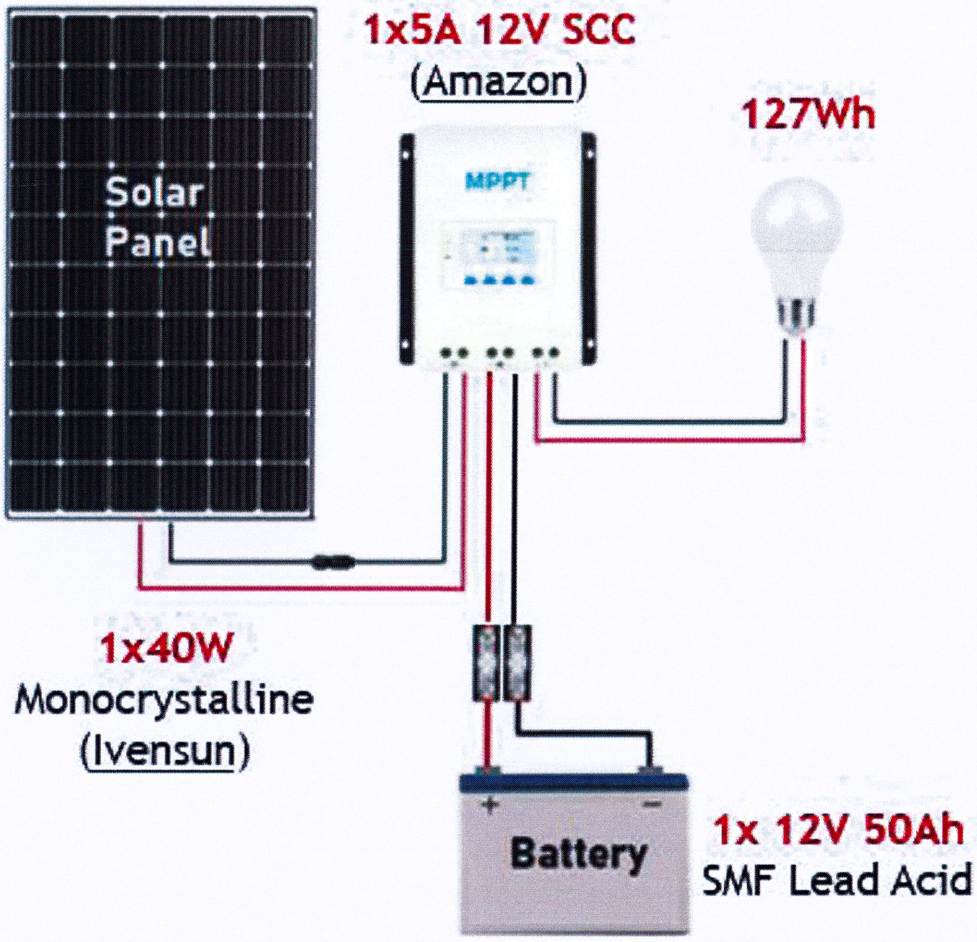


Figure 81, Diagram of Sized PV System

الملخص

ندرة المياه معضلة عالمية ، وبالتالي البحث عن طرق مستدامة لإنتاج المياه هو أحد أهداف التنمية المستدامة. تبحث الأطروحة التالية في دراسة الجدوىعلى إنشاء نظام لتوليد المياه من الهواء الجوي عن طريق التكثيف في منطقة تحت الأرض على سطح ضحل في البحرين و الذي يعمل بالطاقة الكهروضوئية خارج الشبكة.

مبدأ عمل الجهاز هو أن يكون لديك نظام ينتج الماء من الهواء الجوي (AWG) من خلال إجبار الهواء الدافئ و الرطب تحت الأرض على أعماق ضحلة التي هي أكثر برودة ، مما يتسبب في تكثف بخار الماء عن طريق الوصول إلى نقطة الندى (DWPNT) بسبب انتقال الحرارة. وبالتالي ، فإن اللأهداف الرئيسية هي دراسة تغير درجة الحرارة على عمق ضحل من سطح الأرض طوال العام و الى دراسة مدى فعالية الجهاز و كمية الإنتاج السنوية من الناحية النظرية.

المنهج المتبع للوصول الى الأهداف هو الابتداء باستعمال برنامج COMSOL لمحاكاة نمذج ثلاثي الابعاد (3D) على تغير درجة حرارة سطح الأرض في البحرين على اعماق ضحلة طوال العام بإدخال الفيزياء الضرورية و من بعدها دمجه مع أنبوب نحاسي و حقن بداخله سجلات الطقس السنوية للهواء الجوي في البحرين لمراقبة سلوك الديناميكيا الحرارية و كمية انتاج المياه نظرياً. من بعدها، تتم مقارنة نتائج عينة COMSOL لكمية انتاج المياه مع النموذج المبسط الذي يأخذ بعين الاعتبار المعادلات الميكانيكية التي تشمل انتقال الحرارة، الديناميكية الحرارية و ميكانيكية الموائع. و في الأخير، تحديد حجم مكونات النظام الكهرضوئية خارج الشبكة (Off Grid PV) باحتساب حمل الجهاز باستعمال المعادلات الكهربائية.

و على هذا الضوى، النتائج المكتسبة هي ان درجة الحرارة السطحية تصل من ٥٨ الى ١٨ درجة مئوية خلال العام في فصول الصيف و الشتاء و لاكن تثبت طيلة العام على ٢٥ درجة مئوية مع اختلاف بسيط غير ملحوض من عمق ٦ امتار تحت الأرض. و من خلال محاكاة النموذج المصغر في COMSOL الذي يشمل أنبوب نحاسي بتصميم لفائف (COIL) لزيادة انتقال الحرارة بطول ٣٤ متر و قطر داخلي (ID) بمقدار ما يقارب ٣٢ مليمتر، إمكانية انتاج الجهاز ل ٢٩ لتر من الماء خلال الوصول الى نقطة الندى ٦٩ يوم في السنة وهي مابين فترة منتصف شهر تموز الى بداية شهر أكتوبر (الصيف). تم أيضاً تحديد حجم مكونات النظام الكهرضوئية خارج الشبكة بحسب الحمل و الميطلب هو بطارية بسعة ٥٠ امبير، لوح ٤٠ واط و جهاز تحكم شحن (SCC) بمعدل ٥ امبير.

تم ايضاً ذكر أسباب انحراف النتائج مابين نموذج ثلاثي الابعاد و النموذج المبسط و تقديم التوصيات والمقترحات التي تشمل استخدام البرامج الاخرى لمقارنة النتائج و القيام بتجارب فعلية على ارض الواقع لثبات النتائج.

جامعة البحرين

كلية الهندسة

قسم هندسة الكهرباء و الالكترونيات

جدوى نظام توليد المياه من الهواء الجوي الذي يعمل بالطاقة الكهروضوئية خارج الشبكة عن طريق التكثيف تحت الأرض في البحرين

أطروحة مقدمة كجزء من متطلبات الحصول على درجة الماجستير العلوم في هندسة الطاقة المتجددة

إعداد

يوسف أحمد علوي

20146996

إشراف

د. معمر طالب

د. عمر العباسي

مملكة البحرين

12 يناير 2023